HELLENIC REPUBLIC
National and Kapodistrian
University of Athens

Πρόγραμμα
Μεταπτυχιακών
Σπουδών
Επιστήμες Γης
και Περιβάλλον

Master Thesis

Palaeontological study of craniodental material of Late Miocene rhinocerotids (Mammalia, Rhinocerotidae) from the Island of Samos, Greece

Georgia Svorligkou
BSc Geologist
21809

GEORGIA SVORLIGKOU
BSC GEOLOGIST

ΓΕΩΡΓΙΑ ΣΒΟΡΛΙΓΚΟΥ
ΠΤΥΧΙΟΥΧΟΣ ΓΕΩΛΟΓΟΣ

PALAEONTOLOGICAL STUDY OF CRANIODENTAL MATERIAL OF LATE MIOCENE RHINOCEROTIDS (MAMMALIA, RHINOCEROTIDAE) FROM THE ISLAND OF SAMOS, GREECE

ΠΑΛΑΙΟΝΤΟΛΟΓΙΚΗ ΜΕΛΕΤΗ ΕΥΡΗΜΑΤΩΝ ΚΡΑΝΙΟΔΟΝΤΙΚΟΥ ΥΛΙΚΟΥ ΑΠΟΛΙΘΩΜΕΝΩΝ ΡΙΝΟΚΕΡΟΤΙΔΩΝ (MAMMALIA, RHINOCEROTIDAE) ΑΠΟ ΤΟ ΑΝΩΤΕΡΟ ΜΕΙΟΚΑΙΝΟ ΤΗΣ ΝΗΣΟΥ ΣΑΜΟΥ

Υποβλήθηκε στο ΠΜΣ Επιστήμες Γης και Περιβάλλον
Ειδίκευση: Κλιματικές Μεταβολές και Επιπτώσεις στο Περιβάλλον

Ημερομηνία Προφορικής Εξέτασης:
02/12/2021

Three-Member Advising Board:
Assistant Professor Dr. Socrates Roussiakis, National Kapodistrian University of Athens, Supervisor
Professor Dr. Dimitrios S. Kostopoulos, Aristotle University of Thessaloniki
Associate Professor Dr. Georgios Iliopoulos, University of Patras

Τριμελής Εξεταστική Επιτροπή
Επίκουρος Καθηγητής Δρ. Σωκράτης Ρουσιάκης, Επιβλέπων, Εθνικό Καποδιστριακό Πανεπιστήμιο Αθηνών
Καθηγητής Δρ. Δημήτριος Σ. Κωστόπουλος, Μέλος, Αριστοτέλειο Πανεπιστήμιο Θεσσαλονίκης
Αναπληρωτής Καθηγητής Δρ. Γεώργιος Ηλιόπουλος, Μέλος, Πανεπιστήμιο Πατρών

PALAEONTOLOGICAL STUDY OF CRANIODENTAL MATERIAL OF LATE MIOCENE RHINOCEROTIDS (MAMMALIA, RHINOCEROTIDAE) FROM THE ISLAND OF SAMOS, GREECE – *Master Thesis*

ΠΑΛΑΙΟΝΤΟΛΟΓΙΚΗ ΜΕΛΕΤΗ ΕΥΡΗΜΑΤΩΝ ΚΡΑΝΙΟΔΟΝΤΙΚΟΥ ΥΛΙΚΟΥ ΑΠΟΛΙΘΩΜΕΝΩΝ ΡΙΝΟΚΕΡΟΤΙΔΩΝ (MAMMALIA, RHINOCEROTIDAE) ΑΠΟ ΤΟ ΑΝΩΤΕΡΟ ΜΕΙΟΚΑΙΝΟ ΤΗΣ ΝΗΣΟΥ ΣΑΜΟΥ– *Μεταπτυχιακή Διπλωματική Εργασία*

Citation:
Svorligkou G., 2021. Palaeontological study of craniodental material of Late Miocene rhinocerotids (Mammalia, Rhinocerotidae) from the Island of Samos, Greece. Master Thesis, Program of Postgraduate Studies in Earth Science and Environment. Faculty of Geology and Geoenvironment, National Kapodistrian University of Athens, 115 pp.

This thesis is dedicated to the loving memory of my grandfather, Vassilis Drakatos (1934-2019).

Contents:

Acknowledgments

First and foremost, I would like to thank my family, for the emotional and financial support they provided me with during the culmination of my Master's program and the present work. I wish to express my vast gratitude to my supervisor, Associate Professor Dr. Socrates Roussiakis, for entrusting me with the material from Samos and assisting me during the whole process. For their advice and helpful remarks in correcting this manuscript, I would like to thank the members of my advising board, Professor Dr. Dimitrios Kostopoulos (Aristotle University of Thessaloniki) and Assistant Professor Dr. Georgios Iliopoulos (University of Patras). Further, I am grateful to Professor Emeritus Dr. Georgios Theodorou and Professor Dr. Efterpi Koskeridou (University of Athens), former and current Director of the Athens Museum of Palaeontology and Geology respectively, for providing me access to the Samos material and supporting me through this work. I would like to express my gratitude to Dr. Ursula Göhlich and Dr. Karin Wiltske (Naturhistorisches Museum Wien) for their guidance and hospitality during my SYNTHESYS+ visit (AT-TAF-3924: Systematics and Palaeoecology of Late Miocene Rhinocerotids from Greek and Iranian Localities) in Vienna. I wish to thank my colleague, PhD candidate Panagiotis Kampouridis (Eberhard-Karls University of Tübingen) for providing me data on the Tübingen collection material and kindly proofreading my many drafts. For helping me with editing the photographs, I would like to express my gratitude to MSc Georgios Oikonomakis and BSc Athanassios Maravelias (National Kapodistrian University of Athens). I would like to thank PhD candidate Ioannis Giaourtsakis (Ludwig-Maximilians University of Munich), for sharing his vast knowledge on fossil rhinocerotids with me. For their cordial spirit and kind advice, I wish to thank Dr Alexandros Xafis (University of Vienna), Dr Naomi Apostolaki (University of Bristol), PhD candidate Dionysia Liakopoulou (National Kapodistrian University of Athens), MSc students Stamatina Sklavounou, Panagiotis Filis and Evangelia Alifieri (Aristotle University of Thessaloniki). Finally, I would like to thank fellow MSc students Chrysanthi Kosma, Sofia Matsangou and Maria-Anna Nakasi, as well as BSc geologists Euphemia Panopoulou, Stefania Papamanoli, Eirini Koumoutsea and Maria-Roi Panagiotaki, for supporting me from the beginning of the Master's programme to the end of this thesis - and learning more about fossil rhinos than a non-palaeontologist should ever wish to learn.

Abstract

The rich and diverse Late Miocene fauna of Samos Island, Greece, consists of an impressive number of mammalian taxa, among whom the hornless rhinocerotid *Chilotherium schlosseri* WEBER, 1905 and the two-horned species *Dihoplus pikermiensis* TOULA, 1906 and *Miodiceros neumayri* OSBORN, 1900 are present. In this thesis, antecedently undescribed craniodental material of these three rhinocerotid genera, excavated in 1903 in Samos by Professor Theodoros Skoufos of the University of Athens and stored in the collections of the Athens Museum of Palaeontology and Geology (AMPG), is prepared, examined and evaluated for the first time. Some of the most noteworthy specimens of the collection include an almost complete juvenile *M. neumayri* maxilla, a *C. schlosseri* mandible partially bearing the lower incisors, two partly preserved adult *C. schlosseri* skulls and the skull of an infant *C. schlosseri.* An important number of both isolated and articulated dental and postcranial rhinocerotid specimens also belong to the collection, but their preparation and study were beyond the scope of the present work.

The sympatric presence of the three aforementioned taxa is not a unique feature of Late Miocene Samian faunal assemblage. Veritably, the coexistence of brachydont *D. pikermiensis* and more robust, hypsodont *M. neumayri*, along with an aceratheriine genus such as specialized *Chilotherium* or more primitive browser *Acerorhinus* KRETZOI, 1942, was not uncommon in the Turolian localities of the Greco-Iranian Zoobiogeographic Province.

As far as Samos Island is concerned, the majority of the craniodental rhinocerotid elements studied herein belong to *C. schlosseri*. Due to the small number of craniodental *M. neumayri* and *D. pikermiensis* specimens, no safe conclusion may be drawn on the relative dominance of the tandem-horned rhinocerotids. However, the presence of *C. schlosseri* does point to a more arid, open habitat. Consequently, during the Turolian, Samos habitats resembled somewhat more those of Anatolia and Iran, rather than those of the classical synchronous localities of Pikermi (Attica) and Kerassia (Euboea Island).

Περίληψη

Η πλούσια και ποικιλόμορφη, ηλικίας Ανωτέρου Μειοκαίνου, πανίδα της νήσου Σάμου φέρει πλήθος απολιθωμένων θηλαστικών. Μεταξύ αυτών, ξεχωρίζουν τα κερασφόρα είδη ρινόκερων *Miodiceros neumayri* OSBORN, 1900 και *Dihoplus pikermiensis* TOULA, 1906 καθώς και το μη κερασφόρο είδος *Chilotherium schlosseri* WEBER, 1905. Στα πλαίσια της παρούσας διπλωματικής εργασίας, τμήμα του κρανιοδοντικού υλικού των τριών αυτών ειδών από τη συλλογή του Μουσείου Παλαιοντολογίας και Γεωλογίας του Πανεπιστημίου Αθηνών συντηρείται, καταγράφεται και μελετάται συστηματικά για πρώτη φορά. Το υλικό προέρχεται από τις ανασκαφές που διεξήχθησαν στη Σάμο το 1903 από τον καθηγητή του Πανεπιστημίου Αθηνών Θ. Σκούφο. Μερικά από τα πλέον εντυπωσιακά και καλά διατηρημένα δείγματα της συλλογής περιλαμβάνουν μια σχεδόν πλήρη νεογιλή οδοντοστοιχία *M. neumayri*, ένα κρανίο νεαρού *C. schlosseri* και δύο κρανία ενηλίκων ατόμων του ίδιου είδους. Επιπλέον, η συλλογή περιλαμβάνει μεγάλο αριθμό μετακρανιακού υλικού και των τριών ειδών, των οποίων η συντήρηση και καταγραφή υπερβαίνει τους σκοπούς της εργασίας αυτής.

Η συμπατρική παρουσία των τριών αυτών ρινοκεροτιδών δεν ήταν σπάνια στο Ανώτερο Μειόκαινο της Ανατολικής Μεσογείου. Στην πραγματικότητα, η συνύπαρξη του βραχυδοντικού είδους *D. pikermiensis* με το εύρωστο, υψοδοντικό είδος *M. neumayri* και ένα μη κερασφόρο γένος, όπως το εξελιγμένο *Chilotherium* ή το πιο πρωτόγονο γένος *Acerorhinus* KRETZOI, 1942, ήταν αρκούντως συχνή στην Ελληνο-Ιρανική Ζωοβιογεωγραφική Επαρχία κατά το Τουρώλιο.

Όσον αφορά στη Σάμο, το μεγαλύτερο τμήμα του κρανιοδοντικού υλικού της ανασκαφής Σκούφου που μελετήθηκε στα πλαίσια της παρούσας μεταπτυχιακής διατριβής ανήκει στο είδος *C. schlosseri*. Ο μικρός αριθμός δειγμάτων *M. neumayri* και *D. pikermiensis* δεν αρκεί για να ρίξει φως στη σχετική κυριαρχία μεταξύ των δύο κερασφόρων ειδών. Εντούτοις, η ισχυρή παρουσία του εξειδικευμένου βοσκητή *C. schlosseri* είναι ενδεικτική της ύπαρξης ενός περισσότερο ανοιχτού και ξηρού περιβάλλοντος. Συνεπώς, το οικοσύστημα της Σάμου κατά το Τουρώλιο προσομοίαζε ελαφρώς περισσότερο τα αντίστοιχα της Ανατολίας και του Ιράν από εκείνα που χαρακτηρίζουν τις κλασσικές απολιθωματοφόρες θέσεις της Αττικής, όπως το Πικέρμι και η Κερασιά Ευβοίας.

1. Introduction

1.1 Samos Island

Samos Island is in the eastern Aegean Sea, south of Chios Island, north of Patmos Island and the Islands of the Dodecanese, and separated from the coast of Asia Minor by the 1.6 km wide Mycale Strait. According to renowned Greek geographer Strabo, the name Samos is from Phoenician language, meaning "rise by the shore".

The area of the island is 477.395 km^2, its length is 43 km and its width is 13 km. The island is dominated by two large mountains, Ampelos (locally known as "Karvounis"), rising to 1095 meters, and Kerkis (anc. Kerketeus), with an altitude of 1434 meters.

1.2 Study and excavation of the Samos fossil mammals: unweaving the fabric of legends

The island of Samos is characterized by a notably rich Late Miocene vertebrate fauna, consisting of a great variety of ungulates, carnivores and micromammals. Skeletal remains of mythical dead beasts had been found in the island since the times of Greek antiquity, inspiring the spread of legends. Greek geographer Euphorion (~200 B. C.) reported the myth of the dreadful Neades, gigantic monsters whose roaring would make the earth split, whereas writer Plutarchus (~100 A. D.) explains the reddish-colored soil and the bones situated in the area of Panema (full of blood) as the results of the massacre of the mythical female warriors Amazons by God Dionyssos (Solounias & Ring 2007, Koufos 2009). Since the horse-like skulls of equid *Hipparion* are among the most numerous fossils in Samos, it can be argued that they were interpreted, by the ancient inhabitants, as remains of the horses of the Amazons (Solounias & Mayor 2004). Another intrusion of the Samian fossils in Greek mythology is the Trojan Monster, a peculiar beast depicted on the Hesione vase, a column-crater painted in Corinth, circa 560-540 BC (Museum of Fine Arts, Boston, 63.420). The vase is decorated with an illustration of how the hero Hercules and the Trojan princess Hesione slaughtered a monster that was raiding the coasts of Troy, in Asia Minor. According to Mayor (2000a, b) is similar to the skull of the Late Miocene large giraffid genus *Samotherium* (Fig.1). In an almost ironic manner, the myths and legends concerning the Samos monsters would become the inspiration for British physician and naturalist

Charles Forsyth Major to lead the first large-scale paleontological excavations on the island (Giaourtsakis 2009).

The palaeontological wealth of Samos had sparked the interest of researchers from Europe since the early 1850s, when travelers from Italy exported a number of specimens in Padova (Piccoli et al. 1975). Among these were the first documented fossils of rhinoceroses from the island, stored at the Geological Institute of Padova and reported by P. Leonardi in 1947 (Giaourtsakis 2009). However, the first systematic excavations on the island were conducted in 1885-1887 and 1889 by Charles Forsyth Major, in the sites Adrianos ravine, Potamies ravine and Stefana, under the auspices of a wealthy Swiss family, who founded the mission. The specimens are part of the collection of the Museums of Lausanne, Geneva and Basel, Switzerland (Forsyth Major 1888, 1894), whereas his collection of 1889 was sold to the Natural History Museum of London (Lydekker 1890, fide Koufos 2009).

The fossil dealer B. Sturtz collected and sold Samian fossils to Natural History museums of Vienna, Stuttgart, Frankfurt and London, however the site where the material was collected has not been determined (Schlosser 1904).

German scientists T. Stutzel and A. Hentschel also contributed to the excavations on the island between 1897 and 1902, enriching the collections of the Palaeontological Museum of Munich (Schlosser 1904, Andrée 1926).

In 1901, E. Fraas exported the material he collected in Samos to Stuttgart and Munich. Moreover, Consul of Germany on Samos and wine trader K. Acker exported fossils together with wines (!) to various museums in Germany and Austria (Koufos 2009).

Later on, the famed American “fossil hunter” Barnum Brown excavated a notable number of specimens (Brown 1927), now stored at the collections of the American Museum of Natural History.

As far as Greek researchers are concerned, the Samian doctor Achilleas Stefanidis from Mytilinii village was among the pioneers of excavating and collecting fossils. Stefanidis also delivered some of his collected specimens to University of Athens Professor Iraklis Mitzopoulos, though he never received any feedback; eventually, he gave his collection to C. Forsyth Major the second time the English expatriate came to Samos, in 1887 (Koufos 2009).

In 1903, the curator of the AMPG and, later, University of Athens Professor Theodoros Skoufos was the first to lead an organized excavation in the sites Adrianos,

Katikoumena, Bartzikos and Bailntaki in 1903 (Proceedings of the Rectorate of Athens University, 1904) (Fig. 12). Part of the aforementioned material, stored at AMPG, was first-time prepared and studied for the purposes of the present thesis by the author.

Postdating Skoufos, Aristotle University of Thessaloniki Professor Ioannis Melentis conducted two new excavations at the fossiliferous site Mytilinii-1A (MTLA) of Adrianos ravine, in 1963 and 1985, storing the specimens at the Aegean Museum of Natural History in Mytilinii village (Melentis 1969).

In 1976, Nikos Solounias led new excavations on the island under the auspices of University of Colorado (Black et al. 1980, Solounias & Ring 2007). Solounias was the first to also excavate for small mammals, which were found in locality S3 (Solounias & Ring 2007).

The latest systematic excavations in Samos were led by Aristotle University of Thessaloniki Professors Georgios Koufos and Dimitrios Kostopoulos between 1990 and 2006, shedding light to an immense number of specimens and resolving important issues on the stratigraphy and palaeoecology of the island's fossiliferous localities (Koufos 2009).

Fig. 1: Detail of the clay pot depicting the "Trojan Monster" on the Hesione vase. From Mayor (2000b).

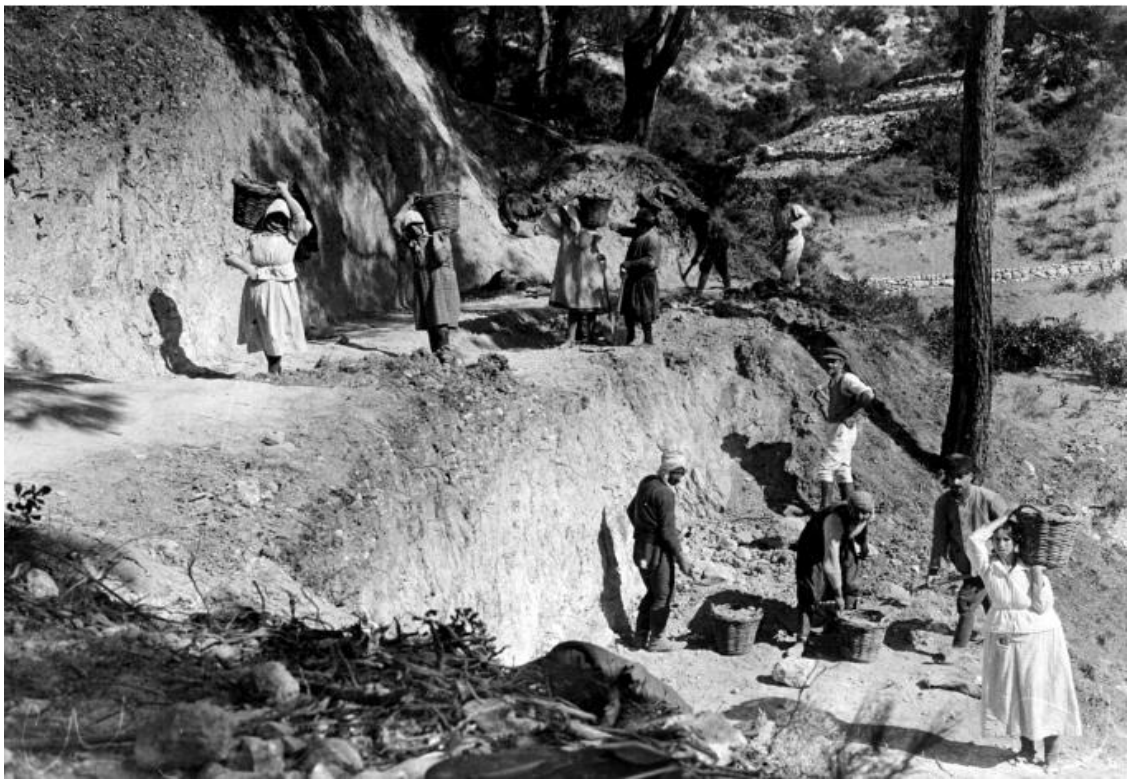

Fig. 2: Refugees from Asia Minor participate in B. Brown's palaeontological excavations in Samos, 1923-24. From Mayor (2000b).

Fig. 3: Barnum Brown (right) excavating bone bed near Mytilini, Samos, Greece, 1923–24. From Mayor (2000b).

Year	Excavator	Locality	Collection	References
1852	Anonymous travellers from Italy	Undetermined	University of Padova	Piccoli et al. 1975
1879	A. Stefanidis	Undetermined	Switzerland?	Forsyth-Major 1888, 1894,
1885-1887, 1889	C. I. Forsyth-Major	Adrianos ravine, Potamies ravine, Stefana	Zoological Museum of Lausanne, Natural History Museum Basel, Natural History Museum Geneva, Natural History Museum of London	Forsyth-Major 1888, 1894, Lydekker 1890
1889-1900	B. Sturtz	Undetermined		
1897-1902	T. Stutzel, A. Hentschel	Undetermined	Palaeontological Museum of Munich	Schlosser 1904, Andrée 1926
1901	E. Fraas	Undetermined	Palaeontological Museum of Munich, Stuttgart State Museum of Natural History	Koufos 2009
1900?	K. Acker	Undetermined	Natural History Museum of Vienna, Natural History Museum of Hamburg, Stuttgart State Museum of Natural History, Natural History Museum of Bern, Natural History Museum Basel, University of Tubingen Palaeontological Collection	Koufos 2009
1903	T. Skoufos	Adrianos, Katikoumena, Bartzikos, Bailntaki	Athens Museum of Palaeontology and Geology	Proceedings of the Rectorate of Athens University1904
1909	T. Wegner	Undetermined	Geomuseum of the University of Münster	Andrée 1921, Wehrli 1941
1921-1924	B. Brown	Adrianos ravine	American Museum of Natural History	Brown, 1924
1963, 1985	I. Melentis	Adrianos Ravine	Aegean Museum of Natural History	Melentis 1969, Koufos 2009
1976	N. Solounias		Carnegie, Pittsburg, University of Colorado	Black et al 1980, Solounias 2007
1990-2006	G. Koufos, D. Kostopoulos	Adrianos Ravine	Laboratory of Palaeontology and Geology, University of Thessaloniki	Koufos 2009

Table 1: The main Samos excavations in chronological order

ΤΑ ΠΑΛΑΙΟΝΤΟΛΟΓΙΚΑ

ΕΥΡΗΜΑΤΑ ΕΝ ΣΑΜΩ

Η ΣΠΟΥΔΑΙΟΤΗΣ ΤΩΝ

ΣΥΝΕΝΤΕΥΞΙΣ ΜΕ ΤΟΝ κ. ΣΚΟΥΦΟΝ

ΕΠΙΤΥΧΙΑ ΤΩΝ ΑΝΑΣΚΑΦΩΝ

Πρὸ ἡμερῶν εἴχομεν ἀναγράψει ὅτι ἐπανῆλθεν ἐκ Σάμου ὁ κ. Σκοῦφος ὅπου εἶχεν ἐνεργήσει παλαιοντολογικὰς ἀνασκαφάς, ἀνευρὼν πλεῖστα πολύτιμα παλαιοντολογικὰ ἀντικείμενα.

Χθὲς τὸ ἑσπέρας ἐπεσκέφθημεν τὸν κ. Σκοῦφον ἐν τῇ οἰκίᾳ του ἵνα μᾶς παράσχῃ τὰς λεπτομερείας τῶν παλαιοντολογικῶν αὐτοῦ ἀνασκαφῶν ἐν Σάμῳ.

Ὁ κ. Σκοῦφος μὲ τὴν χαρακτηρίζουσαν αὐτὸν προσήνειαν μᾶς ἐδέχθη εἰς τὸ γραφεῖον του.

— Παλαιοντολογικὰς ἀνασκαφὰς ἐνήργησα ἐν Σάμῳ, μᾶς εἶπεν ὁ κ. Σκοῦφος, εἰς τρεῖς διαφόρους θέσεις, εἰς Ἀδριανοῦ, Κατοικούμενα καὶ Τσαροῦχι.

Αἱ τρεῖς αὗται θέσεις ἀντιπροσωπεύουσιν ἀκριβῶς καὶ τοὺς τρεῖς γεωλογικοὺς ὁρίζοντας τῶν ἀπολιθωματοφόρων στρωμάτων, οἱ ὁποῖοι ὁρίζοντες μᾶς παρουσιάσθησαν καὶ εἰς τὸ Πικέρμι. Ἡ μόνη διαφορὰ μεταξὺ αὐτῶν εἶνε τὸ πάχος τῶν στρωμάτων, τὸ ὁποῖον ἐν Σάμῳ εἶνε 100 περίπου μέτρων.

Τὰ ὑδατογενῆ στρώματα τὰ φέροντα τὰ ἀπολιθώματα διευθύνονται κατὰ μέσον ὅρον ἐκ Βορρᾶ πρὸς Νότον καὶ κλίνουσιν ὑπὸ γωνίαν 30—70 μοιρῶν ποῦ μὲν πρὸς ἀνατολάς, ποῦ δὲ πρὸς δυσμάς.

Τὰ εὑρήματα τῆς Σάμου

Κατόπιν ὁ κ. Σκοῦφος ἔφερε τὸν λόγον ἐπὶ τῶν εὑρεθέντων ζώων:

— Τὰ ἀνευρεθέντα ζῶα ἐπὶ τῆς νήσου Σάμου, μᾶς εἶπεν, ἔζων εἰς ἐποχὴν (ἄνω μειόκαινος διάπλασις) κατὰ τὴν ὁποίαν ἡ Μεσόγειος Θάλασσα ἀπετέλει χέρσον διακαπτομένην ὑπὸ πολλῶν λιμένων, ἐκ τῶν ὁποίων μία ἦτο καὶ ἡ νῆσος Σάμος. Κατὰ τὴν ἐποχὴν ταύτην ἡ Σάμος συνείχετο ἀμεσώτατα μετὰ τῶν νήσων τοῦ Αἰγαίου Πελάγους, τῆς Ἑλλάδος, τῆς Ἀσίας καὶ Ἀφρικῆς.

Κατὰ μέγα μέρος τὰ ὑδατογενῆ ταῦτα στρώματα τῆς Σάμου ὀφείλουσι τὴν ὕπαρξίν των, τὸ μὲν εἰς σποδὸν ἡφαιστείων, τὸ δὲ εἰς προϊόντα τῆς ἀποσαθρώσεως τῶν πυριγενῶν πετρωμάτων, ἅτινα προϋπῆρχοντο ἐκ τῶν ἡφαιστείων τὰ ὁποῖα ἦσαν ἐν ἐνεργείᾳ κατὰ τὴν αὐτὴν ἄνω μειόκαινον περίοδον παρὰ τὰς ἀκτὰς τῆς Μικρᾶς Ἀσίας καὶ μάλιστα τῆς Σμύρνης.

Τὰ στρώματα ταῦτα μεγάλως σήμερον συντελοῦσιν εἰς τὴν ἀνάπτυξιν τῆς ἀμπέλου εἰς τὴν νῆσον Σάμον καὶ εἰς τὴν γονιμότητα τοῦ ἐδάφους της.

— Ἀνευρέθησαν πολλὰ ζῶα κατὰ τὰς ἀνασκαφὰς ταύτας;

— Αἱ ἐν Σάμῳ ἀνασκαφαί, ἐξηκολούθησεν ὁ κ. Σκοῦφος, καὶ λόγῳ τοῦ ἀριθμοῦ καὶ τῆς ἀρίστης διατηρήσεως τῶν εὑρημάτων, δύνανται νὰ παραβληθῶσι πρὸς τὰς τοῦ Πικερμίου.

Fig. 4: Interview of Th. Skoufos discussing the “success of the palaeontological excavations in Samos on the Greek newspaper “Empros”, October 1903. Courtesy of S. Roussiakis.

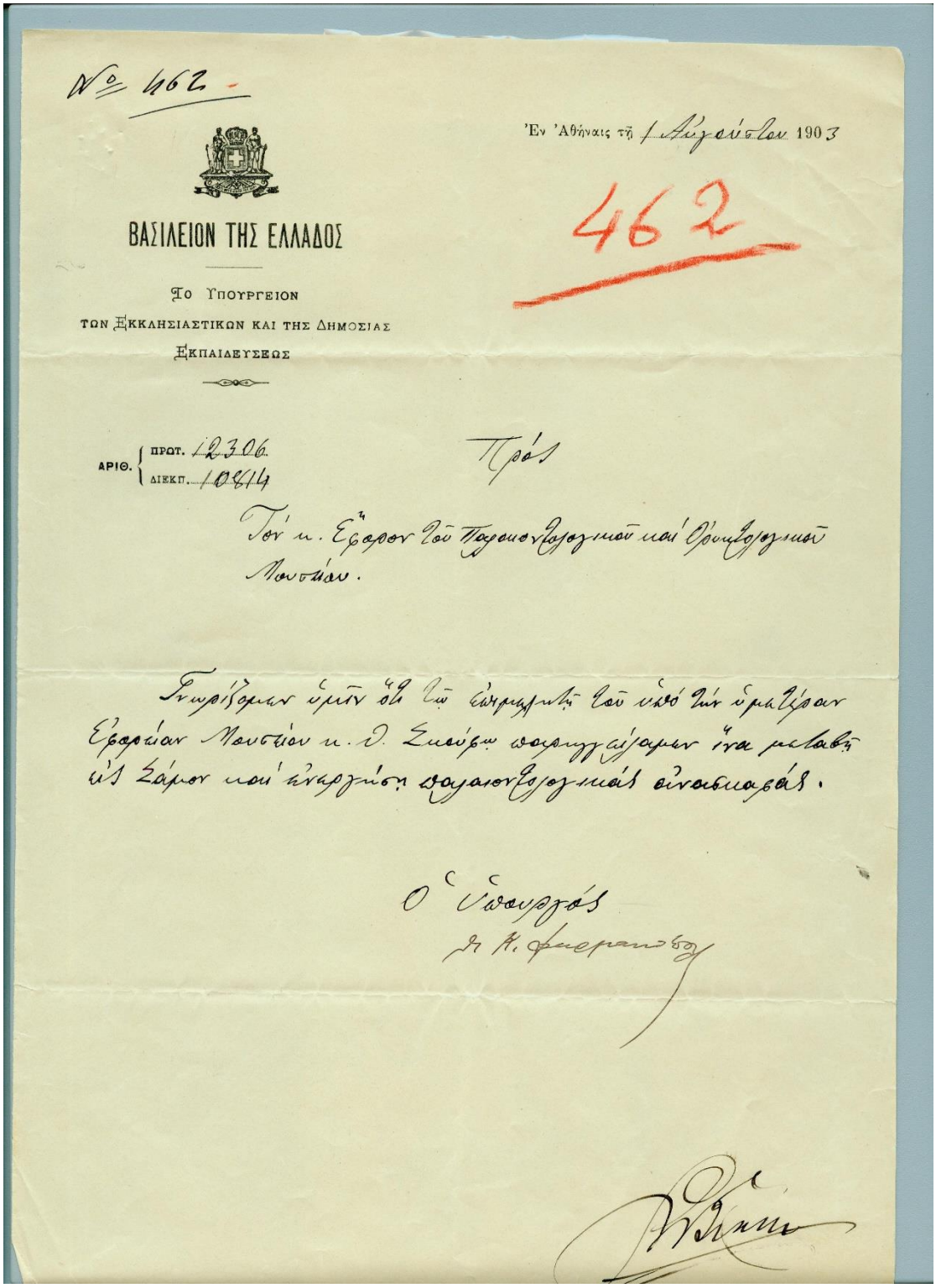

№ 462

Ἐν Ἀθήναις τῇ 1 Αὐγούστου 1903

462

ΒΑΣΙΛΕΙΟΝ ΤΗΣ ΕΛΛΑΔΟΣ

Τὸ Ὑπουργεῖον
ΤΩΝ ΕΚΚΛΗΣΙΑΣΤΙΚΩΝ ΚΑΙ ΤΗΣ ΔΗΜΟΣΙΑΣ
ΕΚΠΑΙΔΕΥΣΕΩΣ

ΑΡΙΘ. { ΠΡΩΤ. 12306
ΔΙΕΚΠ. 10414

Πρός

Τὸν κ. Ἔφορον τοῦ Παλαιοντολογικοῦ καὶ Ὀρυκτολογικοῦ Μουσείων.

Γνωρίζομεν ὑμῖν ὅτι ὡς ἐπιμελητὴς τοῦ ὑπὸ τὴν ὑμετέραν Ἐφορείαν Μουσείων κ. Θ. Σκούφος ἀναλαμβάνῃ ἵνα μεταβῇ εἰς Σάμον καὶ ἐκτελέσῃ ἀνασκαφὰς παλαιοντολογικὰς ἀνακοινοῦμεν.

Ὁ Ὑπουργός
Δ. Κ. Φιλαρέτου

Fig. 5: The assignment of “Samos palaeontological excavtions” to “curator of the Palaeontological and Mineralogical Museum” Theodore Skoufos. Athens, August 1903. From the archives of the AMPG, courtesy of S. Roussiakis.

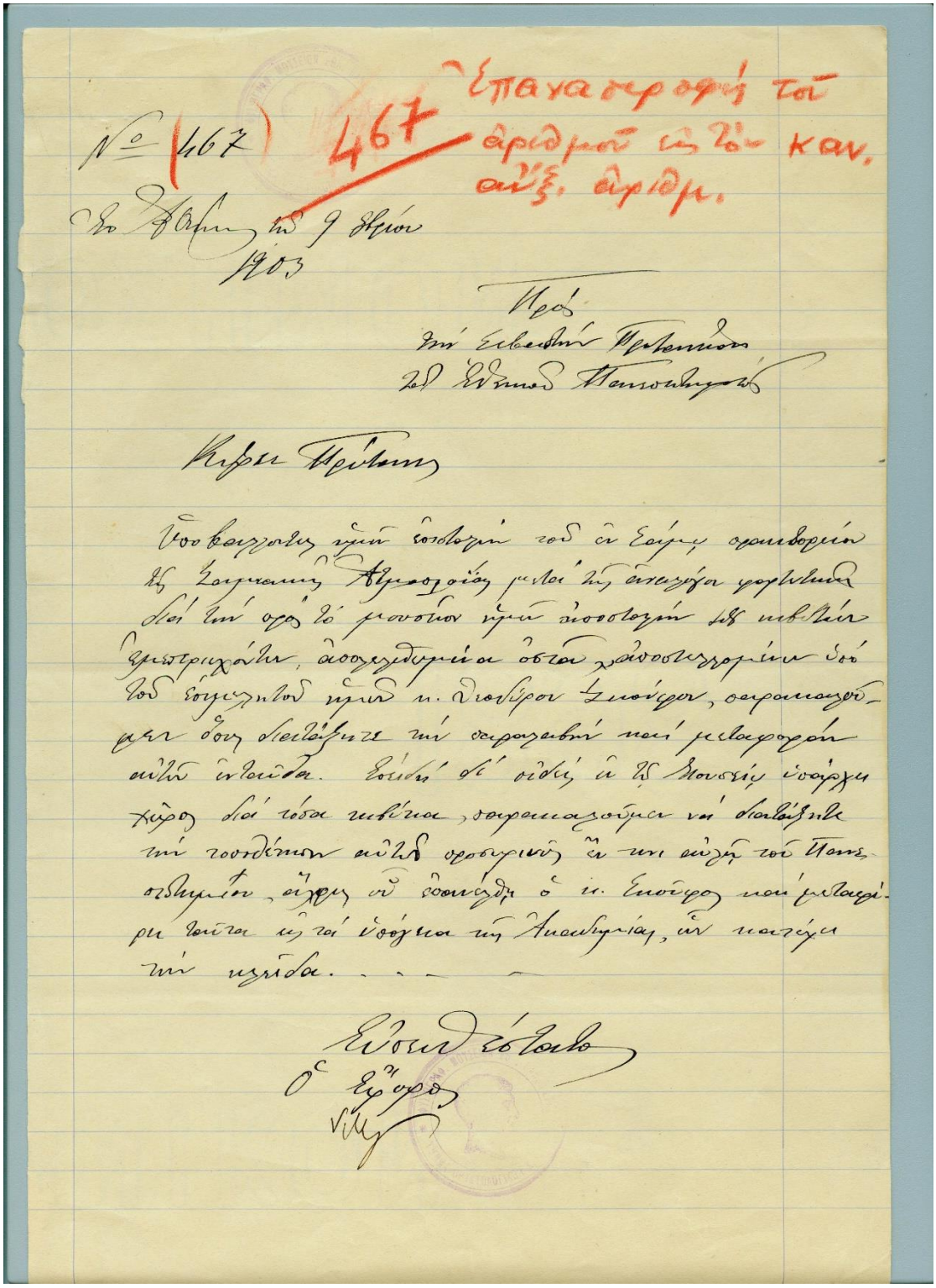

Fig. 6: An update on the Samos excavation: the curator of the Palaeontological and Mineralogical Museum infroms the Dean of the University of Athens that “T. Skoufos has delivered 48 boxes of fossils to the Museum (…) Due to their great number, the boxes are to be put at the Museum’s garden, up to the return of Mr Skoufos, who has a key to the museum’s basement, where the boxes are to be located”. October 1903. From the archives of the AMPG, courtesy of S. Roussiakis.

1.3 Geological and Stratigraphical Settings

The location of Samos within the South-Eastern Balkans geotectonic system has yet to be clarified, with the island being considered either as a part of the Atticocycladic Zone (Alther et al. 1982, Mporonkay 1995) or of the Asia Minor Menderes Massif (Papanikolaou 1979). However, more recent views favor the attribution of Samos to the Atticocycladic Zone, due to the lack of counterparts of the Menderes nappes to the Aegean region (Ring et al. 1999a, Gessner 2000).

The Pre-Neogene basement of the island includes mainly marbles and an allocthonous unit of Mesozoic non metamorphic rocks (Theodoropoulos 1979). Papanikolaou (1979) described 5 tectonic units:

- The **Kerketeas Unit,** consisting of ~1000m of marbles, followed by ~50m of yellow phyllites.

- The **St. John Unit,** a tectonic slice of basic metavolcanic rocks, situated between the Kerketas Unit and the overlaying Ambelos unit.

- The **Ambelos Unit,** which includes alternate marbles along with sipolines and mica-schists.

- The tectonically overlaying **Vourliotes Unit,** consisting of marbles and mica-schists.

- The non-metamorphic **Kallithea Unit,** which includes ~400m of Middle – Late Triassic basic volcanic rocks, postdated by a thinner series of Late Triassic – Jurassic limestones.

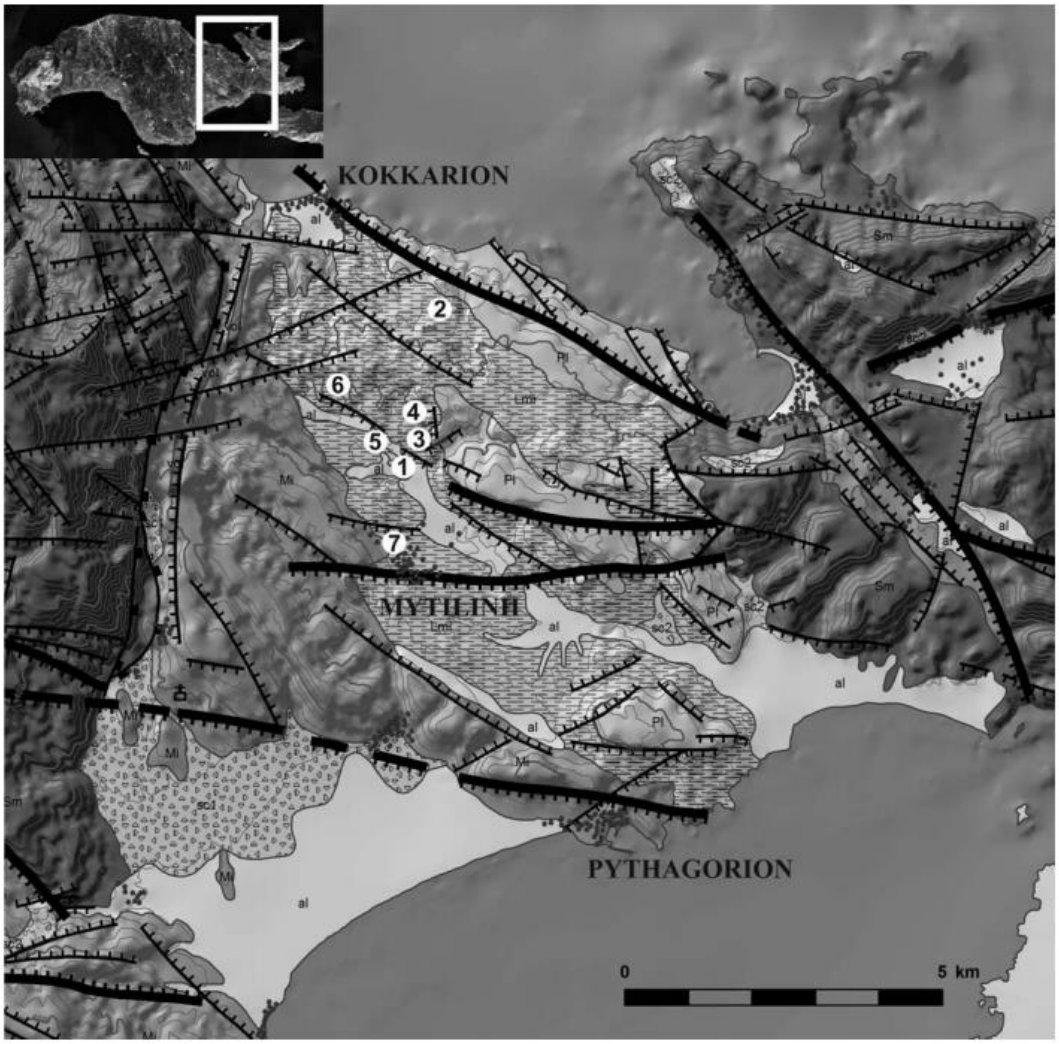

Fig. 7: Geological map of the Mytilinii Basin with location of the old and new fossiliferous sites (geological map from Mountrakis et al. 2003). Sm: Upper tectonic unit of Samos consisting of schists, sericite phyllites, quartzites and intercalations of marbles; Mi: Lower Neogene Group, including the Basal Fm, Mavradzei Fm and Hora Fm; Lmi: Mytilinii Fm; Pl: Kokkarion Fm; sc1-sc2: scree deposits; al: alluvial deposits. **Fossiliferous sites: 1. MLN – Q2 – Stefano; 2. MTN–? Q6; 3. MYT– Q3 –? Potamies; 4. MTL – 1 (A-D) – Q1 – Adriano; 5. Q4; 6. Q5; 7. Qx**. From Koufos et al. 2011.

Three Neogene depressions disrupt the metamorphic layers – forming three respective units: The Karlovassion Basin, the Mytilinii Basin and the Paleokastron Basin (Mountrakis et al. 2003). The Karlovassion and Mytilinii Basins are connected by a passage named the Pyrgos Basin, and considered part of the Western Anatolia complex of horst and graben tectonic system (Kostopoulos et al. 2009). All basins are

primarily filled with Neogene deposits, with thin Quaternary sediments limited to flat areas.

The illustrious fossiliferous strata of Samos are part of the Mytilinii Formation, situated in the northwestern part of Mytilinii Basin. The latter is characterized by a complicated stratigraphy, which has been an issue of study since the 19th century (Kostopoulos et al. 2009 and references therein). For the purposes of the present thesis, the stratigraphy proposed for the Mytilinii Basin by Kostopoulos et al. (2009, Fig. 8) shall be followed.

- The **Basal Formation**, Early to Middle Miocene. A formation of red-brown sands, gravels and conglomerates, uncomformably overlaying the Pre-Neogene basements. The probable depositional environment is a flood plain.

- The **Mavradzei Formation**, Middle to Late Miocene. Bituminous lacustrine limestones bearing fossil gastropods, with intercalations of organic clay. Basalt flow and lahar type volcanoclastic sediments are found on the upper part of this formation, probably correlated to the Middle-Late Miocene southeastern Aegean volcanism (Fytikas et al. 1984), whereas the depositional environment may be described as alluvial-fan facies with vegetated swamps and marshes passing laterally into lacustrine conditions.

- The **Hora Formation**, Vallesian. Laminated lacustrine limestones with intercalations of thin tuffaceous clay beds. This formation represents a deepening of the previous lacustrine environment.

- The **Mytilinii Formation**, Turolian. Brownish-reddish fluviolacustrine volcanoclastic sediments. The renowned mammal fossils belong to this formation. The depositional environment may correspond to subaerial hyperconcetrated flows in complex with ephemeral lake and overflow deposits.

- The **Kokkarion Formation**, Latest Miocene to Pliocene. Alternation of lacustrine limestones, clays and tuffaceous sands.

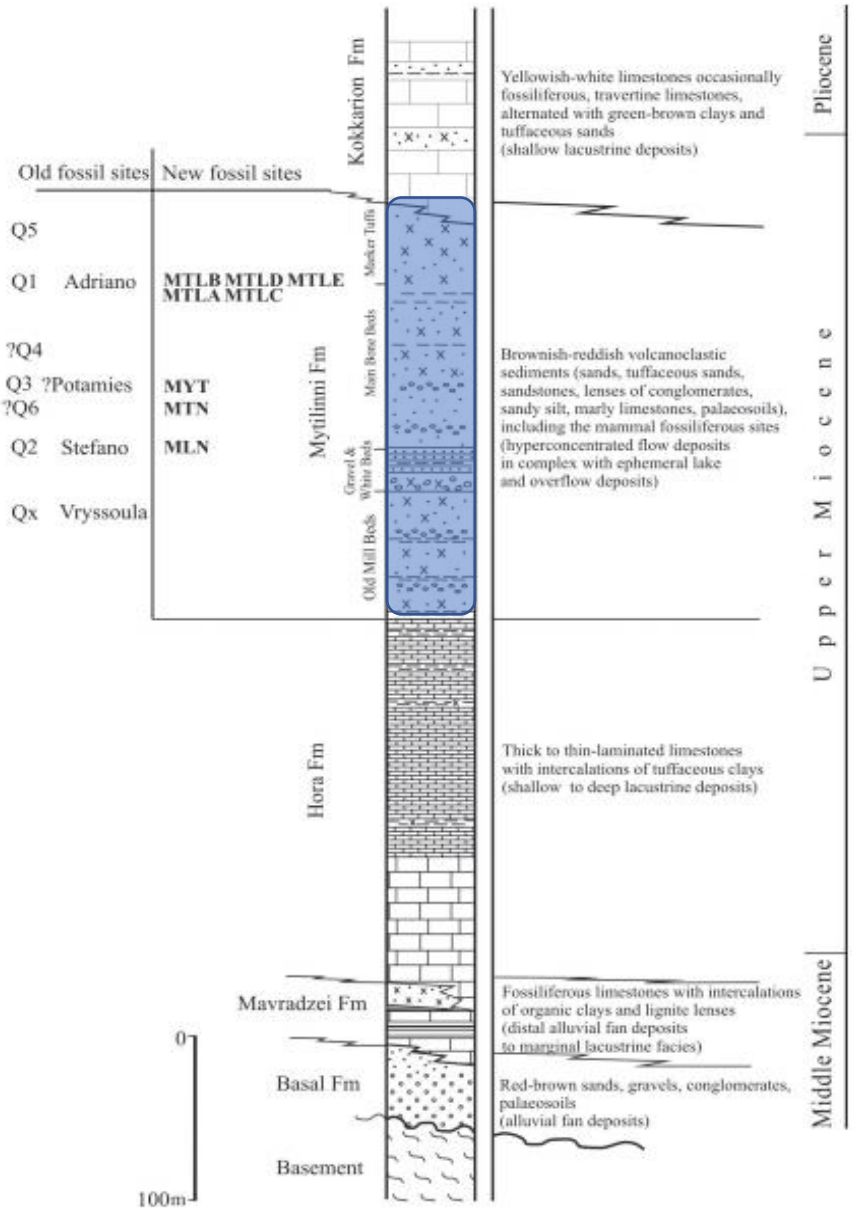

Fig. 8: Composite stratigraphic column including the lithology, chronology and sedimentary environments of the Neogene deposits of Mytilinii Basin. In blue color are the stratigraphic position of the vertebrate fossil sites of Mytilinii Fm. (Modified from Kostopoulos et al. 2009).

One major problem concerning the study of the Samos fauna concerns the inadequate stratigraphic data. Numerous excavations were led by different scientists, each one using their own methods for documenting their findings. Consequently, the same locality can be found in the literature under different names. As an example, Forsyth-Major marked the fossiliferous localities he excavated as “Stefano”, “Potamies” and “Adriano”, based on local place-names, whereas Brown used codes

starting with Q, for "quarry" (Q1-6, QX) (Koufos et al. 2009a). Additionally, many specimens originate from unknown fossiliferous horizons, as is the case with the AMPG material. After the extensive excavations between 1999 and 2006, Koufos et al. (2009a, 2011) recognized 4 fossil horizons at least in the Mytilinii Formation in 3 new named fossiliferous localities, starting from the base and on to the top:

- **Mytilinii-4 or MLN**, located in Potamies ravine. The biostratigraphic and magnetostratigraphic data point to a late early Turolian age (late MN 11).

- **Mytilinii-3 or MYT**, also located in Potamies ravine, at the basal part of the main fossiliferous beds of the formation. The biostratigraphic and magnetostratigraphic data indicate an early MN 12 age.

- **Mytilinii-1 or MTL**, located in Adrianos ravine. This locality includes quite a few fossiliferous sites, alphabetically coded MTLA, MTLB, MTLC, MTLD, and MTLE. According to both magnetostratigraphic and biostratigraphic data, the locality has a late middle Turolian age (late MN12).

For the scope of this work, the correlation of new and old fossiliferous localities proposed by Kostopoulos et al. (2009) was followed. This correlation is presented here:

- Adrianos Ravine / "Adriano" / MTL, MN12, 7.13-7.17 Ma
  - MTLA
  - MTLB
  - MTLC
  - MTLD = Q1
  - MTLE

- Potamies Ravine
  - MYT = Q3 = "Potamies", MN12, 7.3 Ma
  - MLN = Q2 = "Stefano", MN11, ~7.5 Ma

- <u>Mytilinii Basin</u>

- QX = Vryssoula, MN11, 8-7.6 Ma

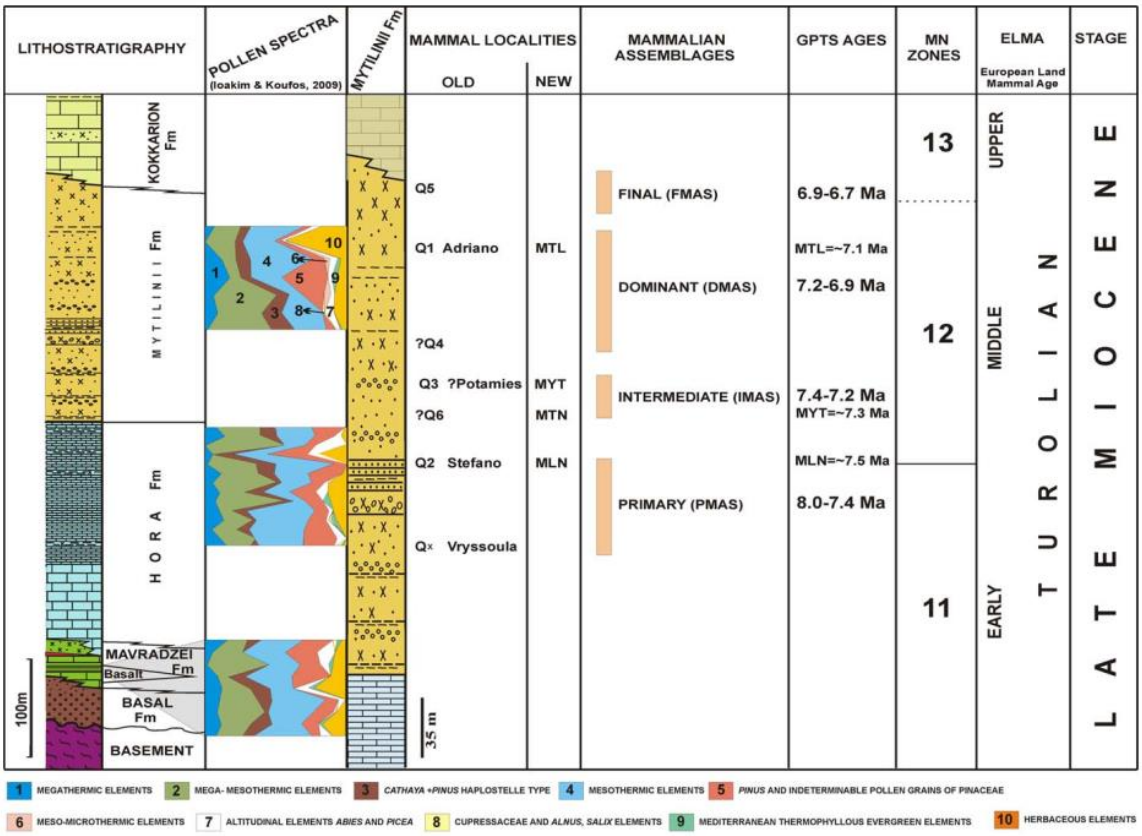

Fig. 8: Litho-, bio- and chrono-stratigraphy of the Neogene deposits of the Mytilinii Basin, Samos, Greece. From Koufos et al. 2011.

The respective faunal composition of Mytilinii-1 (MTLA, MTLB, MTLC), Mytilinii-3 (MYT) and Mytilinii-4 (MLN) localities, as registered in Koufos et al. (2009a, 2011), Vlachou (2013) and Kostopoulos (in press) is presented upon the following boards. The species studied in this thesis are in bold letters.

Mytilinii-4/MLN

Carnivora	Perissodactyla	Artiodactyla
Hyaenictitherium cf. *wongii*	*Hipparion* aff. *proboscideum*	*Palaeotragus rouenii*
Protictitherium crassum	*Hipparion* aff. *prostylum*	*Palaeotragus* sp.
	Miodiceros neumayri	*Samotherium boissieri*
		Gazella pilgrimi
		Tragoportax sp.
		Miotragocerus sp.
		Palaeoryx palassi

Mytilinii-3/MYT

Perissodactyla	Artiodactyla
Miodiceros neumayri	*Samotherium major*
Dihoplus pikermiensis	*Sporadotragus parvidens*
Ancylotherium pentelicum	*Gazella pilgrimi*
Hipparion sp.	*Skoufotragus zemalisorum*
Hipparion aff. *forstenae*	*Palaeoryx?* sp.
Hipparion cf. *prostylum*	*Majoreas?* sp.
Hipparion cf. *matthewi*	*Majoreas woodwardi*

Mytilinii-1/MTLA

Rodentia	Carnivora	Proboscidea
Pseudomeriones pythagorasi	*Adcrocuta eximia*	*Zygolophodon turicensis*
'Karminata' provocator	*Hyaenictitherium* cf. *wongii*	
Spermophillinus cf. *bredai*	*Machairodus giganteus*	
	Metailurus parvulus	
	Parataxidea maraghana	
Tubulidentata	**Perissodactyla**	**Artiodactyla**
Amphiorycteropus gaudryi	***Miodiceros neumayri***	*Microstonyx major*
	Dihoplus pikermiensis	*Palaeotragus rouenii*
	Ancylotherium pentelicum	*Samotherium major*
	Hipparion brachypus	*Helladotherium duvernoyi*
	Hipparion dietrichi	*Urmiatherium rugosifrons*
	Hipparion cf. *matthewi*	*Miotragocerus valenciennesi*
	Hipparion aff. *forstenae*	*Tragoportax rugosifrons*
	Hipparion cf. *proboscideum*	*Gazella capricornis*
		Gazella pilgrimi
		Gazella mytilinii
		Palaeoryx pallasi
		Palaeoryx majori
		Skoufotragus laticeps
		Sporadotragus parvidens

Mytilinii-1/MTLB

Rodentia	Carnivora	Proboscidea
Pseudomeriones pythagorasi *Spermophillinus* cf. *bredai* *Pliospalax* cf. *sotirisi*	*Plioviverrops orbignyi,* *Hyaenictitherium wongii*	*Choerolophodon pentelici*
Tubulidentata	**Perissodactyla**	**Artiodactyla**
Amphiorycteropus gaudryi	***Miodiceros neumayri*** *Ancylotherium pentelicum* *Hipparion brachypus* *Hipparion dietrichi* *Hipparion* cf. *proboscideum* *Hipparion* cf. *matthewi* *Hipparion* aff. *forstenae*	*Palaeotragus rouenii* *Palaeotragus* sp. *Samotherium major* *Miotragocerus valenciennesi* *Gazella pilgrimi* *Gazella* cf. *capricornis* *Gazella mytilinii* *Sporadotragus parvidens* *Skoufotragus laticeps* *Palaeoryx pallasi* *Palaeoryx majori* *Urmiatherium rugosifrons*

Mytilinii-1/MTLC

Carnivora	Hyracoidea	Artiodactyla
Hyaenictitherium cf. *wongii*	*Pliohyrax graecus*	*Samotherium major* *Miotragocerus valenciennesi* *Gazella* cf. *capricornis* *Palaeoryx majori*

1.4 Previous works on Samos rhinocerotids

Due to the extensive excavations led by international scientific teams, Samian fossils are spread among an impressive number of collections around the globe, from Germany and Paris to New York. With the exception of the fossils recently unearthed by the Aristotle University of Thessaloniki, only a fraction of the initially excavated material remains stored in Greek museums.

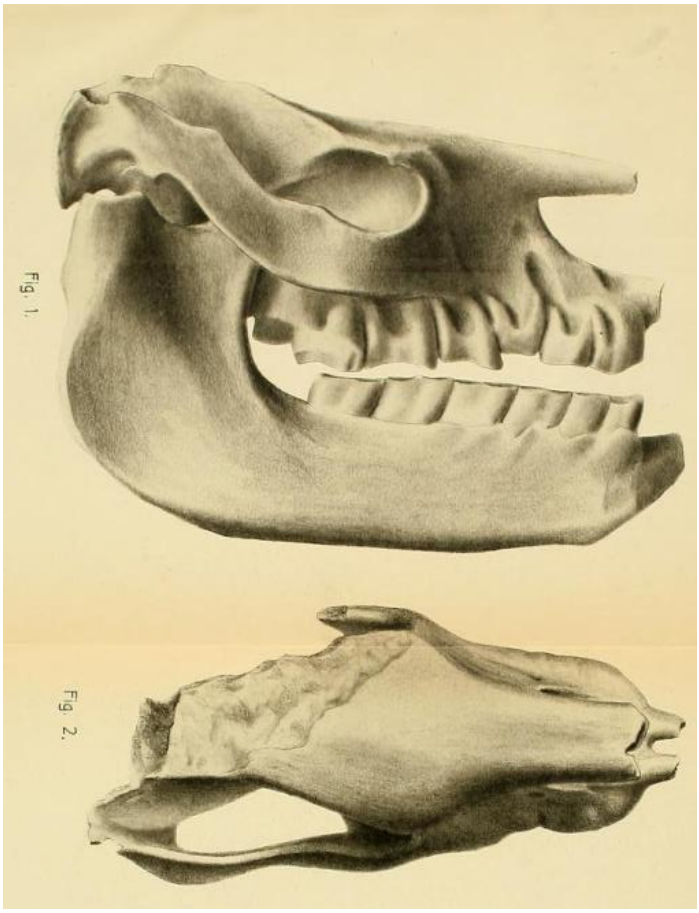

Fig. 9: Sketches of the skull (Fig.1: lateral view and Fig.2: dorsal view) of *C. samium* from Samos Island, Greece. From Weber (1905).

Rhinocerotid fossils from Samos have been reported from many collections: C. Forsyth Major reported certain findings from his long lasting excavations (Forsyth Major 1894). Weber (1904, 1905) described and illustrated a noteworthy number of specimens, including one *Rhinoceros schleiermacheri* KAUP, 1834 and one *Rhinoceros pachygnathus* WAGNER, 1848 skull, two *Aceratherium schlosseri* and two

Aceratherium samium skulls, as well as a great number of mandibles, deciduous teeth and postcranial material. Later on, Andrée (1921) illustrated a hornless rhinocerotid skull and a complete mandible he attributed to his newly erected species *Aceratherium wegneri* ANDRÉE, 1921, as well as a skull and isolated teeth that he attributed to *Aceratherium angustifrons* ANDRÉE, 1921. Unfortunately, all Samian material stored in Munich was lost during WWII bombings (Giaourtsakis 2009). Drevermann (1930) reported two skulls from Samos, attributed to *Chilotherium schlosseri* WEBER, 1905 and *Atelodus pachygnathus* respectively, stored at Seckenberg Museum, Frankfurt. Leonardi (1947) reported a *Chilotherium wegneri* skull bearing the almost complete dentition, missing only P1, stored at the Geological Institute of Padova; the same specimen was later described by Piccoli et al. (1975). Lately, Giaourtsakis (2009) studied and described ample material from Samos excavated during the latest expeditions led by the Aristotle University of Thessaloniki, including an adult *M. neumayri* skull, two juvenile skulls of the same species and postcranial material belonging to both *M. neumayri* and *Dihoplus pikermiensis*. The complete lack of material belonging to *Chilotherium* is also pointed out by Giaourtsakis (2009). Kampouridis et al. (2021) studied the *'C. wegneri'* material excavated by T. Wegner in 1909, attributing it to *C. schlosseri.* Most recently, Giaourtsakis (2021) reviewed the fossil record of rhinocerotids from Greece, including a revision of the late Miocene rhinos form Samos, and assigned the Dicerotina to the new genus *Miodiceros,* based on differences on the cranial and appendicular skeleton from the extant African rhinocerotid genera *Diceros* and *Ceratotherium*.

Rhinocerotid specimens from Samos were also reported in collective works, such as the report of a *Diceros pachygnathus* skull in NHMW collections by Thenius (1955) and a skull of the same species illustrated by Viret on his contribution to J. Piveteau's Traité de Paléontologie (1952). Melentis (1968) reported a *Miodiceros neumayri* skull from the Aegean Museum of Natural History collection, whereas Geraads (1988) included a *Ceratotherium neumayri* skull from Staatliches Museum für Naturkunde Stuttgart collection and a *Dicerorhinus pikermiensis* skull fragment from the collections of Geologisch-Paläontologisch Museum of Munster in his work on the morphological distinction among Late Miocene Greek rhinocerotids.

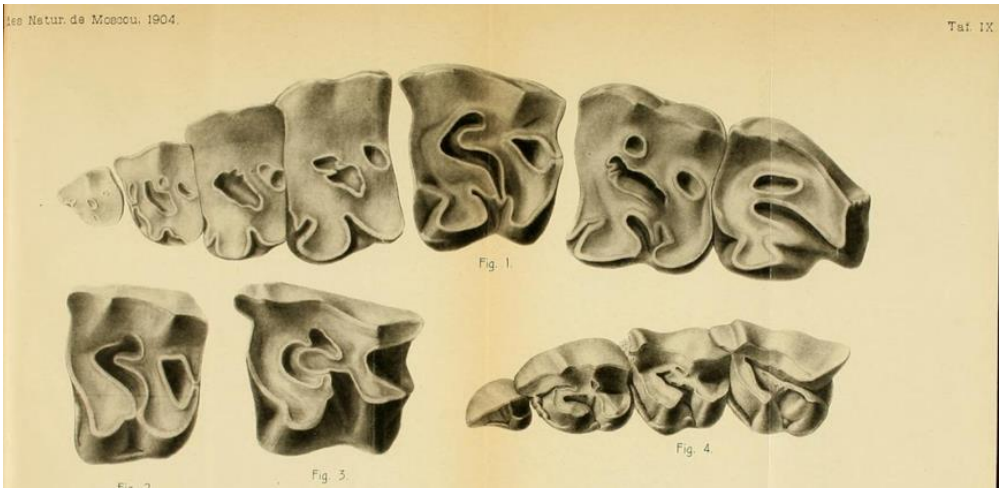

Fig. 10: Sketches of the upper permanent (Fig.1-3) and deciduous (Fig. 4) dentition of *C. schlosseri* from Samos Island, Greece. From by Weber (1905).

1.5 Phylogeny and Taxonomy of Extant Rhinocerotids

For millions of years, the rhinoceroses roamed Africa, Asia, North America and Europe, comprising one of the most diverse families among the Perissodactyla. The impressive diversity that characterizes the fossil record of the Rhinocerotidae family has shrunken to only five remaining species: the White Rhinoceros *Ceratotherium simum* BURCHELL, 1817 and the Black Rhinoceros *Diceros bicornis* LINNAEUS, 1758 both live in sub-Saharan Africa, the Indian Rhinoceros *Rhinoceros unicornis* LINNAEUS, 1758 found in India and Nepal, the Javan Rhinoceros *Rhinoceros sondaicus* DESMAREST, 1822 and the Sumatran Rhinoceros *Dicerorhinus sumatrensis* FISCHER, 1814 both live in Indonesia (Dinerstein 2011). Although all herbivores, they have adapted to different ecological niches and display contrasting dietary preferences: *C. simum* is an obligate grazer and open habitat dweller, *D. bicornis* is a forest-dwelling browser, the grazer *R. unicornis* prefers savannahs and open plains, the browser *R. sondaicus* favors closed habitats and *D. sumatrensis* is a folivore, favoring closed habitats (Hullot et al. 2019). Deplorably, the five extant species are brought to the verge of extinction due to poaching and obliteration of their natural habitats.

There are three main hypotheses concerning the phylogeny of extant rhinoceroces. The morphological hypothesis, first proposed by Simpson (1945) and Loose (1975), separates the extant genera in two subfamilies based on the number of horns. Consequently, the tandem-horned genera *Diceros*, *Ceratotherium* and

Dicerorhinus form the subfamily Dicerorhininae and the one-horned Asian genus *Rhinoceros* represents the subfamily Rhinocerotinae. The hypothesis is supported by the study of mitochondrial DNA (Morales & Melnick 1994, Fig. 11) as well as the cytochrome b gene (Hsie et al. 2003). According to geographic split hypothesis, mainly supported by Pocock (1945), Groves (1983) and Heissig (1981, 1989), the three Asian genera are considered as sister taxa and clustered together to the subfamily Rhinocerotinae and tribe Rhinocerotini, regardless of the number of horns. On the other hand, the African genera form the subfamily Dicerinae. The study of mitochondrial cytochrome b and rRNA genes by Tougard et al. (2001) supported this hypothesis. It is stimulating that the contradicting hypotheses are supported by different analysis of the same proxy, the cytochrome b, by Hsie et al. (2003) and Tougard et al. (2001). However, the difference in the final results may be explained by the use of partial fragments of the cytochrome-b gene by the first study group and of full lengths by the latter (Hsie et al. 2003). The third hypotheses, supported by Guérin (1980), Prothero and Schoch (1989) and Cerdeño (1998) bases the taxonomy of the extant genera on both morphological features and geographic distribution. Consequently, the extant Sumatran rhino belongs to the Dicerorhinini tribe and the Dicerorhinina subtribe, the Indian rhino and the Javan rhino form the Rhinocerotini tribe and Rhinocerotina subtribe, and the black and white African rhinos cluster together to form the Dicerotini tribe and the Dicerotina subtribe. Together these tribes form the subfamily Rhinocerotinae OWEN, 1845 of the "true (modern) horned rhinoceroses". The radiation of the three tribes is considered to have taken place early in the family's evolutionary history, leading to the present controversies (Giaourtsakis 2009).

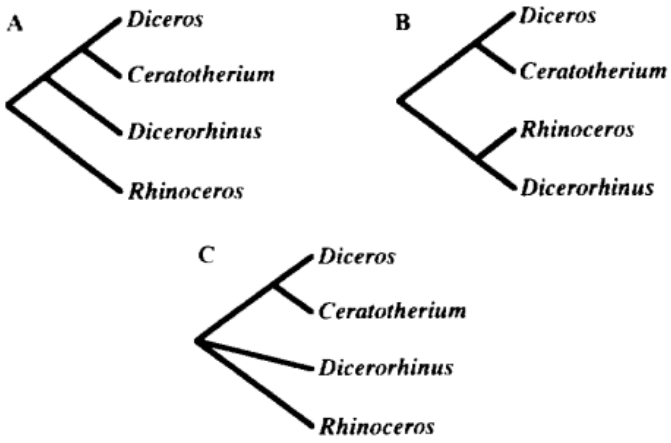

Fig. 11: The main approaches on the extant rhinocerotid genera systematics: A. Simpson (1945); B. Groves (1983); C. Prothero and Schoch (1989b). From Morales & Melnick (1994).

2. Material and Methodology

2.1 Material and Methods

As previously discussed, Samos Island's fossiliferous localities had been a pole of attraction to palaeontologists and fossil hunters from around the world, resulting to a spread of the acquired material in various museums in Europe and the USA. As a result, only a small fraction of the excavated material is stored in the collections of two Greek museums: Aegean Museum of Natural History in Mytilinii village and Athens Museum of Palaeontology and Geology. The material studied under the scope of the present thesis belongs to the collections of the latter. It was excavated in 1903 by University of Athens Professor Theodoros Skoufos. According to the Proceedings of the Rectorate of Athens University (1904) (Fig. 12), "the Museum's curator T. Skoufos (…) lead palaeontological excavations close to the sites Adrianos, Katikoumena, Bartzikou and Baildaki of the small town Mytilinii, shedding light to three fossiliferous layers. (…)[The layers] consist of trachitic tuff (…) in clay, sand or conglomerate form (…)There are immeasurable findings of animals; among them the most important are: of the carnivores the *Machairodus*, the *Lycaena*, the *Hyaena* and the *Ictitherium*, of the ruminants the *Protoryx*, the *Prostrepsiceros*, the *Palaeoeras*, the *Criotherium*, the *Palaeotragus*, the *Samotherium*, the *Helladotherium*, the *Camelopardalis*, of the omnivores the Erymathian pig, of the ungulates the *Hipparion*, of the pachyderms the *Rhinoceros*, the *Mastodon*, the *Deinotherium*, of the ancylopods the *Chalicotherium*, of the tubulidentates the *Orycteropus*, of the rodents the *Hystrix*, of the reptiles the Tortoise, of the birds various bone parts and, for the first time, fossilized eggs (Palaeovum)" (translated from Greek).

Two types of fossil matrix are observed: one type can be described as a tuffaceous conglomerate in variant coccometry levels, whereas the other type is resembling a yellowish calcitic sandstone (Appendix D).

Skoufos' material is stored in the collections of the AMPG. Part of the fossils were stored in boxes, while some specimens were still wrapped with newspapers and layers of hay dating back to the excavation era. The majority of the material was not prepared, still bearing the tuffaceous matrix.

The stratigraphic correlation of the specimens is problematic, since the material has not been ascribed to a specific locality. It is only known that it was excavated close to Mytilinii village. There is no information on the precise site every fossil was found

at, however. It may be supposed that the harder, thicker tuffaceous conglomerate and the softer marl and shales indicate a correlation with different fossiliferous horizons.

The preparation of the specimens took place in the AMPG facilities, by GS. The tools utilized were a hammer, needles of varying thickness, an INGCO Industrial model AC20248 air compressor and a Dremel engraver. It is worth mentioning that a large number of very well-preserved postcranial specimens is also still stored, though unprepared, at the AMPG collection.

Cranial and mandibular measurements follow van der Made (2010) (Appendix A, Fig. A1-2). These measurements include the classic measurements from Guérin (1980) as well as a lot more. Anatomical conventions follow Getty (1975) and Baron (1999), taking into account the recommendations of NAV (2005). Dental terminology follows Antoine et al. (2010) and dental measurements follow van der Made (2010) (Appendix A, Fig. A3). The capital letters P and M indicate the upper premolars and molars respectively and the lowercase letters p and m are used for the respective lower cheek teeth.

Measurements ranging from 0-150 mm were taken using a digital caliper to 0.01 mm and rounded to the nearest 0.1 mm. For larger measurements, a linear caliper with a precision of 0.1 mm was applied. All measurements are given in millimeters (mm). The terminology used for tooth description follows Antoine et al. 2010 (Appendix A, Fig. A4).

Institutional abbreviations

AMPG: Athens Museum of Palaeontology and Geology, Athens, Greece
NHMA: Aegean Museum of Natural History, Mytilinii, Samos, Greece
AUTH: Aristotle University of Thessaloniki, Greece
NHMW: Naturhistorisches Museum Wien, Vienna, Austria
MNHN: Muséum National d' Histoire Naturelle, Paris, France
NKUA: National and Kapodistrian University of Athens
GPIT: Geologisch-Paläontologisches Institut der Universität Tübingen, Germany

περὶ διορισμοῦ τοῦ τελειοφοίτου Β. Χαΐμαντᾶ ὡς βοηθοῦ τοῦ Μουσείου ἀντὶ τοῦ διδάκτορος Ν. Πάτση, διορισθέντος ὑποτρόφου ἐν Ἑσπερίᾳ πρὸς εὐρυτέρας σπουδάς.

Ὁ δὲ Ἐπιμελητὴς τοῦ Μουσείου Θ. Σκοῦφος συνεπείᾳ τοῦ ὑπ' ἀριθμ. $\frac{12,306}{10,814}$ ἐγγράφου τοῦ ἐπὶ τῆς Παιδείας Ὑπουργείου μετέβη εἰς Σάμον, ἔνθα ἐνεργήσας παλαιοντολογικὰς ἀνασκαφὰς παρὰ τὰς θέσεις Ἀδριανός, Κατοικούμενα, Μπαρτζίκου, καὶ Μπαϊλντάκι τῆς κωμοπόλεως Μυτιληνοί, ἔφερον εἰς φῶς τρεῖς συγκεκριμένας ἀπολιθωματοφόρους διαστρώσεις. Τὸ πάχος τῶν ἐν τῷ μεταξὺ τῶν ἀπολιθωματοφόρων τούτων διαστρώσεων στρωμάτων ὑπερβαίνει κατά τινας δεκάδας μέτρων τὰ ἀντίστοιχα τοῦ Πικερμίου καὶ ἀποτελοῦνται οὐχὶ ἐκ πλαστικῆς ἐρυθρᾶς γῆς μετὰ ἐπαλλασσόντων φακοειδῶν κροκαλοπαγῶν διαστρώσεων, ἀλλ' ἐκ τόφφου τραχειτικοῦ ποῦ μὲν ἀργιλομιγοῦς, ποῦ δὲ ἀσβεστολιθικοῦ ἢ ἀργιλομιγοῦς ἅμα καὶ ἀσβεστολιθικοῦ, ἐν πηλοπαγεῖ, ψαμμιτικῇ ἢ καὶ κροκαλοπαγεῖ καταστάσει.

Αἱ διαστρώσεις αὗται ἔχουσι διεύθυνσιν κατὰ μέσον ὅρον ἐκ Β. πρὸς Ν. μὲ κλίσιν 30-70° ποῦ μὲν πρὸς ἀνατολὰς ποῦ δὲ πρὸς δυσμάς, οὕτως ὥστε νὰ σχηματίζωσι σάγματα καὶ λεκάνας, πολλαχῶς διακοπτόμεναι ὑπὸ τεκτονικῶν ρηγμάτων

Τὰ ἀνευρεθέντα ζῷα εἶνε ἀναρίθμητα· ἐξ αὐτῶν τὰ σπουδαιότερα εἶνε τὰ ἑξῆς: Ἐκ τῶν σαρκοφάγων ὁ Μαχαιρόδους, ἡ Λυκύαινα, ἡ Ὕαινα καὶ τὸ Ἰκτιθήριον, ἐκ τῶν μηρικαστικῶν ὁ Πρωτόρυξ, ὁ Προστριψίκερως, ὁ Παλαιορέας, τὸ Κριοθήριον, ὁ Παλαιότραγος, τὸ Σαμοθήριον, τὸ Ἑλλαδοθήριον, ἡ Καμηλοπάρδαλις κτλ. ἐκ τῶν παμφάγων ὁ Ἐρυμάνθιος χοῖρος, ἐκ τῶν ὁπληφόρων τὸ ἱππάριον, ἐκ τῶν παχυδέρμων ὁ Ρινόκερως, ὁ Μαστόδους, τὸ Δεινοθήριον, ἐκ τῶν ἀγκυλοπόδων τὸ χαλικοθήριον, ἐκ τῶν νωδῶν ὁ Ὀρυκτερόπους, ἐκ τῶν τρωκτικῶν ἡ Ὕστριξ, ἐκ τῶν ἑρπετῶν ἡ Χελώνη, ἐκ τῶν πτηνῶν διάφορα τμήματα ὀστῶν καὶ διὰ πρώτην φορὰν ὠὰ ἀπολελιθωμένα (Palaeovum).

Ἡ δὲ ἐν τῷ φροντιστηρίῳ διεξαχθεῖσα ἐργασία ἔχει ὡς ἑξῆς: ἐν μὲν ταῖς πρακτικαῖς ἀσκήσεσιν συμμετέσχον 117 φοιτηταὶ τοῦ Φυσικοῦ καὶ Μαθηματικοῦ τμήματος τῆς Φιλοσοφικῆς σχολῆς καὶ τοῦ Φαρμα-

Fig. 12: Extract of the Proceedings of the Rectorate of Athens University (1904), reporting the most important findings of T. Skoufos' excavations in Samos. From the Archives of the AMPG, courtesy of S. Roussiakis.

2.2 Nomenclatural Notes

The occurrence of two different horned rhinoceros' species during the Late Miocene in Greece has been reported since the first systematic excavations at Pikermi, Attica (Gaudry 1863, Weber 1904). However, both taxa suffer from some complex nomenclatural issues caused by frequent misidentifications and systematic discrepancies. The first rhino species described from Greece was named *Rhinoceros pachygnathus* WAGNER, 1848, based on a mandible from Pikermi. This taxon was repeatedly used in the past to refer to the dicerotine rhino from the Late Miocene of Greece (today known as *Miodiceros neumayri*). However, its holotype, stored at the Palaeontological Museum of Munich, is actually the fragmentary mandible of a juvenile Dihoplus pikermiensis (Heissig 1975).

In his extensive work on cranial and postcranial material from many Pikermian faunas (including Pikermi itself and Samos), Geraads (1988) assigned the tandem-horned rhinocerotids to either *Dihoplus pikermiensis* (former *Dicerorhinus orientalis*) or *Ceratotherium neumayri* (former *Diceros pachygnathus*) due to certain cranial similarities of the latter species with the genus *Ceratotherium*. This taxonomic status has been retained by an important number of researchers for almost two decades (Geraads & Koufos 1990, Kaya 1994, Heissig 1996, Fortelius et al. 2003a, Giaourtsakis 2003, Antoine & Saraç 2005). Moreover, Geraads (2005) considered *Ceratotherium neumayri* to be the common ancestor of extant African rhinoceroses *Diceros bicornis* and *Ceratotherium simum*, as an intermediate species in terms of both ecology and morphology: *C. neumayri* was an ancestral mixed feeder, leading to a lineage of grazers (*Ceratotherium*) and another lineage of browsers (*Diceros*), after the Miocene-Pliocene boundary.

However, according to Giaourtsakis et al. (2009), the fossil record of African rhinocerotids indicates that the two extant lineages split in Africa before the Miocene-Pliocene boundary, with *Miodiceros neumayri* representing a separate, monophyletic evolutionary lineage, expanding out of Africa and lacking Pliocene descendants. Besides, the authors suggest that the cranial similarities of *Miodiceros neumayri* with *Ceratotherium* pointed out by Geraads (1988) actually point to early convergences. Thus, Giaourtsakis (2021) proposed the monospecific genus *Miodiceros for Miodiceros neumayri*.

The nomenclature of *Dihoplus pikermiensis* has also been a cause of disagreement amidst palaeontologists. This conservative rhinocerotid, typical of the Greek locality Pikermi, has been attributed to the genera *Dicerorhinus* GLOGER, 1841 (Guérin 1980, 1982, 1989) and *Stephanorhinus* KRETZOI, 1942 (Heissig 1989, 1996, Fortelius et al. 2003). However, the Plio-Pleistocene forms of *Stephanorhinus* share two synapomorphies *D. pikermiensis* definitely lacks: the loss of upper incisors and the ossification of the nasal septum (Geraads & Spassov 2009). Moreover, certain vital similarities have been reported from the craniodental morphology of *D. pikermiensis* and large sized Central and Western Europe species *Dihoplus schleiermacheri* (Giaourtsakis 2003, Giaourtsakis et al. 2006). The derivation of *D. pikermiensis* from *D. schleiermacheri* has also been supported by Geraads and Spassov (2009). Since the nomenclatural issues remain to be resolved, in the present study, the Dicerorhinini rhinoceroses from Samos shall be attributed to *Dihoplus pikermiensis*, following Giaourtsakis (2003) and Geraads & Spassov (2009), whereas the Dicerotini rhinoceroses from Samos shall be referred to as *Miodiceros neumayri*, following Giaourtsakis (2021).

The taxonomic identification of hornless rhinos of the Samos faunal assemblages has also been an issue of disagreement among scientists for more than a century. As previously mentioned, the presence of these animals was first reported by Weber (1905) who described them as the new species *Aceratherium schlosseri* and *Aceratherium samium*. However, the type material of *A. samium* is de facto problematic: a very old individual from an unknown horizon of Samos, with markedly worn teeth (Fortelius et al. 2003). Andrée (1921) used the same genus name to describe *A. wegneri* and *A. angustifrons*, whereas three years later Ringström (1924) included all the previous species to novel genus *Chilotherium*, as *C. schlosseri, C. samium, C. wegneri* and *C. angustifrons*. Heissig (1975) suggested the attribution of *C. wegneri* and *C. angustifrons* to *C. schlosseri* and *C. kowalevskii* PAVLOW, 1913 respectively. Giaourtsakis (2009) suggested that *C. wegneri* and *C. angustifrons* might represent junior synonyms of either *C. schlosseri* or *C. kowalevskii*. Kampouridis et al. (2021) supported that both species erected by Andrée (1921) are junior synonyms of *C. schlosseri*. Giaourtsakis (2021) also supported that *C. wegneri* and *C. kowalevskii* represent junior synonyms of *C. schlosseri*. In the recent literature, the synonymy of *C. kowalevskii* and *C. schlosseri* has been strongly recommended (Giaourtsakis 2009, Antoine & Sen 2016, Pandolfi 2016), though Giaourtsakis (2021) preferred to keep the

Chilotherium material from Samos and Grebeniki as distinct species, pending a revision of the Grebeniki material. For the purpose of this thesis, only *C. schlosseri* shall be considered for the Samos Chilotheriini, following Fortelius et al. (2003).

3. Systematic Palaeontology

3.1 Subfamily Rhinocerotinae

Order Perissodactyla OWEN 1848

Family Rhinocerotidae GRAY 1821

Subfamily Rhinocerotinae OWEN 1845

Tribe Dicerotini RINGSTRÖM 1924

Genus *Miodiceros* GIAOURTSAKIS 2021

***Miodiceros" neumayri* OSBORN 1900**

3.1.1 Upper Deciduous Dentition

Material: AMPG-SAM501, juvenile skull (Fig. 13)

Description

AMPG-SAM501 (Fig. 13) is an incomplete *M. neumayri* cranium. However, the dentition is preserved in a surprisingly good condition. It consists of a rising, almost totally unworn M1 and worn deciduous D4-D2 on both toothrows. On the right hemimaxilla, the D1 is also preserved. The specimen belongs to a juvenile individual, as can be deduced by its relatively small size and the presence of both deciduous and permanent dentition.

The sole D1 present is moderately preserved. The tooth only bears a weak paracone fold and lacks a metacone fold. As a result, the ectoloph profile is noticeably less wavy than on the rest of the dentition. The parastyle is more pronounced than the metasyle. There are no labial cingula. In occlusal view, the protocone is weakly constricted and the protoloph is slightly curved. The hypocone is not preserved. A miniscule crista can be observed. The median valley appears to be open. Mesially, the tooth bears a weakly expressed yet continuous cingulum.

The left D2 is in better state of preservation than the right one. The paracone fold is markedly strong, especially on the left tooth, whereas the metacone fold is

Fig. 13: AMPG-SAM501, *M. neumayri* maxilla, occlusal view. Scale: 5 cm.

weaker. The ectoloph profile is slightly wavy. The parastyle and metastyle are both rounded, yet the parastyle is somewhat longer and sharper. No labial cingulum is present. In occlusal view, the protocone and hypocone are unconstricted. A rather small crochet and crista are present. The protoloph is wide and the metaloph narrow and roughly straight. The median valley is open and wide. In lingual view, a continuous cingulum can be observed, but not a distinct hypostyle. Both a mesial and a distal cingulum are present.

On both preserved toothrows, the D3s are in a remarkable stage of preservation. The paracone fold is markedly well-developed, terminating at the basis of the tooth. On the other hand, the metacone fold is faintly expressed, gradually weakening and terminating at the middle of the tooth. As a result, the ectoloph profile is markedly wavy. The parastyle is short, with a rounded tip. The metastyle is longer, curved and sharper. No observable labial cingulum is present. In occlusal view, the protocone and hypocone are both unconstricted. The crista and crochet are well developed, joined to the formation of a deep medifossette. The protoloph is straight and wide. The median valley is open. Lingually, a marked adamantine style is formed, a feature common in *M. neumayri* upper dentition. No lingual cingula are preserved. Both mesially and distally, however, continuous cingula are present.

On the right D4, the adamantine layer of the ectoloph is almost totally missing, scarcely preserved at the basis of the tooth. As is the case for D3, the left D4 is also characterized by a prominent paracone fold that extends up to the tooth's base, and a much weaker metacone fold that terminated roughly at the middle of the tooth, resulting to a wavy ectoloph profile. The metastyle is only partly preserved, yet it can be deduced that it was longer and sharper than the parastyle. As the rest of the deciduous dentition, the D4 also lack labial cingula. In occlusal view, there are certain similarities with the previously described D3: the protocone and hypocone are unconstricted and the crochet is long. However, there are no preserved cristas, thus no medifossette is formed. The protoloph is straight and the metaloph is slightly constricted. The median valley is open. In lingual view, a marked cingulum can be traced, forming a distinct peak at the entrance of the lingual valley. In both mesial and distal view, strong continuous cingula are observed.

The only present molar is M1. It is only partly visible since it is in rising stage. On the right toothrow, however, it has risen to a higher level, thus facilitating a clearer observation. The tooth has a rectangular outline. Due to the strong paracone and metacone fold, the ectoloph bears a wavy profile. The metastyle is more curved, longer and sharper, than the parastyle. There aren't any labial cingula. Due to the very early wear stage, the only observable features of the occlusal surface are the unconstricted protocone and hypocone and the presence of a long crochet.

Comparison

Numerous distinctive characters between the deciduous dentition of the two tandem-horned rhinocerotids of the Late Miocene Greco-Iranian province *M. neumayri* and *D. pikermiensis* are discussed in Giaourtsakis et al. (2006) and Giaourtsakis (2009), based on specimens from Kerassia, Euboea Island and Mytilinii, Samos Island, respectively. It is noteworthy that AMPG-SAM501 expresses several of the features characterizing *M. neumayri*: the D1 has a reduced metaloph and a curved protoloph, whereas in *D. pikermiensis* the metaloph is long and the protoloph is straight. D2 is characterized by a well-developed paracone fold, while in *D. pikermiensis* the same fold is faintly expressed. On the same tooth, the metacone fold is weak and present only on its upper part; in *D. pikermiensis*, the metacone fold is stronger and terminates at the basis of D2. AMPG-SAM501 does not bear a postfossette on D2, whereas *D. pikermiensis* always bears a large and wide postfossete on the D2. Finally, there is no distinct hypostyle on the basis of the tooth, as happens in *D. pikermiensis.* As far as D3 and D4 are concerned, the protocone is not constricted in AMPG-SAM501, as happens in *D. pikermiensis*; both a crista and a medifossete are present in D3, contrary to *D. pikermiensis*; the metacone fold is gradually weakening to terminate above the base of the teeth, whereas in *D. pikermiensis* this fold is stronger and continues to the basis of the tooth.

In conclusion, it should be safe to attribute AMPG-SAM501 to *M. neumayri*, on the basis of the numerous aforementioned dental characters.

Tribe Dicerorhinini RINGSTRÖM 1924

Genus *Dihoplus* BRANDT 1878

***Dihoplus pikermiensis* TOULA 1906**

3.1.2 Adult Mandible

Material: AMPG-SAM502A, B**,** mandible (Fig. 14)

Description

AMPG-SAM502 (Fig. 14) is an exquisitely preserved mandible, bearing two almost complete tooth rows. Only the right hemimandible also preserves a small part of the ascending ramus. The specimen is also missing the coronoid processes and the mandibular condyles. The mandibular symphysis is moderately preserved. Due to the prominent rarity of well-preserved adult rhino mandibles (Giaourtsakis et al. 2006), the present specimen is particularly interesting. The size of the bone and the wearing of the dentition are indicative of an adult individual.

The mandibular body is robust, with a slightly convex caudal border. The foramen mentalis is observable on the right hemimandible; it is oval-shaped and situated in front of p2. The mylohyoid line, located on the body's medial surface, forms a longitudinal shallow depression. The mandibular angle, more curved than angulated, is obtuse. In lateral view, the partly preserved masseteric fossa is distinct and the masseteric ridge is well defined. As can be seen on the right hemimandible, the masseteric fossa's depression fades out a little before the level of m3.

In medial view, the pterygoid fossa is not very deep. The mandibular foramen is not preserved. In ventral view, the mandibular symphysis is extended up to a point below the root of p2. In lateral view, the caudal border of the symphysis is smoothly elevated, forming an obtuse angle with the horizontal ramus.

There is no sagittal crest on the mandibular symphysis. The partly preserved rostral border of the symphysis is well defined and convex. In anterior view, the two remnants alveoli of the second incisors can be observed on the rostral border of the symphysis, as shallow depressions.

Fig. 14: AMPG-SAM502, *D. pikermiensis* mandible, dorsal view. Scale: 5 cm.

As far as the dentition is concerned, the left hemimandible bears an almost complete toothrow including m3 to p2, while on the right hemimandible p2 and p3 are almost totally broken. There are no cement traces preserved on the teeth. On the other hand, numerous root etchings can be traced, mainly on the occlusal surface of the molars.

A gradual opening of the trigonid and talonid can be observed in the posterior direction.

On the left hemimandible, the sole preserved p2 is small. Its mesial part, including the paralophid and the mesial valley, is broken. The remaining part of the trigonid is sharp. The talonid is more rounded. The protoconid is wide. The entoconid is somewhat more constricted than the metaconid. The posterior valley is open.

On the same heminadible, the p3 is characterized by an obtuse trigonid, in contrast with the oblique, more V-shaped, talonid. The paralophid is very short and smoothly curved. The protoconid is markedly wide. The metaconid is not constricted, while the endoconid bears a very faint constriction. The mesial valley is very small and open. The distal valley is also open and features a miniscule groove.

The p4s are adequately preserved on both hemimandibles. On this tooth, both the trigonid and the talonid are slightly oblique, sharp and V-shaped. The paralophid is short. The protoconid is wide. The metaconide is notably wide, especially on the left p4, with a faintly expressed constriction. The entoconid is unconstricted. The mesial valley is smaller and more acute than the distal valley, which is more smoothly curved. Both valleys are open.

The second and third molars bear certain morphological similarities: the trigonid is oblique and somewhat V-shaped, whereas the talonid is more obtuse, though also V-shaped. The paralophid is markedly reduced, whereas the protoconid is very wide, especially on the left m2. The metaconid and entoconid is unconstricted and straight. The mesial and distal valleys are open, the latter being wider than the former.

On the right heminadible, the m1 is partly broken and deeply worn, with calcite crystals visible on the cracks. Thus, any description must be based on the left m1. The trigonid is V-shaped, whereas the talonid is more U-shaped. The paralophid is narrow, short and straight. The metaconid is notably narrow and unconstricted, as is the entoconid. The mesial valley is as open as the distal valley and roughly at the same size and shape.

There are no observable cingula present on any tooth.

Comparison

The most prominent characters that immediately facilitates the attribution of the specimen to the Rhinocerotinae subfamily are its large size and its narrow symphysis.

As shall be discussed in the following chapters, the mandible of the Aceratheriinae subfamily's representatives is generally smaller and slenderer, whereas a massively wide mandibular symphysis is amidst the most prominent apomorphies of the *Chilotherium* genus.

The main differences in the mandibular morphology of the two tandem-horned Pikermian fauna rhinos have been documented and established by Giaourtsakis et al. (2006) and Giaourtsakis (2009), based on well-preserved material from Kerassia, Euboea Island and Mytilinii, Samos Island. Moreover, certain marked morphological characters that differentiate various Dicerorhinini skulls and mandibles are also described by Pandolfi et al. (2015), in the examination of material from Zala Subbasin, Hungary. In *Miodiceros neumayri*, the mandibular angle is generally obtuse (see Giaourtsakis 2009, Plate 3, Fig. 1), whereas in *Dihoplus pikermiensis* specimens it tends to be more acute (see Giaourtsakis et al. 2006, Fig. 4a). The interalveolar margin's ridge is weaker in *M. neumayri*, compared to *Dihoplus pikermiensis* (Giaourtsakis et al. 2006, Fig. 4B). As far as the mandible symphysis is concerned, the ventral border is more smoothly elevated in *Dihoplus pikermiensis*, the caudal border tends to end before the level of p3 and the part in front of p2 is longer (Giaourtsakis et. al 2006, Fig. 4B). On the other hand, in *M. neumayri*, the caudal border of the symphysis is at the level of p3 or behind it (Pandolfi et al. 2015) and a sagittal crest is present on the ventral part of the symphysis (see Giaourtsakis 2009, Plate 3, Fig. 2C). Finally, the symphysis of *Dihoplus pikermiensis* bears small, fully formed permanent second lower incisors i2, (as seen in Pandolfi et al. 2015, Fig. 5D) or, in case the latter are not preserved, well defined alveoli (as seen in Giaourtsakis et al. 2006, Fig.3c). On the contrary, *M. neumayri* does not preserve incisors into adulthood (as seen in Pandolfi et al. 2015, Fig. 5A).

The Miocene-Pliocene Rhinocerotini are characterized by a generally conservative lower dentition morphology (Pandolfi et al. 2015). The rarity of adequately preserved, adult rhinocerotid mandibles from the Late Miocene of Greece and the general uniformity of Rhinocerotinae lower dentition has restricted the documented differentiating characters between *M. neumayri* and *D. pikermiensis* mandibles and lower teeth in a small number: In *M. neumayri*, the teeth tend to be more hypsodont and sometimes bear traces of cement, the trigonid and talonid are somewhat more angular, the trigonid and talonid valleys rather open and U-shaped and the ectoflexid deeper and angular (Giaourtsakis et al. 2006). Besides, *Dihoplus*

pikermiensis lower teeth lack both lingual and labial cingula, though may bear mesial ones (Pandolfi et al. 2015) and tend to bear a slightly longer paralophid in the molars (Giaourtsakis et al. 2009). The teeth of AMPG-SAM502 are not hypsodont and do not bear cement, lingual or labial cingula. Furthermore, the trigonid and talonid tend to be smooth and the trigonid and talonid valleys are mostly narrow and V-shaped (see also Giaourtsakis et al. 2006, Fig. 4b-c, *D. pikermiensis* lower dentition).

As a result, the presence of visible alveoli on the mandible, the termination of the symphysis at the level of p2 and the morphology of the dentition clearly facilitate the attribution of the specimen to *Dihoplus pikermiensis.*

3.2 Subfamily Aceratheriinae

Subfamily Aceratheriinae DOLLO 1885

Tribe Chilotheriini QIU ET AL. 1987

Genus *Chilotherium* RINGSTRÖM 1924

***Chilotherium schlosseri* WEBER 1905**

3.2.1 Juvenile Cranium

Material: AMPG-SAM504 (Fig. 15)

Description

The only juvenile *Chilotherium schlosseri* skull present in the AMPG collection is AMPG-SAM504 (Appendix C, Fig. 33). Its markedly small size, compared to adult specimens, as well as the presence of the completely unworn, rising permanent M1 on the right hemimaxilla lead to the conclusion that the specimen belongs to an individual of very young age. The right hemimaxilla also preserves DP4, DP3 and DP2, whereas the left one only bears DP3 and DP2. Only the anterior part of the skull is preserved, consisting of the maxilla, the frontal bones, the lacrymal bone and the palate. A trace of the foramen lacrymalis can also be observed. The temporal and occipital region are completely missing, as well as the zygomatic bones. The frontals are hornless and flattened, with a gentle compression.

Incompletely preserved as it is, the specimen's dentition can facilitate an adequate description. The right toothrow preserves DP4, DP3 and DP2 and the left one only DP3 and DP2. The complex patterns of the enamel, present on the whole dentition, are typical for *Chilotherium* teeth.

On the left toothrow, the roots of the missing teeth are observable. The buccal wall of DP2 is more or less broken on both sides. Small traces of cement are preserved lingually, close to the entrance of the median valley and the basis of the hypocone. The tooth bears a constricted protocone with a straight lingual margin and a less constricted hypocone with a sharper lingual margin, as well as a weak, badly preserved, lingual

cingulum. The antecrochet is more marked than the crochet. A postfossette is also present.

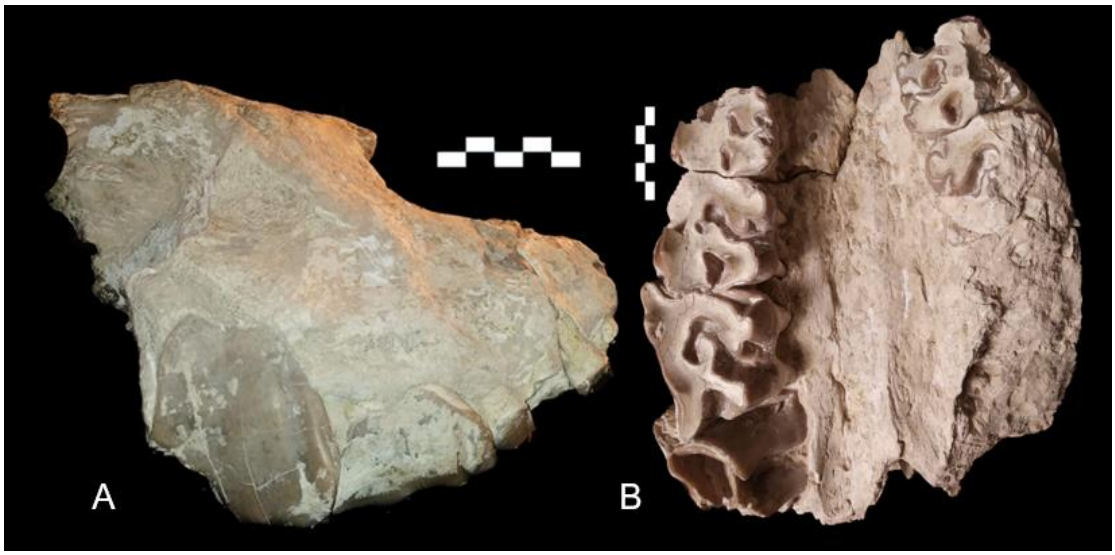

Fig. 15: SAM504, juvenile *C. scholosseri* skull, in (A) lateral and (B) occlusal view. Scale: 5 cm.

The buccal wall and the posterior half of the left DP3 is also broken. Cement traces are present at the opening of the lingual valley. The protocone constriction is strong. The protocone lingual margin is straight. There is a short, yet lingually expanded, antecrochet. On the better preserved right DP3, there are traces of cement. The weak hypocone constriction is also visible. The hypocone and protocone terminate lingually at roughly the same level. There are traces of a broken lingual cingulum. Other than the antecrochet, a short and rounded crochet is also observable on the right tooth, as well as a small crista.

The right DP4 is the most well-preserved tooth of the specimen. It has an extensive cement layer labially, as well as smaller traces lingually, close to the median valley, and mesially. It has strong, continuous cingula mesially, distally and lingually. The protocone and hypocone terminate roughly at the same level. The protocone is strongly constricted, with a straight lingual margin. The antecrochet is marked and lingually expanded. The crochet is well-developed. The metastyle is more elongated than the parastyle and extends lateriodistally.

The rising, almost completely unworn, permanent M1 is lacking its posterior part. In labial view, it preserves thin cement traces. The parastyle is thin and elongated.

The protocone is markedly constricted. A continuous cingulum is present mesially, though not lingually.

Comparison

Incompletely preserved as it is, AMPG-SAM504 bears certain marked *Chilotherium* characters: the gently depressed hornless frontals, the narrow dorsal cranial surface before the highly placed orbita and the short distance between the nasal incision and the partly preserved orbita. Unfortunately, NHMW-2020/0014/0006 (Appendix C, Fig. 45), a skull of an infant *C. persiae*, is also in a bad stage of preservation, making comparisons between the two specimens very difficult. However, few metrical comparisons have been achieved. In AMPG-SAM504, the distance from the nasal incision to the anterior rim of the orbit is 50 mm, whereas the same distance in 2020/0014/0006 is 67.6 mm. The nasal cavity of NHMW-2020/0014/0006 is 41.7 mm wide, whereas in AMPG-SAM506 it is 51.3mm.

The juvenile specimen of *A. neleus* AMPG-PA.4653/91 from Pikermi, Attica, reported by Giaourtsakis et al. (2018), is lacking the hypsodont M1 that characterizes AMPG-SAM504. Moreover, it has slightly concave frontals, instead of the gently depressed, flat frontals of AMPG-SAM504. The dorsal cranial surface is also narrower before the orbita in AMPG-SAM504 than in *A. neleus*, and the parietal crests are wider in AMPG-SAM504 than in *A. neleus* (Giaourtsakis et al. 2018, Fig. 1, personal observations, AMPG). Moreover, the nasal incision of PA.4653/91 is 46.2 mm. Due to the heavy damaged anterior region of the skull, the width of the nasal cavity of AMPG-PA.4653/91 could not be measured.

As far as *A. neleus* is concerned, there are certain characters that differentiate the juvenile teeth of the two species. Comparing AMPG-SAM504 with juvenile *A. neleus* skull AMPG-PA.4653/91 from Pikermi (Giaourtsakis et al. 2018, personal observations, AMPG), the most prominent difference is the weak protocone constriction observed in the dentition of *A. neleus*, in comparison with the strong protocone constriction of AMPG-SAM504. Moreover, the teeth of AMPG-PA.4653/91 do not appear to bear cement coating; in contrast, AMPG-SAM504 bears cement coating, of varying extent, on the whole preserved dentition. The D2 of AMPG-PA.4653/91 bears a deep prefossette and postfossette, but there is no crista, the crochet is almost absent and the antecrochet is short and wide. In AMPG-SAM504, the

antecrochet is more pronounced (due to the missing mesial part of the tooth it cannot be observed whether a prefossette was originally present). The D3 of *A. neleus* from Chomateri does not have a crista, the crochet is marked and the antecrochet is weak, whereas in AMPG-SAM504 the antecrochet is lingually extended and the crochet is weaker, almost joining the small crista. Finally, the main differences between the two specimens D4 is the absence of an antecrochet and the weak metastyle from AMPG-PA.4653/91, while AMPG-SAM504 bears a prominent antecrochet and a longer metastyle.

The *C. persiae* skull NHMW-2020/0014/0006 (Appendix C, Fig. A13), as previously discussed, is not in a good stage of preservation. However, its dentition, though worn and incomplete, has permitted an almost direct comparison with AMPG-SAM505. There are several differences between *C. persiae* and *C. schlosseri* deciduous dentition, among whom the main are the following: in D2 of AMPG-SAM504, the protocone constriction is very strong, the crista and crochet are joined, the antecrochet, though small, is still marked and there is a postfossette. On the other hand, NHMW-2020/0014/0006 has a weaker antecrochet and the crista and crochet are not joined. The D3 of AMPG-SAM504 bears a stronger protocone constriction and a much weaker, almost absent, metastyle than the D3 of NHMW-2020/0014/0006. Finally, the D4 of AMPG-SAM504 bears a marked protocone constriction, a long crochet with a rounded tip and a notably long metastyle, whereas the D4 of NHMW-2020/0014/0006 has a shorter and weaker metastyle, a sharper crochet and almost no protocone constriction. However, it is most probable that those differences appear only due to the different wear stages of the two specimens. As a result, it can be deduced that any difference on the dentition between juvenile *C. schlosseri* and *C. persiae* cannot be used for the moment as diagnostic between the two species.

3.2.2: Adult Crania

Material: AMPG-SAM503, anterior half (Fig. 21C); AMPG-SAM505, anterior half (Fig. 17); AMPG-SAM506, anterior half (Fig. 18, 21B); AMPG-SAM508, occipital region (Fig. 20A); AMPG-SAM509, occipital region (Fig. 20B); AMPG-SAM510, occipital region (Fig. 20C); AMPG-SAM513 (Fig. 16, 20D, 21A)**,** complete skull missing nasal and premaxillary regions; AMPG-SAM515, skull fragment (Fig. 19).

Although a large number of the specimens under study consists of *Chilotherium* skulls, most of them are in a bad preservation stage: specimens AMPG-SAM508 (Fig. 20A), AMPG-SAM509 (Fig. 20B) and AMPG-SAM510 (Fig. 20C) only bear a badly preserved occipital region, AMPG-SAM515 (Fig. 19) only preserves the right half of the anterior region and AMPG-SAM503 (Fig. 21C), which belongs to an aged individual, only preserves the anterior region and part of a markedly worn dentition. The best-preserved specimen is AMPG-SAM513 (Fig. 16, 20D, 21A), an almost complete adult *Chilotherium* skull, bearing M3-P3 on the right hemimaxilla and M2-P2 on the left one. The specimen is missing the nasal and premaxillary bones and both first premolars. The right zygomatic bone is broken, whereas the left one is only partway saved. The temporal region is preserved as well as the sphenoide bone. The occipital region is preserved almost in its entirety: the occipital bone is complete; the occipital condyles are moderately preserved and the post-tympanic apophysis is present on the left side of the skull. Neither the foramen infraorbotalis nor the foramen lacrymalis can be traced. Another noteworthy skull is AMPG-SAM506 (Fig. 18, 21B), bearing the most exquisitely preserved *Chilotherium* dentition of the collection, though preserving only its anterior part. Consequently, descriptions are largely based on the exquisitely preserved specimen AMPG-SAM513, with variations otherwise noted.

The only dentitions available for study are those preserved on specimens AMPG-SAM503, AMPG-SAM506 and AMPG-513 (Fig 21). AMPG-SAM503 only preserves a partial left toothrow, consisting of M3-P4. AMPG-SAM513 preserves M3-P2 on the left toothrow and M3-P3 on the right one. The teeth are in a mediocre preservation stage, the molars being almost crushed. Therefore the description of the upper permanent dentition is based on AMPG-SAM506.

Description

AMPG-SAM513 is amidst the most noteworthy fossils of the AMPG collection, due to its very good preservation. The skull is dolichocephalic and obliquely compressed due to taphonomic processes, as are all the skulls included in the studied material. There are no horn bosses. The frontoparietal region is gently depressed and the frontoparietal crests are well-separated. On the left side, the partly preserved zygomatic arch is wide; this trait is easier to observe on specimen AMPG-SAM509. The nasal notch is deep, terminating above the mesial border of M1. The rostral margin of the orbit is located above the middle of M2 and close to the nasal notch. In posterior view, the occipital region is wide. Its upper part is fan shaped. The occipital condyles are strong, and saddle shaped.

Fig. 16: AMPG-SAM513, *C. schlosseri* skull, lateral view. Scale: 5 cm.

Another notable *Chilotherium* fossil of the AMPG collection is AMPG-SAM505 (Fig. 17): the anterior part of a cranium with an associated mandible, preserved in very hard tuffaceous conglomerate (Svorligkou et al. 2019). The upper dentition consists of an almost complete toothrow, including M3-P2. The mandible preserves m3-p3. The specimen is laterally compressed and entrapped in very hard tuffaceous sediment. The nasals and the anterior part of the frontals are broken. The preserved part bears no horn boss. A gentle depression can be observed, especially on the right side of the frontal, on the region above the orbital fossa; the latter is placed

highly on the skull and its rostral margin is above M1. The nasal notch terminates above the mesial half of P4. The preserved anterior part of the zygomatic is strong. The foramen infraorbitalis is egg-shaped, situated very close to the nasal notch. As far as the mandible is concerned, the ascending rami, the coronoid process and the mandibular condyles are not preserved. Only the posterior part of the symphysis is preserved, though in a bad stage. The mandibular body is straight and slenderer than horned rhinocerotids. The symphysis is wide, typical in *Chilotherium*, and terminates on the level of the middle of p4. The foramen mentalis is placed in front of p2. Due to the preservation stage of the specimen, only the buccal view of the dentition can be examined. In this view, the teeth appear to bear prominent buccal cingula.

Fig. 17: AMPG-SAM505, *C. schlosseri* skull, lateral view. Scale: 5 cm.

Fig. 18: AMPG-SAM506, *C. schlosseri* skull, lateral view. Scale: 5 cm.

Fig. 19: AMPG-SAM515, *Chilotherium schlosseri* skull fragment, lateral view. Scale: 5

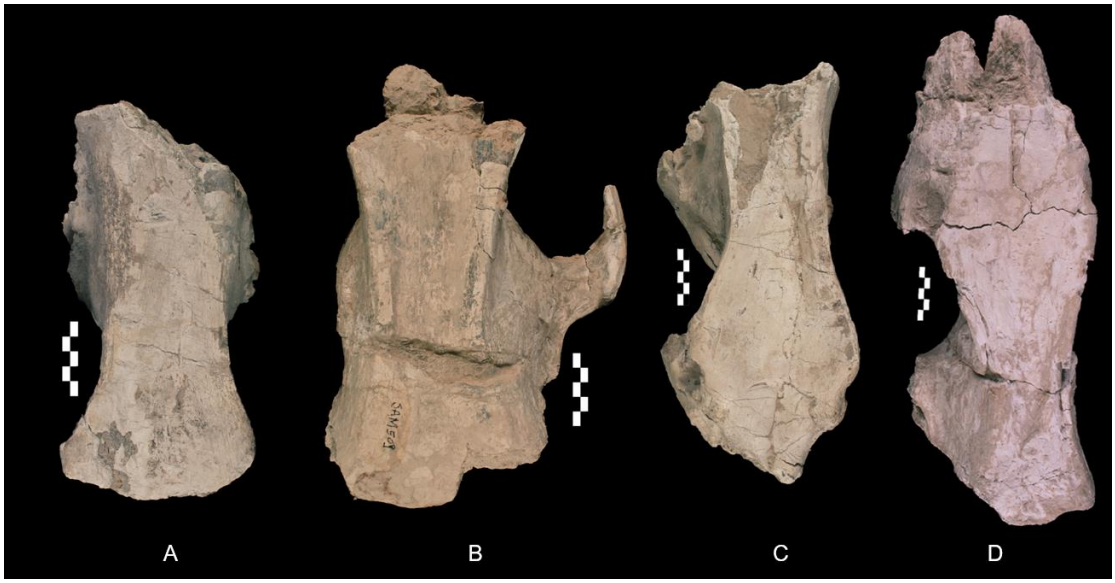

Fig. 20: AMPG-SAM508 (A), AMPG-SAM509 (B), AMPG-SAM510 (C) and AMPG-SAM513 (D), *C. schlosseri* skulls, dorsal view. Scale: 5 cm.

The upper dentition of AMPG-SAM506 is almost complete, missing only the first premolars. The teeth partly preserve the cement. In occlusal view, all the teeth have a roughly quadrangular outline, except for the more triangular M3.

The left P2 preserves traces of cement labially. The protocone and hypocone are connected by a wide bridge and have very weak constriction, whereas on the right P2 the protocone and hypocone are separated. This could be explained by wearing of the enamel due to the individual's aging. These teeth are small, with a quadrangular outline, and preserve traces of cement labially. The right P2 also preserves part of a lingual cingulum. They preserve a postfossette. A small, pointed crista is also present, though more visible on the left tooth. The crochet is also small. The crista and crochet are not joined. The antecrochet is smooth and rounded. The medisinus is open. The parastyle extends mesially. The mesial part of the ectoloph is curved.

The P3s preserve cement traces both labially and, to a lesser degree, lingually. The protocone has a curved lingual margin. The hypocone constriction is much weaker. The antecrochet is smooth and rounded. There is no crista. The crochet is markedly curved. The postfossette is wide. The paracone and metacone folds are weak. A lingual cigulum is present, preserved in a better stage on the right P3. The parastyle is short, the metastyle is slightly longer and sharper. The lingual groove is very small, v-shaped on the right P3 and more rounded on the left one. The median valley is narrow.

On the P4s, the presence of cement traces is strong both labially, close to the neck, and lingually, at the protocone and hypocone basis. The protocone and hypocone, both weakly constricted, are roughly of the same size. The lingual margin of the protocone is almost straight. No lingual cingulum is preserved. The antecrochet is small. The paracone fold is light. The crochet is very well developed and markedly curved. On the contrary, the crista is miniscule. The postfossette is large and roughly triangular. The posterior wall is strong. The median valley is open lingually. The parastyle is stronger than the metastyle.

The left M1 preserves more cement traces labially, mainly at the basis, than the right one. These teeth bear the most marked protocone constriction on the whole dentition. The hypocone is also constricted, more markedly on the right side than on the left. These teeth bear the most prominent antecrochets of the whole dentition: they are very strong and curved lingually. There is no crista. The crochet is marked and curved labially. The postfosette is triangular. The posterior wall is partly broken. The paracone fold is very weak, almost absent. The parastyle is broken on both sides. There is a lingual groove on the protocone, as well as a weak, partly preserved lingual cingulum.

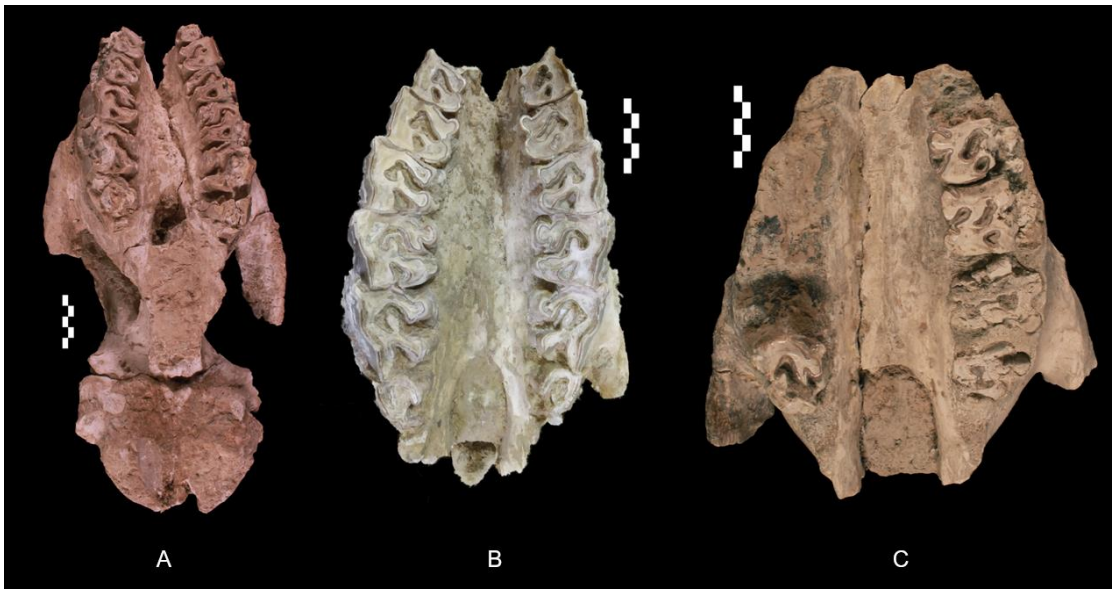

Fig. 21: AMPG-SAM513 (A), AMPG-SAM506 (B) and AMPG-SAM503 (C), *C. schlosseri* skulls, occlusal view. Scale: 5 cm.

On the right M2, the cement traces cover a large part of the labial side of the tooth, whereas they are smaller on the left one. The M2s bears a very sharp, mesially extended parastyle. The metastyle is long. The protocone is notably more constricted than the hypocone and has a roughly straight lingual margin. The crochet is very large and markedly curved labially, almost tear shaped. There is no crista. The antecrochet is present, though weak and rounded. There is no posterior wall. The posterior valley has a triangular outline. A lingual cingulum, in better preservation stage on the right M2, is present on both teeth.

The M3 preserves miniscule cement traces labially. It has a sharp parastyle. The ectoloph and metaloph are fused together, thus explaining the triangular outline of the tooth. The paracone fold is very weak. The crochet is partly broken, thin but long and curved. There is no visible antecrochet preserved. A weak lingual cingulum is present. The posterior valley is wide.

Comparison

The immediate attribution of AMPG-SAM513 to the genus *Chilotherium* is possible due to certain observable features: the hornless, flattened frontal region, with a very gentle longitudinal compression; the narrow cranial surface before the highly placed orbita; the short distance between the nasal incision and the rostral margin of the orbita. AMPG-SAM505 also exhibits a series of salient features that indicate its attribution to the genus *Chilotherium*: the frontal bones are flattened and bear no horns; the notch of the nasal bones is notably retracted; the orbital fossa is placed highly on the skull; the distance between the orbital fossa and the nasal notch is very short; the symphysis is wide; the teeth bear buccal cingula.

As previously mentioned, the two hornless rhinocerotid genera of the Greek Pikermian Faunas are *Chilotherium* and *Acerorhinus*. The latter is interpreted as a less derived hornless rhinocerotid form, represented by *A. neleus*, first reported from the locality of Kerassia, Euboea Island (Athanassiou et al. 2014). As a result, there are certain cranial and dental differences between the two species, due to their different phylogeny and palaeoecology. The flattened frontal region of AMPG-SAM513 is much different from the concave dorsal profile of *A. neleus* (as seen in Athanassiou et al. 2014, Plate 1, Fig. 3a-b). The cranial surface before the orbit is wider in *A. neleus*, whereas the parietal crests are less widely separated (as seen in Athanassiou et al. 2014,

Plate 2, Fig. 1a). The distance between the nasal incision and the rostral margin of the orbital fossa, which is always shorter in hornless genera than in the horned ones, is 77 mm (sin.) and 88 mm (dex.) in *A. neleus* (Athanassiou et al. 2014, Table 1), whereas in AMPG-SAM513 it is 63.5 mm (dex.) and 72.8 mm (sin.). Finally, the occipital region of *A. neleus* is more elongated vertically and bell-shaped, while it is wider and trapezium-like in AMPG-SAM513.

It is difficult to compare AMPG-SAM513 *to C.samium*, due to the latter's problematic nomenclature and lack of any preserved specimens. Only one sketch of an old individual's upper dentition is available by Weber (1905), and the type material is lost. Fortelius et al. (2003) described *C. samium* as being at a comparable evolutionary stage as *C. wimani,* but because of the problematic taxonomy of *C. samium,* they proposed to restrict this name to its type material. The limited diagnostic features of *C. samium* skulls are the following: the frontals are slightly convex, the parietal crests are very highly placed (Weber 1905) and the zygomatic arches are not very expanded, a morphology closer to the Asian *C. wimani* (Borsuk-Bialynicka 1980). In comparison, the AMPG skulls have slightly concave frontals; when preserved, the zygomatic arches are widely expanded and the parietal crests are well-separated.

Chilotherium persiae POHLIG, 1886, though not reported from Greece, is another common Late Miocene hornless rhinocerotid of the Eastern Mediterranean. It has been described from Maraghah, Iran, along with tandem-horned *M. neumayri*, huge elasmothere *Iranotherium morgani* MECQUENEM, 1908 and acerathere *Persiatherium rodleri* PANDOLFI, 2015 (Pandolfi 2015 and references therein). It has been made possible to directly observe certain differences between *C. persiae* and *C. schlosseri* skulls preserved in NHMW: The frontal region, though also hornless, is even flatter in *C. persiae* NHMW-2020/0019/0003 (Appendix C, Fig. A11) than in *C. schlosseri* NHMW-1911/0005/0128 (Appendix C, Fig. A9) and AMPG-SAM513. The cranium does not get very narrow before the orbita in *C. persiae*. The nasal incision is smoother and more rounded in *C. schlosseri* NHMW-1911/0005/0128 than in *C. persiae* skulls NHMW-2020/0014/0093 and NHMW-2020/0014/0097. The zygomatics are very strong and almost completely straight, whereas in *C. schlosseri* they are shorter and exhibit an abrupt curve at the level of the postorbital process (compare *C. persiae* NHMW-2020/0014/0097, NHMW-2020/0014/0008 and NHMW-2020/0014/0093 to *C. schlosseri* NHMW-1911/0005/0128).

AMPG-SAM506 bears the best-preserved upper teeth among the collection's chilotheres. The presence of well-developed antecrochets on the upper dentition is one of the most characteristic apomorphies of the genus (Geraads and Koufos 1990), along with the marked protocone constriction on the molars, the reduced lingual cingulum on the preserved premolars, the lingual bridge connecting the hypocone and protocone on P2, indicating late wear stage and an older age, the lack of labial cingulum and crista on upper molars (Deng 2006b, Antoine & Sen 2016, Pandolfi 2016, Sun et al. 2018). Moreover, the strong antecrochets that are parallel to the ectoloph and the elongated crochets that characterize the derived chilotheres, such as *C. schlosseri* (Deng 2006b, Antoine & Sen 2016, Sun et al. 2018) are also present on the specimen. In comparison, the antecrochet of more primitive *C. samium* is moderate (Geraads & Spassov 2009).

Taxon	Min	Max	N
C. schlosseri	87	90	5
C. samium	~40	-	1
C. kowalevskii	40	66	10
C. persiae	32	50	4
C. habereri	42	60	9
C. anderssoni	50	63	5
C. wimani	28	64	10
C. primigenius	18	-	1
AMPG specimens	57.1	83.8	3

Table 2: Minimim distance (in mm) between the parietal crests in *Chilotherium* spp. From Kampouridis et al. 2021, completed with own data.

Moreover, the AMPG dentitions are very similar to the *C. schlosseri* illustrated by Weber (1905, Tafel IX). On the P2 of AMPG-SAM506, the medifosette is open and the protocone constriction is somewhat weak, as in Weber (1905, Tafel IX, Fig. 1). On the same illustration, on the P3, there is no closed medifosette; it is unclear if this is associated with the specimen's advanced wear stage. In AMPG-SAM506 the medifosette is also open. The connection between the protocone and the hypocone is only a little narrower than in AMPG-SAM506. On the P4 illustrated by Weber (1905, Tafel IX, Fig. 1), the medifosette is almost closed, and in the *C. schlosseri* P4 MNHN.F.TRQ339 from Turkey (Antoine & Sen 2016, Fig. 2B-D), the medifossette

will close in a later wear stage. The latter also appears to be the case with AMPG-SAM506. Another similarity of these specimens is that they have a short crista. The paracone fold is stronger in AMPG-SAM506 and MNHN.F.TRQ339 than in Weber's illustration. The M1 of *C. schlosseri* from Samos (Weber 1905, Tafel IX, Fig. 1) and Turkey (Antoine & Sen 2016) share with AMPG-SAM506 the sharp, elongated antecrochet, the long crochet and the open medifosette. In AMPG-SAM506, the antecrochet is almost parallel to the ectoloph, as described by Antoine & Sen (2016) for *C. schlosseri* from Turkey. In AMPG-SAM513 it is more curved to the lingual direction, exactly as in the *C. schlosseri* dentition illustrated by Weber (1905, Tafel IX, Fig. 1). The M2 and M1 in Weber's illustration (1905, Tafel IX, Fig. 1) both feature closed medifosettes, which is not the case for AMPG-SAM506. The partly preserved M2 KÇ 297 from Turkey (Antoine & Sen 2016, Fig. 2E) has an open medifosette.

The main differences between the AMPG dental material and *A. neleus* from Kerassia and Pikermi are the following: the protocone constriction of the AMPG specimens is markedly strong, whereas in *A. neleus* it is much weaker (Athanassiou et al. 2014, Plate 2 Fig. 1b, Plate 3 Fig. 1b). *Acerorhinus neleus* bears very strong, continuous cingula and very small medifossettes on the premolars (Athanassiou et al. 2014, Plate 2 Fig. 1b), whereas AMPG-SAM506 only preserves a weaker lingual cingulum only on P3 and no medifossettes on any tooth. In P3-P4 of A. *neleus*, the crochet is shorter and more rounded (Athanassiou et al. 2014, Plate 2 Fig. 1b, Plate 3 Fig. 1b) compared to the more elongated crochet on the respective teeth of AMPG-SAM506. The molars of the two specimens bear more differences than the premolars. The M1 and M2 of AMPG-SAM506 bear very strong, elongated antecrochet and crochet, whereas *A. neleus* has a much weaker antecrochet, a more rounded crochet on M1 and weaker protocone and hypocone constrictions (Athanassiou et al. 2014, Plate 1 Fig. 4b). Moreover, AMPG-SAM506 first and second molar have notable constrictions on the protocone and the hypocone, that *A. neleus* teeth lack (Athanassiou et al. 2014, Plate 1 Fig. 4b, Plate 3 Fig. 1b). The M2 of AMPG-SAM506 also has a longer metastyle and a marked mesial elongation of the parastyle than *A. neleus* (Athanassiou et al. 2014, Plate 1 Fig. 4b). The M3 of AMPG-SAM506 is badly preserved, yet appears to lack the crista that is observed on *A. neleus* (Athanassiou et al. 2014, Plate 3 Fig. 1b) and to bear a more pronounced crochet (see Athanassiou et al.

2014, Plate 1 Fig. 4b, Plate 3 Fig. 1b). These data can safely exclude the attribution of the AMPG upper dentition material to *A. neleus*.

Despite belonging to the same genus, AMPG collections *C. schlosseri* is also different from *C. persiae*. In terms of upper dentition, the main differences are the following: The protocone constriction is marked in both species, however the lingual margin of the protocone is straighter in AMPG-SAM506 than in *C. persiae* from Maraghah (compare with *C. pesiae* skulls NHMW-2020/0014/0005 and NHMW-2020/0014/0003, Appendix C, Fig. A11). The P2 of *C. persiae* NHMW-2020/0014/0099 bears a longer and more marked crochet and a more pointed crista than the AMPG specimens. Moreover, the protocone and hypocone are connected by a lingual bridge, which is not the case in AMPG-SAM506 or *C. schlosseri* skull NHMW-1911/0005/0128. The P3 of *C. persiae* MNHN.F.MAR3053 (Appendix C, Fig. A19) has a stronger and more curved crochet and a slightly more pronounced paracone fold than AMPG-SAM506. The lingual bridge connecting the protocone and hypocone may be present on the P3 of both species (AMPG-SAM506 and *C. persiae* specimens NHMW-2020/0014/0099, NHMW-2020/0014/0008) or may be absent (*C. persiae* skull MNHN.F.MAR3053), and cannot therefore be used as a distinctive character. The hypocone tends to expand lingually up to a pointy edge in *C. persiae* (see MNHN.F.MAR3822, Appendix C, Fig. A18) but not in *C. schlosseri* AMPG-SAM506.

Additionally, the P4 of *C. persiae* is somewhat smaller and with a weaker crochet than AMPG-SAM506, yet the antecrochet tends to be more developed (*C. persiae* MNHN.F.MAR3822). The antecrochet on the M1 of *C. persiae* skulls MNHN.F.MAR3822 and NHMW-2020/0014/0008 expands lingually and vertically, almost touching the hypocone, whereas in AMPG-SAM506 it is more elongated and mesialingually expanded, never in contact to the hypocone. Additionally, the hypocone of the *C. persiae* specimen MNHN.F.MAR3822 is curved mesialingually, a feature also observable in *C. persiae* skull NHMW-2020/0014/0002 but absent from AMPG-SAM506. The M2 of *C. persiae* MNHN.F.MAR3822 has a markedly longer and stronger antecrochet than AMPG-SAM506, a feature also observed in *C. persiae* NHMW-2020/0014/0003. Finally, *C. persiae* is the only chilothere to bear a somewhat quadrangularly outlined M3 (Ringström 1924).

		M. neumayri	*D. pikermiensis*	*C. schlosseri*	*A. neleus*
D1	Overall size	Slightly reduced	Normal	Tooth not preserved on specimen	Slightly reduced
	Protoloph	Very long, bends posterolingually blocking up the entrance of medisinus.	Regular, vertical, does not bend	Tooth not preserved on specimen	Regular, vertical, does not bend
	Metaloph	Reduced, very short	Regular, long	Tooth not preserved on specimen	Regular, long
D2	Lingual cingular pillar	Present	Absent	Absent	Absent
	Protocone constriction	Not constricted	Slightly constricted	Markedly constricted	Slightly constricted
	Size of Postfossette	Very small and narrow if present	Large, wide	Small, narrow	Large, narrow
	Hypostyle	Not developed/distinct from posterior cingulum	Present, distinct from posterior cingulum	Not developed	Not developed
	Paracone Rib	Very strong, usually double	Strong, always single	Not preserved on tooth	Moderate, single
	Metacone Rib	Absent or faint only at the top of the crown, then fades out and disappears	Present, clearly marked and continuous down to the basis of the crown	Not preserved on tooth	Weak
D3-D4	Lingual cingular pillar	Present in front of the entrance of medisinus	Absent	Absent	Absent
	Protocone constriction	Not constricted	Slightly constricted	Strongly constricted	Slighlty constricted
	Crista	Always present	Always absent	Small	Absent
	Medifosette	Usually present	Always absent	Absent	Absent
	Metacone Rib	Absent or faint only at the top of the crown, then fades out and disappears	Present, clearly marked and continuous down to the basis of the crown	Very faint	Absent

Table 3: The main distinctive characters on the deciduous upper dentition of the three Samos rhinocerotids and *A. neleus*. Columns on *M. neumayri* and *D. pikermiensis* from Giaourtsakis et al. 2006, column on *C. schlosseri* based on AMPG specimen AMPG-SAM505, column on *A. neleus* based on PA4653/91 (see Giaourtsakis et al. 2018).

3.2.3 Adult Mandible

Material: adult mandible AMPG-SAM500 (Fig. 28)

Description

Among the specimens under study, the only adult *Chilotherium schlosseri* mandible is AMPG-SAM500 (Appendix C, Fig. 28). It is a moderately preserved mandible, missing both ascending rami and the caudal half of the mandibular body, though preserving the symphysis. The left hemimandible preserves a partial toothrow, including p2 and the mesial half of p3, whereas the right hemimandible retains p2, p3 and part of the p4. The roots of the lower incisors i1 and parts of i2 are also preserved.

The teeth partially preserve their cement. The mandibular body is not very robust, bearing a distinctly concave dorsal profile. Its base is nearly straight beneath the level of m3 to p2, gradually bending towards the symphysis. The angle between the body and the symphysis is obtuse.

The mandibular symphysis itself is very wide, terminating posteriorly at the level of p3. In lateral view, the foramen mentalis opens in front of p3. In the rostral part of the symphysis, a light sagittal linear groove is formed. In dorsal view, the specimen demonstrates a long diastema with a marked crista along the interalveolar margin.

The premolars do not have vertical external roughness. The p2 bear a pronounced, acute trigonid. The paralophid is straight and sharp, though not forked. The metaconid is weakly constricted. The mesial valley is open and U-shaped. A continuous lingual cingulum is present.

The p3 have a well-developed, V-shaped ectolophid groove, terminating before the level of the neck. The trigonid is more acute on the left p3 than on the right one. The talonid, observable only on the right p3, is smooth and rounded. The metalophid is slightly constricted. The entoconid is only preserved on the right p3, where it is developed without a constriction. The paralophid is somewhat abruptly curved. The distal valley is open and larger than the mesial one. A weak continuous lingual cingulum is present.

Due to breaking and very deep level of wearing, the right p4 is inadequately preserved to facilitate a detailed description.

The lower incisors are partly visible. The left one preserves a larger part than the right one. It is tusk-like, straight and wide close to the basis, getting progressively narrower. It can be deduced that the incisors grew divergently.

A small part of the roots of the i1 is also preserved, somewhat easier to observe on the left side of the symphysis. It is small and somewhat meniscus shaped.

Fig. 22: AMPG-SAM500, *C. schlosseri* mandible in occlusal (A) and rostral (B) view. Scale: 5 cm.

Comparison

Since the mandible and lower teeth of *Chilotherium* is markedly uniform within the genus, it is not recommended to base a specific attribution on such specimens (Ringström 1924). However, AMPG-SAM500 shares a series of salient features with NHMW-1911/0005/0032 and NHMW-1911/0005/0033 (Appendix C, Fig. A14 and Fig. A16 respectively) two adult mandibles labeled as *C. schlosseri*: the notable widening of the mandibular symphysis with a markedly concave dorsal profile; the obtuse angle
between the mandibular body and the symphysis; the long diastema between i2 and p2, marked by a thin crista.

The markedly wide symphysis is one of the most important apomorphies of the genus *Chilotherium* (Ringtrom 1924), thus immediately excluding an attribution to *A.*

neleus (also compare to Athanassiou et al. 2014, Plate 2, Fig. 2c & 2d). Other differences between AMPG-SAM500 and *A. neleus* are the following: the diastema along the interalveolar margin appears more curved in AMPG-SAM500 (see Athanassiou et al. 2014, Plate 2, Fig. 2d, and Plate 3 Fig. 3). In the same work, this diastema is measured at 35.5 (sin) and 43.2 in *A. neleus*, whereas in AMPG-SAM500 it is 52.4 mm (sin.) and 50.4 mm (dex.) approximately. In lateral view, the mesial part of the symphysis, bearing the incisors, is straighter in AMPG-SAM500 than in *A. neleus* (see Athanassiou et al. 2014, Plate 2, Fig. 2a & 2b).

Mandibles of *C. persiae* from Maragheh, Iran, also tend to have a wide mandibular symphysis (personal observation, NHMW). However, in NHMW-2020/0014/0096 (Appendix C, Fig. A15) and NHMW-2020/0014/0100 (Appendix C, Fig. A17), two adult *C. persiae* mandibles, the symphysis is shorter, terminating at the mesial half of p2. Specimen NHMW-2020/0014/0036 is the only adult *C. persiae* mandible still preserving a strong ridge on the interalveolar margin, very similar to that of AMPG-SAM500. The anterior, incisors-bearing, part of the symphysis is also more curved in NHMW-2020/0014/0096. It should be noted that the curving of the anterior part of the symphysis is more marked in juvenile *C. persiae* mandibles (e.g. specimen MNHN.F.MAR3859 and MNHN.F.MAR3889, Appendix C, Fig. A20, A21 respectively) than in adult mandibles; it could be deduced that this trait is intertwined with the individual's ontogenetical stage, since the straighter, stronger anterior part of the symphysis probably facilitates the development of the tusks.

As already mentioned, the lower teeth of the species belonging to *Chilotherium* exhibit a large degree of uniformity, with occurring variations often caused by intraspecific variability. However, the lower dentition under study shares many prominent features with *C. schlosseri* mandible NHMW-1911/0005/0032: the well-developed paralophid on the p2, the prominent, V-shaped ectolophid groove terminating before the neck on the p3, the weak lingual cingulum on the premolars and the strong, tusk-like, divergent i2. The tusks are among the most impressive features of the specimen and a prominent apomorphy of the genus. They expose very strong sexual dimorphism, having been used as a tool of sexual domination by the male individuals (Chen et al. 2010). Sadly, the tusks of AMPG-SAM500 are broken, thus not immediately revealing the individual's sex. However, the width at the basis is measured at 27mm on the left incisor and at 30.3 at the right one. In a male *C. schlosseri* i2 (GPIT/MA/12983) from the latest Miocene of Staniantsi, Bulgaria (Kampouridis

2020), the width at the basis of the tusk is measured at 55 mm, whereas in a female i2 (GPIT/MA/13400) from the same locality the width is 35 mm (Kampouridis, pers. comm.). Also, the tusks are 46 mm wide in the *C. wegneri* type mandible (*C. schlosseri* sensu Kampouridis et al. 2021). Consequently, it can be deduced that AMPG-SAM500 likely belongs to a female individual.

A number of differences can be found between the lower permanent dentition of AMPG-SAM500 and *A. neleus* from Kerassia: the latter has cement traces only on the labial side of the teeth, a less acute trigonid on p3, more narrow and oblique distal valleys and a less prominent paralophid on the premolars and no lingual cingulum (see Athanassiou et al. 2014, Plate 2, Fig. 2c & Plate 3, Fig. 2a). Moreover, *A. neleus* has a labial cingulum on the premolars that AMPG-SAM500 lacks (Athanassiou et al. 2014). The ectolophid groove on the premolars is sharper in AMPG-SAM500 than in *A. neleus*, whereas the trigonid of the latter is more rounded on the premolars (see Athanassiou et al. 2014, Plate 2, Fig. 2c & Plate 3, Fig. 2a). In comparison with adult *C. schlosseri* mandible NHMW-1911/0005/0032, which preserves its wide, rather shovel-like tusks, the incisors of *A. neleus* are weaker and pointier (see Athanassiou et al. 2014, Plate 2, Fig. 2a & 2d and Plate 3, Fig. 3).

As previously discussed, the mandibles of *C. schlosseri* and *C. persiae* do not exhibit marked differences. As far as the lower dentition is concerned, the main differences observed between AMPG-SAM500 and NHMW *C. persiae* specimens NHMW-2020/0014/0096, NHMW-2020/0014/0100 and NHMW-2020/0014/0036 are the following: the ectolophid groove, though also V-shaped, is more oblique in *C. persiae*; the metaconide of the premolars of *C. persiae* is more oblique and bears a slightly stronger constriction. Finally, the second incisors of *C. persiae*, though also strong and divergent, are dagger-like, with pointy ends, rather than the more shovel-like second incisors preserved on the NHMW *C. schlosseri* adult mandible 1911/0005/0032 (Appendix D, Fig. A14).

4. Discussion

4.1 Biostratigraphical Remarks

4.1.1 Rhinocerotinae

The most primitive representatives of the subtribe Dicerotina belong to African species *Paradiceros mookiri* HOOIJER, 1968 from the Middle Miocene of Kenya, Morocco and Uganda (Hooijer 1968, Guerin 1976, 1994). The Dicerotina subtribe is poorly documented in the Late Miocene of Africa, yet notably common in synchronous Eastern Mediterranean, mainly represented by *Miodiceros neumayri* and *Dihoplus pikermiensis*.

The tandem-horned *Miodiceros neumayri* is amidst the most common perissodactyls of the Late Miocene. It migrated in Eurasia during the late Vallesian (MN8), in Esme Ackacoy locality of Turkey (Koufos 2003). It has been reported from Late Miocene localities of Iran (Thenius 1955), Anatolia (Heissig 1975, Geraads 1994), Bulgaria (Geraads & Spassov 2009), the former USSR, Hungary, Austria and Italy (Giaourtsakis 2003).

Along with *Dihoplus pikermiensis*, *Miodiceros neumayri* is another common perissodactyl of Eastern Mediterranean "Pikermian" faunas. In Greece, it has been reported from Pikermi, Attica (Wagner 1848, Gaudry 1862, Guérin 1980, Geraads 1988), Kerassia, Euboea Island (Giaourtsakis et al. 2006, Athanassiou et al. 2014), Vathylakkos (Arambourg & Piveteau 1929), Ravin des Zouaves (Koufos 1980), Pentalophos (Geraads and Koufos 1990), Thermopigi and Platania (Tsoukala 2018) in Macedonia. Samos and Pentalophos are the sole Greek fossiliferous localities where *M. neumayri* coexisted with *C. schlosseri*.

Dihoplus pikermiensis is the other most frequently documented tandem-horned rhinocerotid of the Greek Late Miocene. Its type locality is Pikermi (Roth & Wagner 1854, Gaudry 1862, Geraads 1988) and it has also been reported from Samos (Weber 1904, Geraads 1988), Kerassia and Halmyropotamos, Euboea Island (Melentis 1968, 1969, Giaourtsakis et. al 2006) and Thermopigi, Serres (Tsoukala 2018).

In the AMPG material, both tandem-horned species are present. The interspecific dominance of *M. neumayri* over *D. pikermiensis* has been established in

literature based on the Aristotle University of Thessaloniki large scale excavation material (Giaourtsakis 2009). However, the small quantity of the material studied herein and the lack of stratigraphical data did not allow for a conclusion on the relative distribution of the Dicerotina representatives.

4.1.2 Chilotheriini

Asia is the undoubted cradle of evolution for the Chilotheriini tribe, China bearing the largest number of species during the Miocene. The first *Chilotherium* fossils are described from the Middle Miocene Siwalik Hills fauna of Pakistan and belong to *C. intermedium* LYDEKKER, 1884 (Majid et al. 2011). The genus expands into China during the Vallesian (middle to late MN9), with the appearance of primitive species *C. primigenius* DENG, 2006. *Chilotherium* is also amidst the most common vertebrates of the "Hipparion Red Clay" localities (sensu Flynn et al. 2011), occasionally emerging as the dominant taxon (Deng 2006a). The dominant species of the Chinese Turolian is *C. wimani* RINGSTRÖM, 1924 (Deng 2006a, b, Sun et al. 2018). Middle Turolian (MN12) species *C. habereri* SCHLOSSER, 1903 and *C. anderssoni* RINGSTRÖM, 1924 are also thriving, whereas the end of the Late Miocene (MN12-13) is marked by the presence of the highly specialized C. *licenti* SUN, LI & DENG, 2018. It is noteworthy that despite the proximity of the hornless genera *Chilotherium*, *Acerorhinus* KRETZOI, 1942 and *Shansirhinus* KRETZOI, 1942, the exclusively Asian hornless genus *Shansirhinus* is a sister group to *Chilotherium* (Deng 2005). As far as the rest of the Asian continent is concerned, *C. xizangensis* JI, HU & HUANG, 1980 is mentioned from the Late Miocene of Thibet and *C. persiae* from the classic "Pikermian Fauna" of Maragha locality, Iran (Pohlig 1886).

It has been proposed that the migration of Asian *C. habereri* into Anatolia during the Turolian eventually brought about the first chilotheres in Europe (Heissig 1975). Nevertheless, the genus is first reported in Europe in the Vallesian of Pentalophos locality, Chalkidiki, Greece. The aforementioned fossils were initially attributed to the new species *"Aceratherium"* (*Chilotherium) kiliasi* (Geraads & Koufos 1990). However, this diagnosis was later firmly doubted, with part of the material attributed to *Chilotherium samium* and the rest to *Acerorhinus zernowi* (Heissig 1996, 1999; Giaourtsakis 2003). In any case, Pentalophos is the exclusive Late Miocene Greek

fossiliferous site were two different hornless rhinocerotid genera ever coexisted and represents the oldest record of *Chilotherium* in Europe (Giaourtsakis 2003).

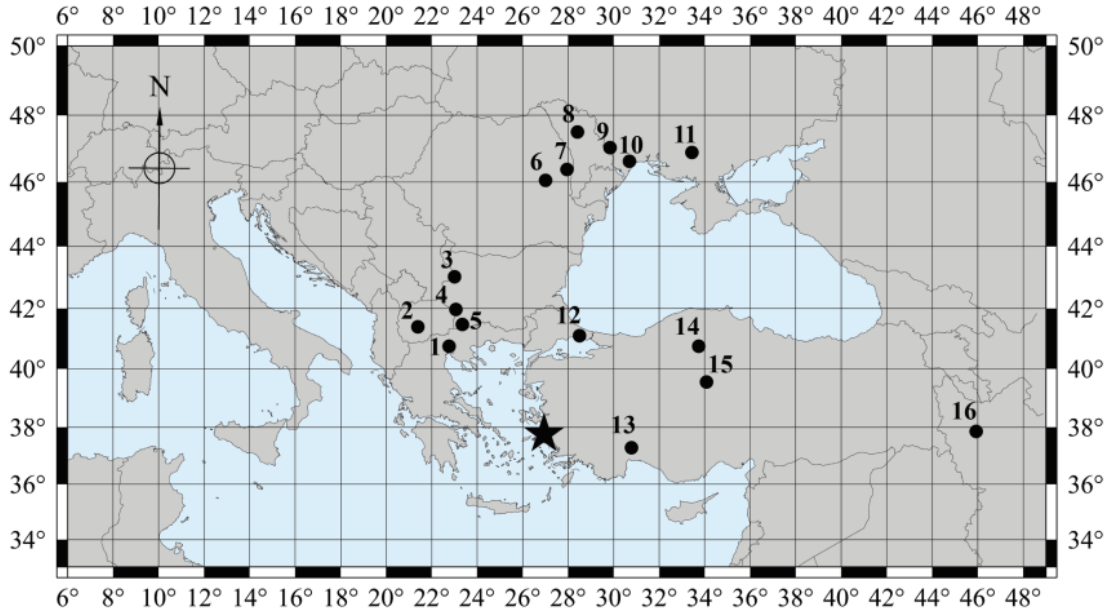

Fig. 23: Distribution of *Chilotherium* spp. in the Balkan-Iranian province. The black star represents Samos (Greece) (Weber 1905; Andrée 1921). 1, Pentalophos (Greece) (Geraads and Koufos 1990); 2, Morievo region (North Macedonia) (Spassov et al. 2018); 3, Staniantsi region (Bulgaria) (Kampouridis 2020); 4, Oranovo region (Bulgaria) (Kampouridis 2020); 5, Kromidovo (Bulgaria) (Geraads and Spassov 2009); 6, Reghiu (Codrea 1996); 7, Pogana (Romania) (Codrea 2011); 8, Raspopeni (Moldova) (Geraads et al. 2020); 9, Grebeniki (Pavlow 1913); 10, Odessa (unknown locality) (Niezabitowski 1913); 11, Berislav (Ukraine) (Korotkevich 1958b); 12, Küçükçekmece (Antoine and Sen 2016); 13, Kayadibi (Geraads et al. 2020); 14, Sinap (several horizons) (Fortelius et al. 2003); 15, Akkaşdağı (Turkey) (Antoine and Saraç 2005); 16, Maragha (Iran) (Pandolfi 2016). From Kampouridis et al. 2021.

In Europe, the genus *Chilotherium* is mainly reported from the southeastern part of the continent, with a marked presence in the Balkan Peninsula. The genus's biostratigraphy in Eurasia is very problematic, due to taxonomic issues, lack of stratigraphic data from the various localities and incomplete documentation of the specimens (lack of detailed descriptions and illustrations) (Fortelius et al. 2003). The species *C. sarmaticum* KOROTKEVICH, 1958 has been described from the late Vallesian of Ukraine (Korotkevich 1958a & b, 1970, fide Kampouridis 2020) and the upper Miocene of Bulgaria (Spassov et al. 2006, Geraads & Spassov 2009). Moreover, *C. kowalewskii* PAVLOW, 1913 has also been reported from the Turolian of Ukraine

(Pavlow 1913), as well as from Anatolia (Heissig 1996), Moldova (Vangengeim & Tesakov 2008) and Bulgaria (Geraads & Spassov 2009). Ukrainian localities have also yielded specimens of *C. schlosseri* of an estimate Late Sarmatian age (Vangengeim & Tesakov 2007). The species *C.* aff. *zernowi* BORISSIAK, 1914 and *C. eldaricum* TSISKARISHVILI, 1987 are part of various South Caucasus Late Miocene faunal assemblages (Bukhsianidze & Koiava 2018 and references therein). Lately, material attributed to *Chilotherium* sp. has been reported from the Middle Turolian of Northern Macedonia (Spassov et al. 2018) and Bulgaria (Spassov et al. 2019). Finally, as far as the rest of Greece is concerned, *C. schlosseri* consists a sizable fraction of the classic "Pikermian Fauna" of Samos Island.

As previously mentioned, the only unquestionably valid *Chilotherium* species in Greece is, currently, *C. schlosseri*. The craniodental material from the AMPG Samos collection can be referred to this species. There are two possible explanations of *C. samium*'s absence: the first one would be a stratigraphic separation of *C. schlosseri* and *C. samium*, indicationg that the material housed at the AMPG (Th. Skoufos collection) is derived from the layers including only *C. schlosseri*.The second could be the complete lack of *C. samium* from Samos, leading to the conclusion that the species is either invalid, or a synonym to *C. schlosseri*.The last scenario cannot be completely ruled out, since *C. samium* is considered as a problematic species, lacking distinctive characters to separate it from *C. schlosseri*, and also considering the lost holotype. In case of a probable synonymy between *C. schlosseri* and *C. samium*, *C. schlosseri* must be regarded as the valid name, because its type material has a better documentation by Weber (1905) and can be identified with specimens from Samos (Giaourtsakis 2021). Nevertheless, in order to extract a safe conclusion, the numerous postcranial *Chilotherium* specimens from the AMPG collection should definitely be taken into account.

4.2 Palaeoecological Remarks

During the Late Miocene, the terrestrial ecosystems of the Greco-Iranian (sensu de Bonis et al. 1992) or Subparatethyan (sensu Bernor 1984) Zoogeographical Province were characterized by the coexistence of at least three rhinocerotids: one or two hornless genera (*Chilotherium* and/or *Acerorhinus*) along with tandem-horned species

Miodiceros neumayri and *Dihoplus pikermiensis* (Giaourtsakis 2003, 2009, Kostopoulos 2009, Athanassiou et al. 2014,).

Moreover, a gradual expanse of more open, arid habitats towards the eastern Mediterranean localities was observed (Fortelius et al. 2002, Eronen et al. 2009, Stromberg et al. 2007, Koufos et al. 2009, Athanassiou et al. 2014). This transition can be observed in the fossil megaherbivores assemblages of Greece, including rhinocerotids: more than 70% of the tandem-horned rhinocerotid material from the classical Turolian locality of Pikermi, Attica, is attributed to *D. pikermiensis*, *M. neumayri* and *A. neleus* are present in smaller numbers and *Chilotherium* is absent (Giaourtsakis 2003). The Turolian site of Kerassia, Euboea, is also characterized by the relative dominance of *M. neumayri* over *D. pikermiensis*, the only present acerathere being *A. neleus* (Kampouridis et al. 2019, Giaourtsakis et al. 2020). Opposing, Samos Island's fossiliferous assemblages are characterized by the presence of at least one *Chilotherium* species and the absence of *A. neleus*, whereas the dominance of *M. neumayri* over *D. pikermiensis* is apparent (Giaourtsakis 2003, 2009, Svorligkou et al. 2019).

The application of a multiproxy analysis, including both microwear and mesowear on Samos bovids and equids by Koufos et al. (2009a), indicated the ascendency of mixed feeders over grazers and browsers. This result immediately excludes the dominance of both dense forests and open grasslands. On the contrary, it is indicative of favoring an open bushland and a trend to more dry climatic conditions starting from the late early Turolian. This interpretation has also been proposed for other Late Miocene Eastern Mediterranean localities, such as Perivolaki, Thessaly (Koufos et al., 2006), Axios Valley, Macedonia (Merceron et al. 2005) and Bulgaria (Merceron et al. 2006). The research team also studied the species diversity of the island's faunal assemblages, examining the homogeneity, equilibrium, and normality (Koufos et al. 2009b and references therein). According to the results of the same analysis, the faunas of Samos are homogeneous, equilibrated, with normal taxonomic distribution. Although the low number of individuals and species of most assemblages under comparison (Koufos et al. 2009b, Tab. 1) severely affect the Simpson index, most sites indicate relatively equilibrated faunas, the MTL fauna being the most diversified and equilibrated.

Lithologically, the Mytilinii formation corresponds to volcanoclastic fluviolacustine sediments, not favouring the preservation of fossilized pollen grains; as

a consequence, only 14 samples were extracted for palynological study (Kostopoulos et al. 2009, Ioakim & Koufos 2009). The samples are ample with herbaceous plants, while also preserving steppe elements, Mediterranean sclerophyllous plants and, to a lesser degree, Taxodiaceae and *Pinus*. The results indicate the existence of an open vegetation flourishing under a warm to temperate climatic regime (Ioakim & Koufos 2009), in agreement with results from the Greek Turolian localities of Axios Valley, Macedonia (Bonis et al. 1992, Merceron et al. 2005, Koufos 2006b) and Thessaly (Koufos et al. 2006). Moreover, the phytolith assemblages designate the presence of wide tracks with an affluent herbaceous vegetal layer including C3 graminoids (Strömberg et al. 2007). In comparison, the synchronous, proximal to Samos, Anatolian localities in Turkey are also characterized by an open environment, but an arid climate (Bonis et al. 1994). Finally, the results are similar to those of the microwear analysis, which point out an open bushland with thick grass coverage (Koufos et al. 2009), and also correspond to the gradual expanse of more arid open environments towards the eastern Mediterranean.

In a combination work on the Pikermi Biome, Solounias et al. (2010) applied microwear analysis on an ample number of samples from Pikermi and Samos. Their material consisted of bovids, giraffids, equids, rhinocerotids and a colobine monkey. According to this work's results, the ruminants are mainly brachydont and mesodont mixed feeders and the equids hypsodont grazers; the palaeodietary results indicate that the Pikermian Biome was more similar to an extant Indian woodland than an African savanna. Samos is also considered to have been more open than Pikermi, as indicated by the presence of many grazing Hipparionini horses and the absence of fruit and leaf browsing primate *Mesopithecus pentelicus* (Solounias et al. 2010).

The palaeoecological traits of the two Late Miocene hornless rhinocerotids of the Eastern Mediterranean are indicative of the two genera's different habitats and ecological niches. *Chilotherium*, originally a forest-dwelling animal in the beginning of the Miocene, gradually adapted to the increasingly more open, warmer, and less humid habitats of the Late Miocene (Deng et al. 2010, Biasatti et al. 2018). It is considered to have been a selective feeder, whose highly specialized diet, consisted mainly of C_3 grasses and lacked seasonal variability (Biasatti et al. 2018). Additionally, the genus's specialized hypsodontic dentition and shortened limbs have been interpreted as adaptations in order to access low vegetation, since its neck lacked the range of vertical motions that characterizes extant grazing rhinoceroses (Heissig 1989). Another

noteworthy characteristic was the intense phyletic dimorphism of the genus, mainly expressed by the enlarged tusks of the male individuals, used for sexual domination (Chen et al. 2010).

As far as the tandem-horned genera are concerned, *Miodiceros neumayri* was a hypsodont species, with a dentition closer to extant browsing African black rhino *Diceros bicornis* than the highly specialized, true grazer, Asian white rhino *Ceratotherium simum* (Heissig 1975, Geraads 1988, Giaourtsakis 2009). During the Late Miocene, this species underwent a series of evolutionary adaptations for surviving

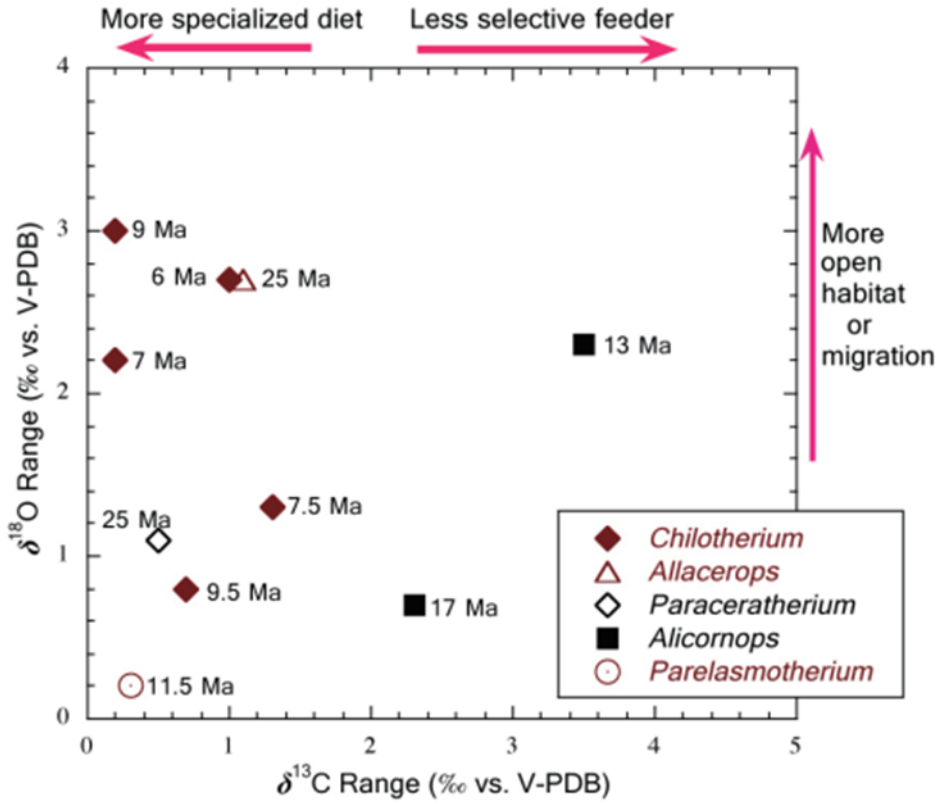

Fig. 24: δ13C range versus δ18O range for rhino individuals of particular genera, including *Chilotherium*, at given geologic ages. From Biasatti et al. (2018).

more open and arid habitats, including a gradual increase in body size and postcranial skeleton robustness and a horizontal elongation and vertical shortening of the skull (Heissig 1975, Giaourtsakis 2009). Thanks to these, the species managed to adapt in the harsh environmental changes of the Late Miocene, surviving on the scarce available food. Although not a true grazer, it could be characterized as a mixed feeder, more adapted to consuming hard, low bush vegetation than grass (Heissig 1999, Giaourtsakis et al. 2006).

Nonetheless, *Dihoplus pikermiensis* is considered a less specialized species, sharing certain features with primitive extant rhino *Dicerorhinus sumatrensis* (Giaourtsakis 2003). It lacks the hypsodont dentition of *M. neumayri* and bears slenderer metapodials (Giaourtsakis et al. 2006, Svorligkou et al. 2018). It can be safely deduced that low-crowned *D. pikermiensis* was a true, selective browser, favoring closed, forested habitats and lacking the craniodental specializations of *Miodiceros neumayri* (Giaourtsakis et al. 2006, Geraads & Spassov 2009).

The interspecific variation previously described may be attributed to the different ecological niches exploited by each species: plesiomorphic, brachydont species *Dihoplus pikermiensis* and *Acerorhinus neleus* favoured more closed and temperate habitats, such as those of Pikermi. Conversely, robust, specialized *Miodiceros neumayri* and *Chilotherium schlosseri* occupied the open, arid niches of more eastern localities of the Mediterranean, including Samos Island and numerous Anatolian sites. Their sympatric presence on the aforementioned localities was probably made possible due to environmentally controlled provincial variations among the species, along with minor dietary competition (Giaourtsakis et al. 2006, Giaourtsakis 2009, Athanassiou et al. 2014).The most noteworthy feature of the studied material is that the majority of craniodental material belongs to *C. schlosseri*, with the two typical tandem-horned Late Miocene rhinocerotids *M. neumayri* and *D. pikermiensis* also represented. However, the material studied in the scope of this thesis is too scarce for any clear conclusion on the interspecific dominance to be drawn.

Although the stratigraphic correlation of the material under study is both problematic and beyond the scope of this work, the different matrix that enclosed the fossils could be indicative of two different fossiliferous horizons, one characterized by the coexistence of *M. neumayri* and *C. schlosseri* and the other characterized by the dominance of *M. neumayri* over *D. pikermiensis*, with *C. schlosseri* being the most abundant species of the thre. Since the two dominant species are generally characterized as robust, specialized grazers, their coexistence could indicate a more open and arid environment for the Late Miocene of Samos, in accordance with the general conclusions found in the literature.

However, the AMPG collection still includes a large number of postcranial rhinocerotid material from the island. A thorough examination of these specimens, along with a detailed stratigraphic correlation, could indeed provide a clearer insight on the palaeoecology and biostratigraphy of the Samian rhinoceroses.

5. Conclusions

The excavation led by T. Skoufos in Samos Island in 1903 brought to light numerous fossils of Late Miocene vertebrates, now stored in the AMPG Collection. This study of the collection's craniodental rhinocerotid elements has validated the presence of three representatives of the Rhinocerotidae family on the island during the Late Miocene: tandem-horned species *M. neumayri* and *D. pikermiensis* and hornless species *C. schlosseri*.

The coexistence of the two tandem-horned genera with a hornless genus (either *Chilotherium* or *Acerorhinus*) is well established in the Turolian of the Greco-Iranian or Sub-Paratethyan Zoobiogeographic Province, based on faunal data from localities such as Pikermi, Attica and Kerassia, Euboea Island. On the other hand, the Vallesian locality Pentalophos, Chalkidiki, remains the sole Greek site where *Acerorhinus* and *Chilotherium* are found sympatric, along with *M. neumayri.*

In the case of Samos, a large part of the craniodental rhinocerotid material of the AMPG collection is attributed to *C. schlosseri*, whereas a relatively smaller number belongs to either *M. neumayri* or *D. pikermiensis.* As a consequence, no conclusion can be drawn on the interspecific dominance of the tandem-horned rhinocerotids. The two distinct types of fossil matrix observed may indicate that the material originated from at least two different fossiliferous horizons of the Mytilinii Formation. Yet, due to the lack of any detailed information about the excavations, it is impossible to correlate the material to any specific fossiliferous horizons.

It can be deduced that all three species, during at least one faunal stage, coexisted in the island. This can be further supported by the different palaeoceological niches of the three rhinocerotids: *M. neumayri* can be interpreted as a mixed feeder, adapted to consuming large quantities of hard, low bush, as a response to the increasingly more open and arid habitats of the Late Miocene; *D. pikermiensis* is considered a less specialized selective browser, occupying closed and forested habitats. Finally, *C. schlosseri,* can be intepreted as a selective feeder, with a highly specialized diet, consisting mainly of C_3 grasses and lacking seasonal variability. Due to these variations in their feeding and habitats, it is safe to assume that, when sympatric, the three species occupied different and independent palaeoecological niches. Furthermore, the marked presence of *C. schlosseri* is indicative of a more arid and open habitat in Samos during

the Late Miocene, somewhat more similar to that of Anatolia, rather than the more forested and humid habitats of Pikermi and Kerassia. However, a more extensive study of the material, including the numerous postcranial specimens stored at the AMPG Collection, shall provide a clearer view of the paleoenvironment of Samos Island during the Late Miocene. Finally, a mineralogical study of the fossil matrix, as well as a comparison with well-calibrated material from the various fossiliferous horizons of the Mytilinii Formation, could prove extremely useful for shedding light to the biostratigraphy of fossil rhinocerotids in Samos Island.

Literature

Alther, R., H. Kreuzer, I. Wendt, H. Lenz, G.A. Wagner, J. Keller, W. Harre and A. Hohndorf. 1982. A late Oligocene-early Miocene high temperature belt in the Attic-Cycladic Crystalline Complex (SE Pelagonian, Greece). Geologisches Jahrbuch 23:97–164.

Andrée, J. 1921. Rhinocerotiden aus dem Unterpliocän von Samos. Paläontologische Zeitschrift 20:189-212.

Andrée, J. 1926. Neue Cavicornier aus dem Pliocän von Samos. Palaeontographica 65:135-175.

Antoine, P. O. 2000. Origine et differenciation des Elasmotheriina parmi les Rhinocerotidae (Mammalia, Perissodactyla): Analyse cladistique et implications biostratigraphiques et paléobiogéographiques – Ph.D. Thesis, Muséum National d'Histoire Naturelle, Paris.

Antoine, P. O. and G. Saraç. 2005. Rhinocerotidae (Mammalia, Perissodactyla) from the late Miocene of Akkaşdağı, Turkey. — [in:] S. Sen (ed.), Geology, mammals and environments at Akkaşdağı, late Miocene of Central Anatolia. Geodiversitas 27(4):601–632.

Antoine, P. O., K. F. Downing, J. Y. Crochet, F. Duranthon, L. J. Flynn, L. Marivaux, G. Métais, A. R. Rajpar and G. Roohi. 2010. A revision of Aceratherium blanfordi Lydekker, 1884 (Mammalia: Rhinocerotidae) from the early Miocene of Pakistan: postcranials as a key. Zoological Journal of the Linnean Society 160(1):139-194.

Athanassiou, A., S. J. Roussiakis, I. X. Giaourtsakis, G. E. Theodorou and G. Iliopoulos. 2014. A new hornless rhinoceros of the genus Acerorhinus (Perissodactyla: Rhinocerotidae) from the Upper Miocene of Kerassiá (Euboea,

Greece), with a revision of related forms. Palaeontographica, Abteilung A: Palaeozoology – Stratigraphy 303(1-3):23-59.

Ballatore, M., G. Merceron and M. Breda. 2017. Inferences on the diet of fossil European rhinoceroses: Palaeoecological inferences from the dental material of Pliocene to Early Pleistocene European rhinoceroses. LAP Lambert Academic Publishing, Germany, 73 pp.

Bernor, R. L. 1984. A zoogeographic theater and biochronologic play: The time/biofacies phenomena of Eurasian and African Miocene mammal provinces. Paleobiologie Continentale 14:121-142.

Biasatti, D., Y. Wang and T. Deng. 2018. Paleoecology of Cenozoic rhinos from Northwest China: a stable isotope perspective. Vertebrata Palasiatica 56(1):45-68.

Black, C. C., L. Krishtalka and N. Solounias. 1980. Mammalian fossils of Samos and Pikermi. Part 1. The Turolian rodents and insectivores of Samos. Annals of Carnegie Museum, 49:359-378.

Bonis, L. de, G. Bouvrain, D. Geraads and G. D. Koufos. 1992. Diversity and paleoecology of Greek late Miocene mammalian faunas. Palaeogeography, Palaeoclimatology, Palaeoecology 91:99-121.

Bonis L. de, G. Bouvrain, D. Geraads, G. D. Koufos, S. Sen and P. Tassy. 1994. Les gisements de mammiféres du Miocéne supérieur de Kemiklitepe (Turquie). 11. Biochronologie, paléoécologie et relations paléobiogeographiques. Bulletin Museum Nationale Histoire Naturelle Paris 16:225–240.

Brown, B. 1927. Samos-Romantic Island of the Aegean. Natural History 27:19-32, New York.

Bukhsianidze, M. and K. Koiava. 2018. Synopsis of the terrestrial vertebrate faunas from the Middle Kura Basin (Eastern Georgia and Western Azerbaijan, South Caucasus). Acta Palaeontologica Polonica 63(3):441–461.

Cerdeño, E. 1996. Rhinocerotidae from the Middle Miocene of the Tung-gur Formation, Inner Mongolia (China). American Museum Novitates 3184:43-86.

Cerdeño, E. 1998. Diversity and evolutionary trends of the family Rhinocerotidae (Perissodactyla). Palaeogeography, Palaeoclimatology, Palaeoecology 141:13–34.

Chen, S., T. Deng, S. Hou, Q. Shi and L. Pang. 2010. Sexual dimorphism in perissodactyl rhinocerotid Chilotherium wimani from the late Miocene of the Linxia Basin (Gansu, China). Acta Palaeontologica Polonica 55(4):587-597.

Codrea, V. 1996. Miocene rhinoceroses from Romania: an overview. Acta Zoologica Cracoviana, 39:83-88.

Codrea, V. A., L. Ursachi, D. Bejan and C. Farcas. 2011. Early Late Miocene Chilotherium (Perissodactyla, Mammalia) from Pogana (Scythian Platform). North-Western Journal of Zoology 7(2):184-188.

Deng, T. 2006a. Neogene rhinoceroses of the Linxia Basin (Gansu, China). Courier Forschungsinstitut Senckenberg 256:43–56.

Deng, T. 2006b. A primitive species of Chilotherium (Perissodactyla, Rhinocerotidae) from the Late Miocene of the Linxia Basin (Gansu, China). Cenozoic Research 5(1-2):93-102.

Deng T. and Z. J. Tseng. 2010. Osteological evidence for predatory behaviour of the giant percrocutid (Dinocrocuta gigantea) as an active hunter. Chinese Science Bulletin 55:1790-1794.

Dinerstein E. 2011. Family Rhinocerotidae (Rhinoceroses) in Wilson D. E., Mittermeier R. A. [eds.] Handbook of the Mammals of the World. Barcelona: Lynx Edicions, 144–181.

Drevermann, F. 1930. Aus der Zeit des dreizehigen Pferdes. Natur und Museum 60 (1): 2-13.

Eronen, J. T., M. M. Ataabadi, A. Micheels, A. Karme, R. L. Bernor and M. Fortelius. 2009. Distribution history and climatic controls of the Late Miocene Pikermian chronofauna. Proceedings of the National Academy of Sciences of the United States of America 106(29):11867-11871.

Forsyth Major, C. 1888. Sur un gisement d'ossements fossiles dans l'île de Samos contemporains de l 'âge de Pikermi. Compte Rendus Hebdomadaire, Séances de la Société Géologique de France 107:1178-1181 [French].

Forsyth Major, C.I., 1891. Considérations nouvelles sur la faune de vertébrés du Miocène supérieur dans l'île de Samos. Comptes Rendus Sommaires Société Géologique de France 113:608–610 [French].

Forsyth Major, C. 1894. Le gisement ossifère de Mytilinii et catalogue d'ossements fossiles recueillis à Mitylini, île de Samos, et déposés au Collège Galliard, à Lausanne. Georges Bridel & Cie. Editeurs: 1-51. [French].

Fortelius, M. and N. Solounias. 2000. Functional characterization of ungulate molars using the abrasion-attrition wear gradient: a new method for reconstructing paleodiets. American Museum of Natural History Novitates 3301:1-36.

Fortelius, M., J. T. Eronen, J. Jernvall, L. Liu, D. Pushkina, J. Rinne, A. Tesakov, I. Vislobokova, Z. Zhang and L. Zhou. 2002. Fossil mammals resolve regional patterns of Eurasian climate change over 20 million years. Evolutionary Ecology Research 4(7):1005-1016.

Fortelius, M., K. Heissig, G. Saraç, and S. Sen. 2003. Rhinocerotidae (Perissodactyla); pp 282-307 in M. Fortelius, J. Kappelman, S. Sen and R. L. Bernor (eds.), Geology and paleontology of the Miocene Sinap Formation, Turkey. Columbia University Press, New York.

Fytikas, M., P. Innocenti, R. Mazzuoli, A. Peccerino, L. Villiari. 1984. Tertiary to Quaternary evolution of volcanism in the Aegean region. Geological Society of London Special Publication 17:687–699.

Gaudry, A. 1862. Animaux fossiles et géologie de l'Attique: d'après les recherches faites en 1855-56 et en 1860 sous les auspices de l'Académie des Sciences. Vol. 1. Savy, Paris [French].

Geraads, D. 1988. Révision des Rhinocerotinae (Mammalia) du Turolien de Pikermi. Comparaison avec les formes voisins. Annales de Paléontologie 74: 13-41 [French].

Geraads, D. and G. D. Koufos. 1990. Upper Miocene Rhinocerotidae (Mammalia) from Pentalophos-1, Macedonia, Greece. Palaeontographica Abteilung A: Palaeozoology-Stratigraphy 210(4-6):151.

Geraads, D. and N. Spassov. 2009. Rhinocerotidae (Mammalia) from the Late Miocene of Bulgaria. Palaeontographica 287:99–122.

Geraads, D., E. Cerdeño, D. G. Fernandez, L. Pandolfi, E. Billia, A. Athanassiou, E. Albayrak, V. Codrea, T. Obada, T. Deng, H. Tong, X. Lu, Š. Pícha, A. Marciszak, G. Jovanovic, D. Becker, J. Zervanova, Y. Chaïd Saoudi, A.-M. Bacon, N. Sévêque, R. Patnaik, J. Brezina, N. Spassov, A. Uzunidis. 2020. A database of Old World Neogene and quaternary rhino-bearing localities. http://www.rhinoresourcecenter.com/about/fossil-rhino-database.php

Gessner, K. 2000. Eocene nappe tectonics and late Alpine extension in the central Anatolide belt, western Turkey – structure, kinematics and deformation history. PhD thesis, University of Mainz, Germany.

Giaourtsakis, I. X. 2003. Late Neogene Rhinocerotidae of Greece: distribution, diversity and stratigraphical range. Distribution and migration of tertiary mammals in Eurasia; A volume in honour of Hans de Bruijn. Deinsea 10:235–253.

Giaourtsakis, I. X. 2009. The Late Miocene Mammal faunas of the Mytilinii Basin, Samos Island, Greece: New Collection. 9. Rhinocerotidae. Beitrag Palaontologie 31:157–187.

Giaourtsakis, I. X. 2021. The Fossil Record of Rhinocerotids (Mammalia: Perissodactyla: Rhinocerotidae) in Greece in E. Vlachos (ed.): The fossil vertebrates of Greece Vol. 2: Laurasiatherians, artiodactyles, perissodactyles, carnivorans and island endemics. Springer – Nature Publishing Group, Cham. https://doi.org/10.1007/978-3-030-68442-6.

Giaourtsakis, I. X., C. Pehlevan and Y. Haile-Selassie. 2009. Rhinocerotidae, pp. 429-468 in Y. Haile-Selassie and G. Woldergabriel (eds.) Ardipithecus kadabba: Late Miocene Evidence from the Middle Awash, Ethiopia, The Middle Awash Series, Volume 2, University of California Press Berkeley and Los Angeles, California University.

Giaourtsakis, I., G. Svorligkou and S. Roussiakis. 2018. A juvenile skull of the hornless rhinocerotid Acerorhinus neleus (Rhinocerotidae, Mammalia) from the Late Miocene locality of Pikermi (Attica, Greece). The Palaeontological Association, 62nd Annual Meeting, 14-17 December 2018, Bristol, UK. Abstract Book, pp. 81.

Giaourtsakis, I. X., G. Theodorou, S. Roussiakis, A. Athanassiou and G. Iliopoulos. 2006. Late Miocene horned rhinoceroses (Rhinocerotinae, Mammalia) from Kerassia (Euboea, Greece). Neues Jahrbuch fur Geologie und Palaontologie Abhandlungen A 239:367–398.

Giaourtsakis, I., P. Kampouridis, S. Roussiakis, G. Svorligkou, N. Kargopoulos, E. Alifieri and G. Theodorou. 2020. Diversity assessment of the family Rhinocerotidae (Mammalia, Perissodactyla) at the Late Miocene locality of Kerassia (Euboea Island, Greece). 2nd Palaeontological Virtual Congress, May 1–15 2020.

Grine, F. E. 1977. Analysis of early hominid deciduous molar wear by scanning electron microscopy: a preliminary report. Proceedings of the Electron Microscopy, Society of South Africa 7:157–158.

Groves, C. P. 1983. Phylogeny of the living species of rhinoceros. Journal of Zoological Systematics and Evolution 21:293–313.

Guérin, C. 1980. Les rhinoceros (Mammalia, Perissodactyla) du Miocene terminal au Pleistocene superieur en Europe occidentale. Comparaison avec les especes actuelles. Documents des Laboratoires de Géologie de la Faculté des Sciences de Lyon 79: 1-1185 [French].

Heissig, K. 1975. Rhinocerotidae (Mammalia) aus dem jungtertiar Anatoliens. Neues Jahrbuch für Geologie und Paläontologie 15:145–151 [German].

Heissig, K., 1981. Probleme bei der cladistischen Analyse einer Gruppe mit wenigen eindeutigen Apomorphien: Rhinocerotidae. Paläontologische Zeitschrift, 55:117–123 [German].

Heissig, K., 1989. The Rhinocerotidae; pp 399-417 in D. R. Prothero and R. M. Schoch, (eds.), The evolution of Perissodactyls. Oxford Monographs on Geology and Geophysics 15, Oxfordshire, UK.

Heissig, K. 1996. The stratigraphical range of fossil rhinoceroses in the Late Neogene of Europe and Eastern Mediterranean, pp. 339-347; in R. L. Bernor, V. Fahlbush, and H.-W. Mittman (eds.), The Evolution of Western Eurasian Neogene Mammal Faunas, Columbia University Press, New York.

Hsieh, H.-M., L.-H. Huang, L.-C. Tsai, Y.-C. Kuo, H.-H. Meng, A. Linacre and J. C.-I. Lee. 2003. Species identification of rhinoceros horns using the cytochrome b gene. Forensic Science International 136:1–11.

Hullot, M., P.-O. Antoine, M. Ballatore, and G. Merceron. 2019. Dental microwear textures and dietary preferences of extant rhinoceroses (Perissodactyla, Mammalia). Mammal Research 64(3):397-409.

Ioakim, C., Koufos, G. D. 2009. The Late Miocene Mammal Faunas of the Mytilinii Basin, Samos Island, Greece: New Collection 3. Palynology. Beitrag Palaontologie 31:27–35.

Kahlke, R.-D and T. M. Kaiser. 2011. Generalism as a subsistence strategy: advantages and limitations of the highly flexible feeding traits of Pleistocene Stephanorhinus hundsheimensis (Rhinocerotidae, Mammalia). Quaternary Science Reviews 30:2250–2261.

Kaiser, T. M. and G. Brinkmann. 2006. Measuring dental wear equilibriums—the use of industrial surface texture parameters to infer the diets of fossil mammals. Palaeogeography, Palaeoclimatology, Palaeoecology 239(3-4):221–240.

Kampouridis, P. 2020. Rhinocerotidae (Mammalia, Perissodactyla) from the Late Miocene of Staniantsi (Bulgaria). Master's Thesis. Eberhard-Karls University of Tübingen, 68 pp.

Kampouridis, P., G. Svorligkou, N. Kargopoulos, and F. J. Augustin. 2021. Reassessment of “Chilotherium wegneri” (Mammalia, Rhinocerotidae) from the late Miocene of Samos (Greece) and the European record of Chilotherium. Historical Biology. DOI:10.1080/08912963.2021.1920939.

Kampouridis, P., S. Roussiakis, N. Kargopoulos, I. Giaourtsakis, G. Dimakopoulos, G. Iliopoulos, G. Svorligkou and G. Theodorou. 2019. Faunal diversity at the Turolian locality of Kerassia (Northern Euboea, Greece). 15th International

Conference of the Geological Society of Greece, Bulletin of the Geological Society of Greece, Special Publications 7:64–65.

Kaya, T. 1994. Ceratotherium neumayri (Rhinocerotidae, Mammalia) in the Upper Miocene of Western Anatolia. Turkish Journal of Earth Sciences (3):13-22.

Kaya, T. and K. Heissig. 2001. Late Miocene rhinocerotids (Mammalia) from Yulafli (Corlu-Thrace/Turkey). Geobios 34 (4):457-467.

Khan, A. M., E. Cerdeño, M. A. Khan, M. Akhtar, and M. Ali. 2011. Chilotherium intermedium (Rhinocerotidae: Mammalia) from the Siwaliks of Pakistan: Systematic Implications. Pakistan Journal of Zoology 43(4):651-663.

Korotkevich, O. L. 1958a: On certain structural features of the limbs in the Sarmatian Chilotherium. Dopovidi Akad. Nauk Ukrainskoi RSR 4:467-470 [Ukrainian].

Korotkevich, O. L. 1958b: A new Chilotherium species from the Sarmatian deposits of the Ukraine. Dopovidi Akad. Nauk Ukrainskoi RSR 12:1372-1376 [Ukrainian].

Korotkevich E. L. 1970: The mammals of the Berislav late Sarmatian hipparion-fauna, in The Natural Environment and the fauna of the past. - Naukova Dumka, Kiev, 5:24-121[Ukrainian].

Kostopoulos, D. S 2009. The Pikermian Event: temporal and spatial resolution of the Turolian large mammal fauna in SE Europe. Palaeogeography, Palaeoclimatology, Palaeoecology 274(1-2): 82-95.

Kostopoulos, D. S. 2021. The fossil record of bovids (Mammalia: Artiodactyla: Ruminantia: Pecora: Bovidae) in Greece in E.Vlachos (ed.): The fossil vertebrates of Greece Vol. 2: Laurasiatherians, artiodactyles, perissodactyles, carnivorans and island endemics. Springer – Nature Publishing Group, Cham. https://doi.org/10.1007/978-3-030-68442-6.

Kostopoulos, D. S., S. Sen and G. D. Koufos. 2003. Magnetostratigraphy and revised chronology of the late Miocene mammal localities of Samos, Greece. International Journal of Earth Sciences 92:779-794.

Kostopoulos, D. S., G. D. Koufos, I. A. Sylvestrou, G. E. Syrides and E. Tsombachidou. 2009. The Late Miocene Mammal Faunas of the Mytilinii Basin, Samos Island, Greece: New Collection. 2. Lithostratigraphy and Fossiliferous Sites. Beitrag Paläontologie 31:13-26.

Koufos, G. D. 2009. The Late Miocene Mammal Faunas of the Mytilinii Basin, Samos Island, Greece: New Collection. 1. History of the Samos Fossil Mammals. Beitrag Paläontologie 31:1-12.

Koufos, G. D., D. S. Kostopoulos and T. D. Vlachou. 2009a. The Late Miocene Mammal Faunas of the Mytilinii Basin, Samos Island, Greece: New Collection. 16. Biochronology. Beitrag Paläontologie 31:397–408.

Koufos, G. D., D. S. Kostopoulos and G. Merceron. 2009b. The Late Miocene mammal faunas of the Mytilinii Basin, Samos Island, Greece: New collection 17. Palaeoecology-Palaeobiogeography. Beitrag Palaontologie 31:409-430.

Koufos, G. D., D. S. Kostopoulos, T. D. Vlachou and G. E. Konidaris. 2009c. The Late Miocene mammal fauna of Samos, Greece. History, Stratigraphy and Localities. 13th Congress RCMNS-2nd-6th September 2009, Naples, Italy, 2-6 September 2009, Acta Naturalia de l'Ateneo Parmense 45:289-290.

Koufos, G. D., D. S. Kostopoulos, T. D. Vlachou, and G. E. Konidaris. 2011. A synopsis of the late Miocene Mammal Fauna of Samos Island, Aegean Sea, Greece. Geobios 44:237–251.

Loose, H. 1975. Pleistocene Rhinocerotidae of W. Europe with reference to the recent two-horned species of Africa and S.E. Asia. Scripta Geologica 33:1–59.

Lu, X. 2013. A juvenile skull of Acerorhinus yuanmouensis (Mammalia: Rhinocerotidae) from the Late Miocene hominoid fauna of the Yuanmou Basin (Yunnan, China). Geobios 46:539-548.

Lydekker, R. 1890. A new mammalian fauna. Nature 43:85-87.

Mayor, A. 2000a. The 'Monster of Troy'vase: the earliest artistic record ofa vertebrate fossil discovery? Oxford Journal of Archaeology 19(1):57-63.

Mayor, A. 2000b. The first fossil hunters: Paleontology in Greek and Roman times. Princeton University Press, Princeton, New Jersey, 361 pp.

Melentis, J. K. 1968. Palaeontological excavations at Samos Island (preliminary report). Proceedings of the Academy of Athens 43:344-349 [Greek].

Morales, J. C. and D. J, Melnick. 1994. Molecular systematics of the living rhinoceros. Molecular Phylogenetics and Evolution 3(2):128-134.

Merceron, G. 2003. Une nouvelle méthodologie pour la quantification de la micro-usure dentaire: application á l'hominoıde fossile Ouranopithecus macedoniensis (Miocene, Grece). Bulletins et Mémoires de la Société d'Anthropologie de Paris 15:300–310 [French].

Merceron, G., C. Blondel, M. Brunet, S. Sen, N. Solounias, L. Viriot and E. Heintz. 2004. The Late Miocene paleoenvironment of Afghanistan as inferred from dental microwear in artiodactyls. Palaeogeography, Palaeoclimatology, Palaeoecology 207(1-4):143-163.

Merceron, G., C. Blondel, L. de Bonis, G. D. Koufos and L. Viriot. 2005. A new method of dental microwear analysis: application to extant primates and Ouranopithecus macedoniensis (Late Miocene of Greece). Palaios 20 (6):551-561.

Mihlbacher, M. and N. Solounias. 2006. Coevolution of tooth crown height and diet in oreodonts (Merycoidodontidae, Artiodactyla) examined with phylogenetically independent contrasts. Journal of Mammalian Evolution 13(1):11-36.

Mihlbacher, M. C., F. Rivals, N. Solounias and G. M. Semprebon. 2011. Dietary change and evolution of horses in North America. Science 331:1178.

Mihlbacher, M. C., D. Campbell, M. Ayoub, C. Chen and I. Ghani. 2018. Microwear–mesowear congruence and mortality bias in rhinoceros' mass-death assemblages. Paleobiology 44:131–154.

Miguel, D. de, M. Fortelius, B. Azanza and J. Morales. 2008. Ancestral feeding state of ruminants reconsidered: earliest grazing adaptation claims a mixed condition for Cervidae. BioMed Central Evolutionary Biology 8(1):1-13.

Mporonkay, K.A., 1995. Geotectonic evolution of Cycladic Islands. PhD Thesis, University of Patras, 193 pp. [Greek].

Mountrakis, D., A. Kilias, E. Vavliakis A. Psilovikos and E. Thomaidou. 2003. Neotectonic map of Samos Island (Aegean Sea, Greece): Implication of geographical information systems in the geological mapping. 4th European Congress on Regional Geoscientific Cartography and Information Systems, Bologna, Italy. Proceedings Volume 1:11–13.

Niezabitowski E. L. 1913. Über das Schädelfragment eines Rhinocerotiden (Teleoceras ponticus Niez.) von Odessa. Bulletin International De I'Academie Des Sciences De Cracovie, Series B.:223–235.

Papanikolaou, D. 1979. Unites tectoniques et phases de deformation dans l'ile de Samos, Mer Egee, Grece. Bulletin de la Societe Geologique de France 19:745-752.

Pavlow, M. 1913-14. Mammifères Tertiaires de la Nouvelle Russie. Nouveaux Mémoires de la Société Impériale des Naturalistes du Moscou, 1ère partie. 17(3):1-67. 2ème partie. 17(4):1-52 [French].

Piccoli, G., F. Franco, O. Bertolotti, M. Bimbatti, P. Buja, L. Cesga and M. Gradenico. 1975. I resti di mammiferi del Neogene di Samos e Pikermi (Grecia) conservationel museo geologico e paleontologico dell' universita di Padova. Memorie degli Istituti di Geologia e Mineralogia dell' Universita di Padova 31:1-39 [Italian].

Peppe, D. J. and A. L. Deino. 2013. Dating Rocks and Fossils Using Geologic Methods. Nature Education Knowledge 4(10):1.

Prothero, D. R. and R. M. Schoch. 2002. Horns, tusks and flippers: The evolution of hoofed mammals. The Johns Hopkins University Press, Charles Village, Baltimore, 384 pp.

Pocock, R. I. 1945. Some cranial and dental characters of the existing species of Asiatic rhinoceroses. Proceedings of the Zoological Society of London 114:437–450.

Ring, U., K. Gessner, T. Gungor, and C. W. Passchier. 1999a. The Menderes Massif of western Turkey and the Cycladic Massif in the Aegean: Do they really correlate? Journal of the Geological Society of London 156:3–6.

Ring, U., S. Laws, and M. Bernett. 1999b. Structural analysis of a complex nappe sequence and lateorogenic basins from the Aegean Island of Samos, Greece. Journal of Structural Geology 21:1575–1601.

Rivals, F., N. Solounias and M. Mihlbacher. 2007. Evidence for geographic variation in the diets of late Pleistocene and early Holocene Bison in North America, and differences from the diets of recent Bison. Quaternary Research 68(3):338-346.

Schlosser, M. 1904. Die fossilen Cavicornia von Samos. Beiträge zur Paläontologie Österreich-Ungarns 17:21-118.

Schulz, E., I. Calandra and T. M. Kaiser. 2013. Feeding ecology and chewing mechanics in hoofed mammals: 3D tribology of enamel wear. Wear 300(1-2):169-179.

Simpson, G. G. 1945. The principles of classification and a classification of mammals. Bulletin of the American Museum of Natural History 85:1-350.

Sen, S. and J. P. Valet. 1986. Magnetostratigraphy of the late Miocene deposits in Samos, Greece. Earth and Planetary Science Letters 80:167-174.

Solounias, N. 1981. The Turolian fauna from the island of Samos, Greece. Contribution on Vertebrate Evolution 6:1-232.

Solounias, N. and U. Ring. 2007. Ancient history of the Samos fossils and the record of earthquakes. Journal of the Virtual Explorer 28(3).

Solounias, N. and G. Semprebon. 2002. Advances in the reconstruction of ungulate ecomorphology with application to early fossil equids. American Museum Novitates 3366:1-49.

Spassov, N., T. Tzankov and D. Geraads. 2006. Late Neogene stratigraphy, biochronology, faunal diversity and environments of South-West Bulgaria (Struma River Valley). Geodiversitas 28(3):477-498.

Spassov, N., D. Geraads, L.Hristova and G. N. Markov. 2019. The Late Miocene mammal fauna from Gorna Sushitsa, southwestern Bulgaria, and the early/middle Turolian transition. Neues Jahrbuch für Geologie und Paläontologie-Abhandlungen 291(3): 317-350.

Spassov, N., D. Geraads, L. Hristova, G. N. Markov, B. Garevska and R. Garevski. 2018. The Late Miocene mammal faunas of the Republic of Macedonia (FYROM). Palaeontographica Abtlung. A: Palaeozoology-Stratigraphy 311(1-6):1-85.

Stefani, C. de and C. I. Forsyth-Major. 1892. Samos. Étude géologique, paléontologique et botanique. G. Bridel, 1892.

Strömberg, C. A. E., L. Werdelin, E. M. Friis and G. Saraç. 2007. The spread of grass-dominated habitats in Turkey and surrounding areas during the Cenozoic: Phytolith evidence. Palaeogeography, Palaeoclimatology, Palaeoecology 250(1-4):18-49.

Svorligkou, G., I. Giaourtsakis and S. Roussiakis. 2019. New material of the hornless rhinocerotid Chilotherium (Mammalia, Perissodactyla) from the Turolian fauna of Samos Island, Greece. 15th International Conference of the Geological Society of Greece, Bulletin of the Geological Society of Greece, Special Publications 7:64-65.

Taylor, L. A., T. M. Kaiser, C. Schwitzer, D. W. H. Muller, D. Codron, M. Clauss and E. Schulz. 2013. Detecting inter-cusp and inter-tooth wear patterns in rhinocerotids. PLoS ONE 8(12):e80921.

Theodoropoulos, D., 1979. Samos Island, geological map 1:50.000 with explanations. Institute for Geological Mining Research, Athens.

Tougard, C., T. Delefosse, C. Hanni and C. Montgelard. 2001. Phylogenetic Relationships of the Five Extant Rhinoceros Species (Rhinocerotidae, Perissodactyla) Based on Mitochondrial Cytochrome b and 12S rRNA Genes. Molecular Phylogenetics and Evolution 19(1):34–44.

Tsombachidou, E., 1999. Stratigraphy and sedimentology of the Mytilinii basin, Samos. Master Thesis, Aristotle University of Thessaloniki, Department of Geology, 95 pp. [Greek].

Tsoukala, E. 2018. Rhinocerotidae from the Late Miocene and Late Pliocene of Macedonia, Greece. A revision of the Neogene - Quaternary Rhinocerotidae of Greece. Revue de Paléobiologie 37(2):609-630.

Ungar, P. S., C. A. Brown, T. S. Bergstrom and A. Walker. 2003. Quantification of dental microwear by tandem scanning confocal microscopy and scale-sensitive fractal

analyses. Scanning: The Journal of Scanning Microscopies. https://doi.org/10.1002/sca.4950250405.

Van Asperen, E. N. and R.-D. Kahlke. 2015. Dietary variation and overlap in Central and Northwest European Stephanorhinus kirchbergensis and S. hemitoechus (Rhinocerotidae, Mammalia) influenced by habitat diversity. Quaternary Science Reviews 107(1):47-61.

Van Couvering, J. A. and J. A. Miller. 1971. Late Miocene and non-marine time scale in Europe. Nature 230:559-563.

Vangengeim, E. A. and A. S. Tesakov. 2008. Late Sarmatian Mammal Localities of the Eastern Paratethys: Stratigraphic Position, Magnetochronology, and Correlation with the European Continental Scale. Stratigraphy and Geological Correlation 16(1):92–103.

Viret, J. 1958. Perissodactyla, pp 368-475 in J. Piveteau (ed.), Traité de Paléontologie 4, Paris (Masson), France [French].

Vlachou, T. D. 2013. Palaeontology, Biochronology and Palaeoecology of the Greek hipparionine horses. PhD Thesis, Aristotle University of Thessaloniki, Department of Geology, 640 pp. [Greek].

Walker, A., H. N. Hoeck and L. Perez. 1978. Microwear of mammalian teeth as an indicator of diet. Science. https://doi.org/10.1126/science.684415.

Wang, H., B. Bai, J. Meng, Y. Wang. 2016. Earliest known unequivocal rhinocerotoid sheds new light on the origin of giant rhinos and phylogeny of early rhinocerotoids. Science Reports 6.

Weber, M., 1904. Über tertiäre Rhinocerotiden von der Insel Samos I. Bulletin de la Société Impériale des Naturalistes de Moscou, 17:477–501.

Weber, M., 1905. Über tertiäre Rhinocerotiden von der Insel Samos II. Bulletin de la Société Imperériale des Naturalistes de Moscou, 18:345–363.

Weidmann, M., N. Solounias, R. Drake, G. Curtis. 1984. Neogene stratigraphy of the eastern basin, Samos Island, Greece. Geobios 17:477-490.

Xafis, A., J. Saarinen, K. Bastl, D. Nagel and F. Grímsson. 2020. Palaeodietary traits of large mammals from the middle Miocene of Gračanica (Bugojno Basin, Bosnia-Herzegovina). Palaeobiodiversity and Palaeoenvironments 100:457-477.

Appendices

Appendix A: Measurements as illustrated by Made 2010

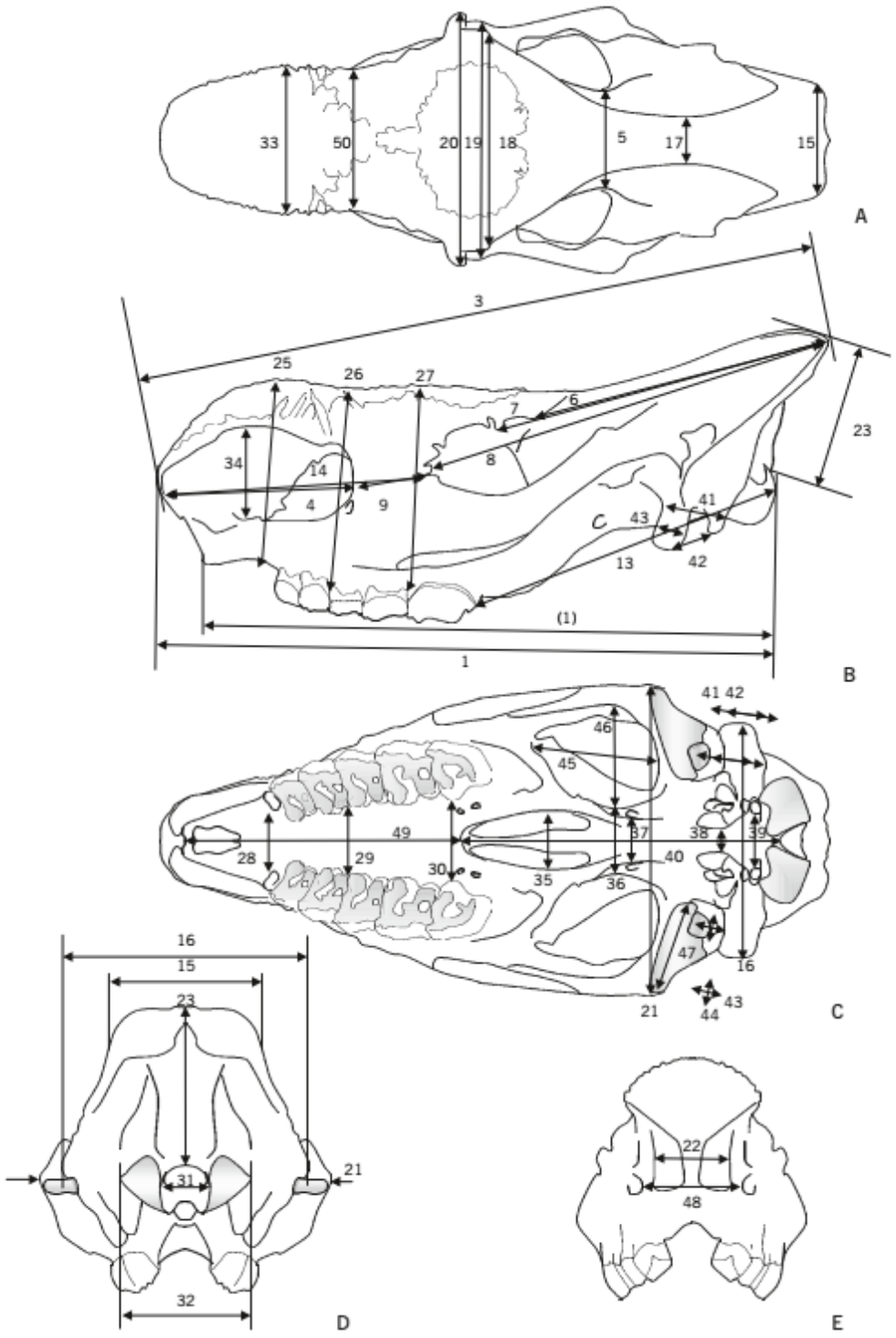

Fig. A1: The way of measuring the skull: A) dorsal view, B) left lateral view, C) inferior view, D) posterior view, E) anterior view.

1) Distance from the tip of the premaxillary to the posterior surface of the occipital condyles in rhinos where the nasal septum is not ossified, identical to measurement 2 in rhinos with an ossified nasal septum.

2) Distance from the tip of a nasal to the posterior surface of an occipital condyle on the same side.

3) Distance from the tip of nasals to the occiput.

4) Length of the nasalincisive notch.

5) Minimal width at the postorbital constriction.

6) Distance from the postorbital process to the occiput (cannot be taken if the postorbital process is not well developed).

7) Distance from the superorbital process to the occiput.

8) Distance from the preorbital process to the occiput.

9) Distance from the nasoincisive notch to the anterior rim of the orbit.

13) Distance from the posterior border of the M3 to the posterior end of the occipital condyle of the same side.

14) Distance from the tip of a nasal to the anterior border of the orbit.

15) Width of the occiput.

16) Width of the skull at the mastoid apophyses.

17) Minimal distance between the frontoparietal crests.

18) Width at the postorbital processes.

19) Width at the supraorbital processes.

20) Width at the preorbital processes.

21) Maximal width at the zygomatic arcs.

22) Width of the entrance of the nasal cavity.

23) Distance of the foramen magnum to the occipital crest.

25) Height of the skull just anterior to the P2, measured parallel to the medial plane.

26) Height of the skull above P4–M1, measured parallel to the medial plane.

27) Height of the skull above the M3, measured parallel to the medial plane.

28) Width of the palate, measured just anterior to the P2.

29) Width of the palate at the level of P4–M1.

30) Width of the palate, measured just anterior to the M3.

31) Width of the foramen magnum.

32) Width of the occipital condyles.

33) Width of the nasals.

34) Height of the nasal aperture.

35) Width of the choanae.

36) Minimal width of the skull in the area of the pterygoid process of the basisphenoid.

37) Distance between the caudal alar foramina.

38) Distance between the lacerum foramina.

39) Distance between the hypoglossal foramina.

40) Distance between the posterior limit of the palate and the foramen magnum.

41) Distance of the front of the retroarticular process to the back of the jugular process.

42) Distance of the tip of the retroarticular process to the tip of the jugular process.

43) DAP of the retroarticular process.

44) DT of the retroarticular process.

45) Length of the space medial to the zygomatic arc.

46) Width of the space medial to the zygomatic arc.

47) Width of the facet.

48) Distance between the infraorbital foramina.

49) Length of the palate measured in the median plane.

50) Minimal width of the nasals behind the area of origin of the nasal horn.

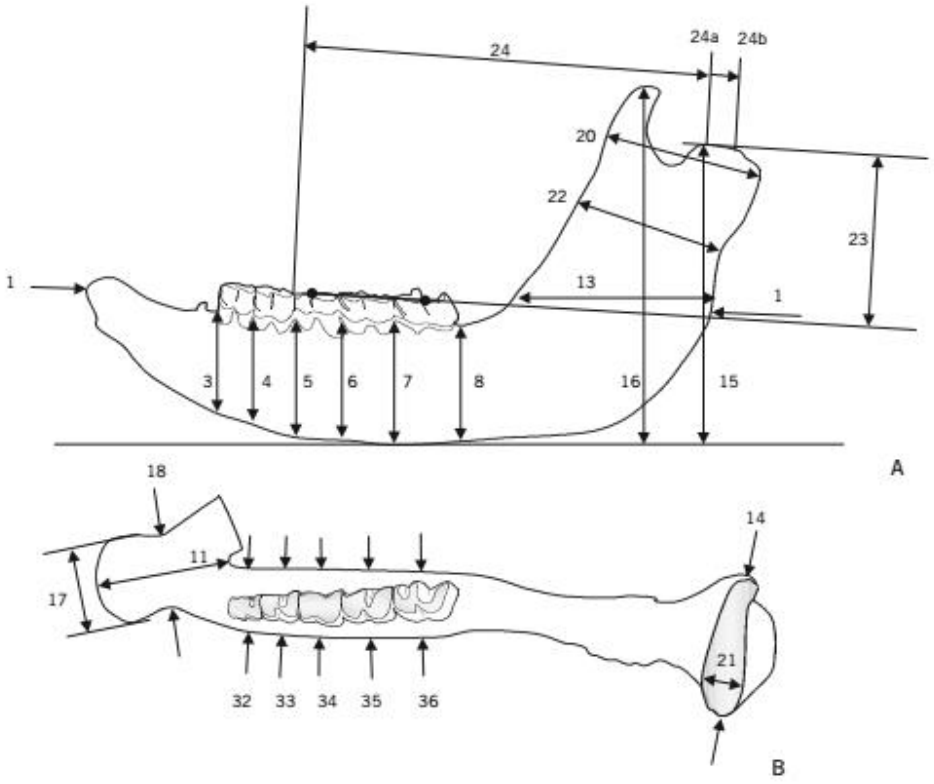

Fig. A2: The way of measuring the mandible: A) buccal view, B) occlusal view. Measurements 1–16 after Guérin (1980).

1) Length of the mandible.

2) Distance of back of symphysis to back of the mandible (not indicated in Guérin's Fig. 4g).

3–8) Depth of the mandible behind P2–M3, measured at the internal side of the mandible and perpendicular to the alveolar border (Guérin, Tab. 3), or at the buccal side and perpendicular to the length of the mandible (measurement 1) (Guérin 198o, Fig. 4g).

9–10) Width of the mandible behind P4 and M2. These values are very similar to the D values taken here and are not given separately

11) Length of the symphysis. Taken here in a similar way as indicated by Van der Made (1996).

12) Not indicated by Guérin (198o, Tab. 3,4g).

13) DAP ramus at occlusal level and parallel to it.

14) DT condyle.

15) Height of condyle above the lower border of the mandible. It should be taken into account that this measurement is subject to the way the mandible is

oriented and thus, may be more variable, especially if measurements taken by different persons are compared.

16) Height of coronoid process above the lower border of the mandible. See remark with measurement 15.

17) Maximal width of the anterior part of the mandible.

18) Minimal width symphyseal area at the place of waisting.

19) Height symphysis (see Van der Made 1996).

20) DAP of the ascending ramus at the level of the condyle.

21) Maximum DAP of the facet of the condyle.

22) Minimal DAP of ascending ramus at about half its height.

23) Height of the condyle above occlusal surface. The height is taken perpendicular to the line that that passes through the lowest points of the occlusal surface in the middle of M1 and M3 (indicated by dots).

24) Distance of the condyle (at its highest point a , or at its posterior border b) behind the front of the M1 and measured parallel to the line through the occlusal surface, described above.

25–30) D = depth of mandible at each cheek tooth: D(P2)... D(M3). It is taken at the lingual side of the mandible and is the shortest distance from the highest point of the mandible below the middle of a tooth to the lower border of the mandible (see Van der Made 1989; Van der Made 1996).

31–36) W = width of the mandible, at each cheek tooth: W(P2)... W(M3). It is taken perpendicular to D. D and W are comparable to measurements 3–1o by Guérin (198o), but are taken as defined by Van der Made (1989; 1996)for ruminants and suoids and are preferred here.

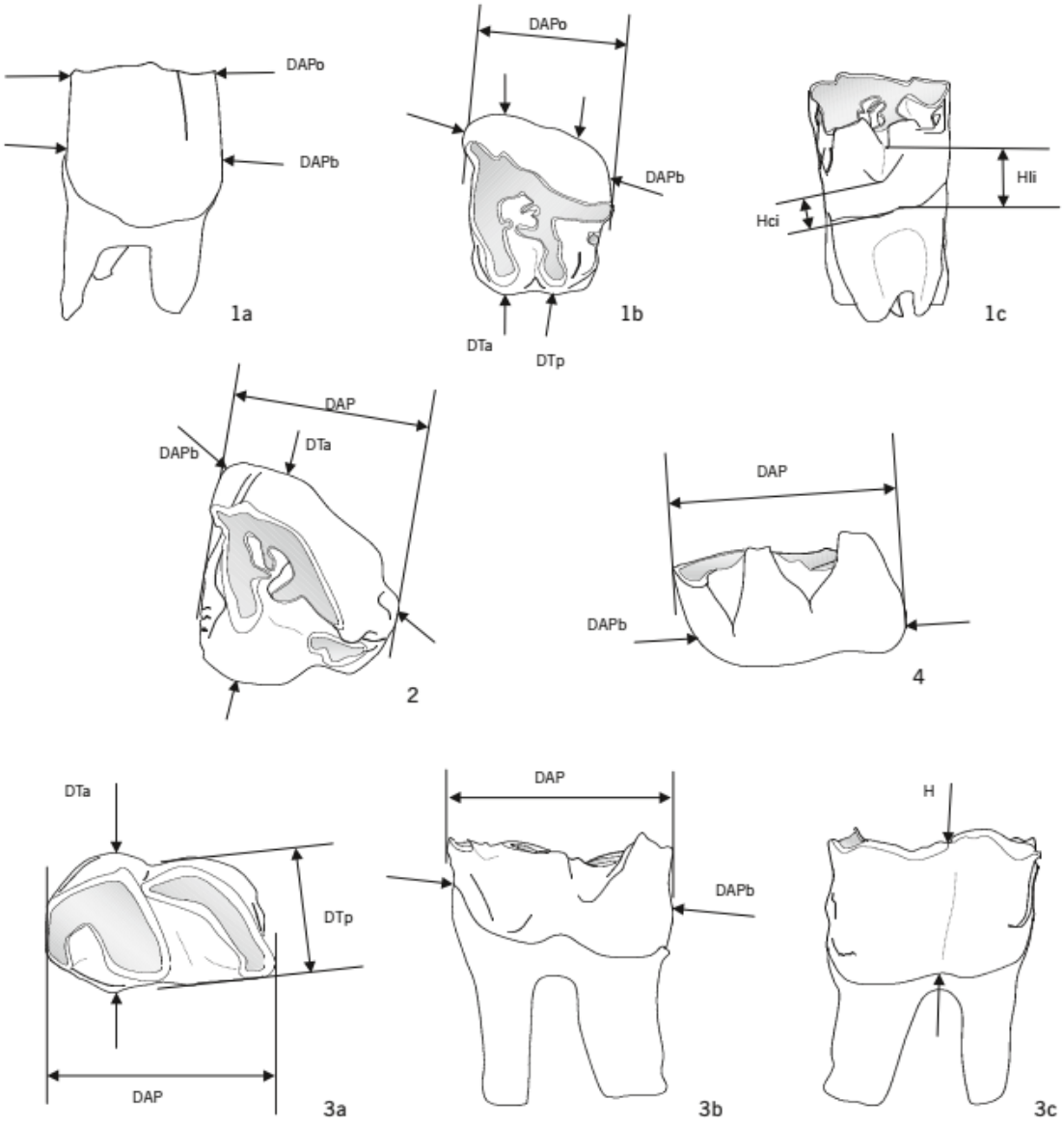

Fig. A3: The way of measuring the teeth. Given as examples: 1) P3, 2) M3, 3) M1 and 4) M3.

DAP = In the Px and M1–2 the maximum DAP measured on the buccal side, usually more or less equivalent to the occlusal DAP, though occasionally the anteriormost point may be a little below the occlusal surface. Compared to the other upper cheek teeth, the M3 has a different shape and in this case, the DAP is taken close to the base, at the level where the crown extends most posteriorly. In the M3, the measurement is perpendicular to the line through the anteriormost parts of the tooth in the middle and at the buccal side at the same level as the posterior measuring point. In the lower teeth, the DAP is the maximum length measured at the lingual side and parallel to the occlusal surface. Usually this will be more or less the occlusal length. In the M3, the basis of the tooth extends much more posteriorly than the occlusal surface. In such a case, the measurement is taken as indicated in Fig. 5, 4.

DTa = the maximum DT of the anterior lobe of the tooth.

DTp = the maximum DT of the posterior lobe of the tooth.

H = in the lower molars, the height of the tooth at the buccal side where the talonid and trigonid meet. It is measured as the distance between the uppermost point of the lower border of the crown and the point where the anterior wing of the hypoconid connects to the back of the protoconid. This measurement is possibly not the best indicator of the functional crown height, but is certainly a measurement that often can be taken, since it is taken at the last point of the upper part of the tooth to be affected by wear.

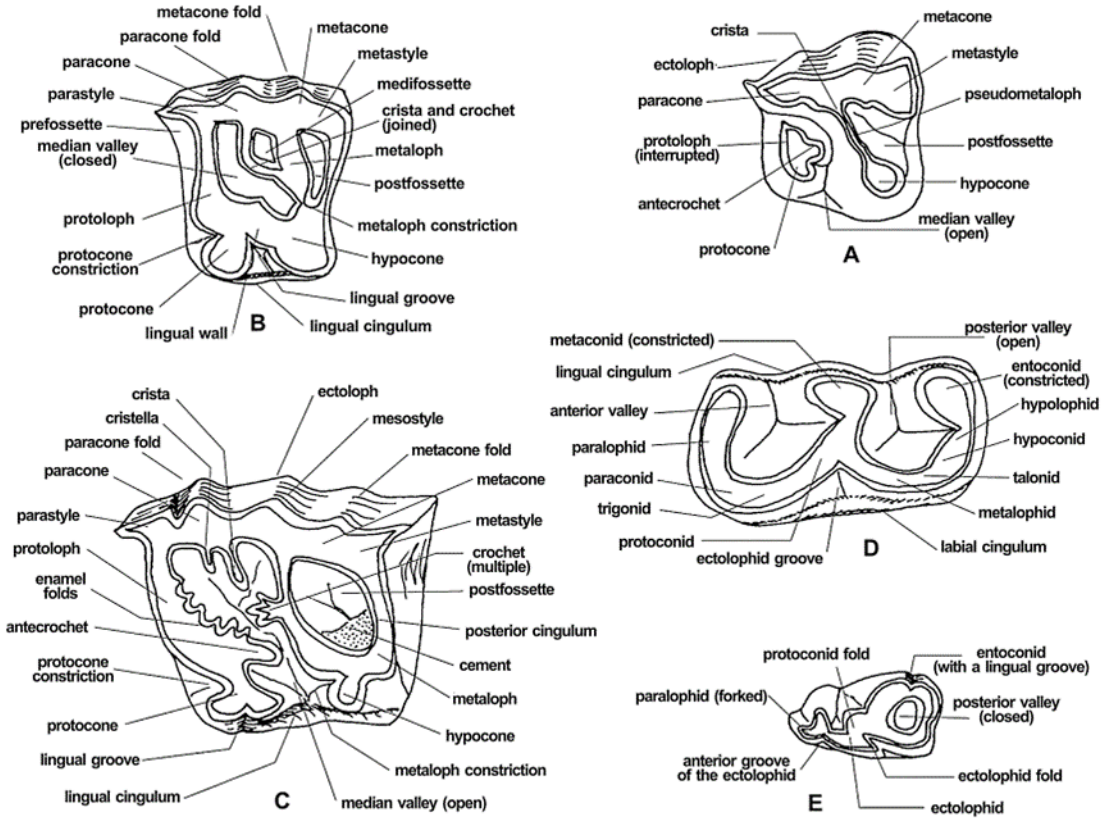

Fig. A4: Dental terminology used for rhinocerotids. A, left P2 (hypothetical); B, left P3 or P4 (hypothetical); C, left upper molar (hypothetical); D, left lower molar (hypothetical); E, left d2. From Antoine et al. 2010.

Appendix B: Measurements of the AMPG material

Code	AMPG-SAM505	AMPG-SAM506	AMPG-SAM503	AMPG-SAM515	AMPG-SAM508	AMPG-SAM509	AMPG-SAM513	AMPG-SAM511	AMPG-SAM510
Species	*C. schlosseri*	*C. schlosseri*	*C. schlosseri*	*C. schlosseri*	*C. schlosseri*	*C. schlosseri*	*C. schlosseri*	*C. schlosseri*	*C. schlosseri*
5	-	-	-	-	-	-	81.9	-	-
6	-	-	-	-	-	-	217.2	-	-
7	-	-	-	-	-	-	241.6	-	-
9	64.2	57.2	65	63.2	-	-	61.8	-	-
13	-	-	-	-	-	-	233.2	-	-
15	-	-	-	-	-	-	118.6	-	-
16	-	-	-	-	115.5	-	-	-	-
17	-	-	-	-	83.8	-	68.8	-	57.1
18	-	-	146.3	-	-	-	136.6	148.3	-
19	-	-	145.7	-	-	-	141.4	148.7	-
20	-	-	145.6	-	-	-	145.1	132	-
21	-	-	235.3	-	-	-	-	-	-
22	-	-	84.8	-	-	-	71.7	-	-
23	-	-	-	-	-	-	111.5	-	-
25	-	49.2	64.9	-	-	-	-	-	-
26	200.9	138	125.2	-	-	-	142.2	-	-
27	204.1	131.7	-	-	-	-	135.7	-	-
28	-	-	55.8	-	-	-	-	-	-
29	-	57.7	59.7	-	-	-	60.4	-	-
30	-	53.6	58.4	-	-	-	60.8	-	-
31	-	-	-	-	44	-	-	-	42.2
32	-	-	-	-	-	-	131.8	-	109.2
35	-	43.4	47.7	-	-	-	-	-	
37	-	-	-	-	-	-	73.6	-	
38	-	-	-	-	25.2	-	-	-	15.1
39	-	-	-	-	76.5	-	-	-	
40	-	-	-	-	-	-	194.2	-	
41	-	-	-	-	52.3	-	-	-	
42	-	-	-	-	35.9	-	-	-	
43	-	-	-	-	18.1	-	-	18.3	
44	-	-	-	-	18.8	-	-	14.1	
46	-	-	57.7	-	-	71.9	-	-	63.8
47	-	-	-	-	40.3	-	-	-	
48	-	-	83.7	-	-	-	77.8	-	

Table 4: Measurements of the adult skulls.

Code	AMPG-SAM506	AMPG-SAM515	AMPG-SAM513	Code	AMPG-SAM506	AMPG-SAM515	AMPG-SAM513
Species	*C. schlosseri*	*C. schlosseri*	*C. schlosseri*	Species	*C. schlosseri*	*C. schlosseri*	*C. schlosseri*
DAPL m3	38.9	-	-	**DAPR M3**	45.9	-	-
DAPL M2	55	-	-	**DAPR M2**	54.2	48.1	-
DAPL M1	45	-	-	**DAPR M1**	42.9	-	41.2
DAPL P4	41.9	-	-	**DAPR P4**	42.1	-	-
DAPL P3	32.5	-	31.7	**DAPR P3**	31.8	-	-
DAPL P2	28.5	-	-	**DAPR P2**	27.4	-	-
DT-a-L M3	31.3	-	42.9	**DT-a-R M3**	42	-	-
DT-a-L M2	49.1	-	55.9	**DT-a-R M2**	51.9	-	-
DT-a-L M1	51.2	-	-	**DT-a-R M1**	51.5	-	52.9
DT-a-L P4	50	-	-	**DT-a-R P4**	49.4	-	-
DT-a-L P3	42.8	-	42.5	**DT-a-R P3**	43.2	-	-
DT-a-L P2	31	-	-	**DT-a-R P2**	32.6	-	-
DT-p-L M2	41.3	-	47	**DT-p-R M2**	45.5	-	-
DT-p-L M1	48.9	-	48.9	**DT-p-R M1**	52	-	51.5
DT-p-L P4	49.9	-	-	**DT-p-R P4**	48.3	-	-
DT-p-L P3	48.2	-	43.3	**DT-p-R P3**	43.3	-	-
DT-p-L P2	43.8	-	-	**DT-p-R P2**	33.8	-	-
DT-p-L P1	33.7	-	-	**DT-p-R P1**	-	-	-
HIL M3	42.1	-	35.2	**HIR M3**	46.6	25.5	-
HIL M2	45.6	-	-	**HIR M2**	38.5	-	-
HIL M1	35.3	-	-	**HIR M1**	31.6	-	32.3
HIL P4	35.6	-	-	**HIR P4**	32	-	35.9
HIL P3	22.7	-	30	**HIR P3**	21.6	-	33.4
HIL P2	22.9	-	-	**HIR P2**	20.8	-	-

Table 5: Measurements of the adult dentitions on left (L) and right (R) side.

Code	AMPG-SAM504	AMPG-SAM501	Code	AMPG-SAM504	AMPG-SAM501
Species	*C. schlosseri*	*M.neumayri*	**Species**	*C. schlosseri*	*M.neumayri*
DAPL M2	-	-	**DAPR m2**	-	-
DAPL M1	-	43.1	**DAPR m1**	48.9	45.5
DAPL d4	-	53	**DAPR d4**	46.2	45.5
DAPL d3	-	45.2	**DAPR d3**	34.9	44.6
DAPL d2	-	35.2	**DAPR d2**	-	34.7
DAPL d1	-	-	**DAPR d1**	-	23.8
DT-a-L m2	-	-	**DT-a-R m2**	-	-
DT-a-L m1	-	22.2	**DT-a-R m1**	43.9	31.9
DT-a-L d4	-	46	**DT-a-R d4**	40.9	50.9
DT-a-L d3	-	44.2	**DT-a-R d3**	36.9	43.8
DT-a-L d2	-	33.4	**DT-a-R d2**	26.4	33.8
DT-a-L d1	-	-	**DT-a-R d1**	-	20.3
DT-p-M2	-	-	**DT-p-R m2**	-	-
DT-p-L m1	-	42.2	**DT-p-R M1**	-	-
DT-p-L d4	-	43.4	**DT-p-R d4**	40.1	43.6
DT-p-L d3	-	38.1	**DT-p-R d3**	36.4	43.7
DT-p-L d2	-	37.9	**DT-p-R d2**	30.8	37
DT-p-L d1	-	-	**DT-p-R d1**	-	-
HmL m2	-	-	**HmR m2**	-	-
HmL m1	-	-	**HmR m1**	55.5	-
HmL d4	-	37.4	**HmR d4**	32.8	33.8
HmL d3	-	32	**HmR d3**	-	32.2
HmL d2	-	23.6	**HmR d2**	-	19.9
HmL d1	-	-	**HmR d1**	-	11.8

Table 6: Measurements of the juvenile dentition, left (L) and right (R) side.

Code	AMPG-SAM500	AMPG-SAM502	AMPG-SAM512	Code	AMPG-SAM500	AMPG-SAM502	AMPG-SAM512
Species	*C. schlosseri*	*D. pikermiensis*	*Rhinocerotinae indet.*	**Species**	*C. schlosseri*	*D. pikermiensis*	*Rhinocerotinae indet.*
3L	38.7	76.2	-	**3R**	40.1	80.6	-
4L	46.1	79.2	78.5	**4R**	47.9	90.1	-
5L	-	87.6	74.9	**5R**	54.1	95.8	-
6L	-	95.1	75.8	**6R**	-	102.7	-
7L	-	101.1	-	**7R**	-	101.1	-
8L	-	101.3	-	**8R**	-	108.8	-
25L	39.5	79	-	**25R**	45.4	90.9	-
26L	42.5	77.3	71.4	**26R**	44.9	89.6	-
27L	-	89.7	63.2	**27R**	54.6	95.3	-
28L	-	94.8	58.9	**28R**	-	102.3	-
29L	-	88.2	-	**29R**	-	102.5	-
30L	-	76.3	-	**30R**	-	104.2	-
31L	36.7	55.7	44.4	**31R**	35.4	47.4	-
32L	40.5	66.4	47.1	**32R**	39.4	44.5	-
33L	-	71.7	47	**33R**	-	69.7	-
34L	-	81.7	45.9	**34R**	-	80.4	-
35L	-	85.2	-	**35R**	-	84.5	-
36L	-	75.4	-	**36R**	-	82.2	-

Table 7: Measurements of the adult mandibles on left (L) and right (R) clade.

Code	AMPG-SAM504	AMPG-SAM501
Species	*C. schlosseri*	*M.neumayri*
9	50	-
19	102.6	-
20	110.4	-
22	51.3	-
26	116.3	-
28	37.6	55.4
29	56.6	66.1

Table 8: Measurements of the juvenile skulls

Code	AMPG-SAM506	AMPG-SAM515	AMPG-SAM513
Species	*C. schlosseri*	*C. schlosseri*	*C. schlosseri*
M1-M3	126.8	-	122.7
P2-P4	99.7	-	91.5
P3-P4	71.4	-	73.2

Table 9: Measurements of the permanent toothrows

Code	AMPG-SAM500	AMPG-SAM502	AMPG-SAM512
Species	***C. schlosseri***	***D. pikermiensis***	***Rhinocerotinae indet.***
11	95.4	-	-
17	114.5	-	-
18	88.5	85.9	-
19	31	-	-

Table 10: Measurements of the mandibular body

Appendix C: Photographic documentation of the Naturhistorisches Museum Wien (NHMW) and Muséum National d' Histoire Naturelle specimens used as comparative material

Fig. A5: 1911/0005/0045, *M. neumayri* adult skull, in occlusal view. Samos Island, Greece. Scale: 4cm.

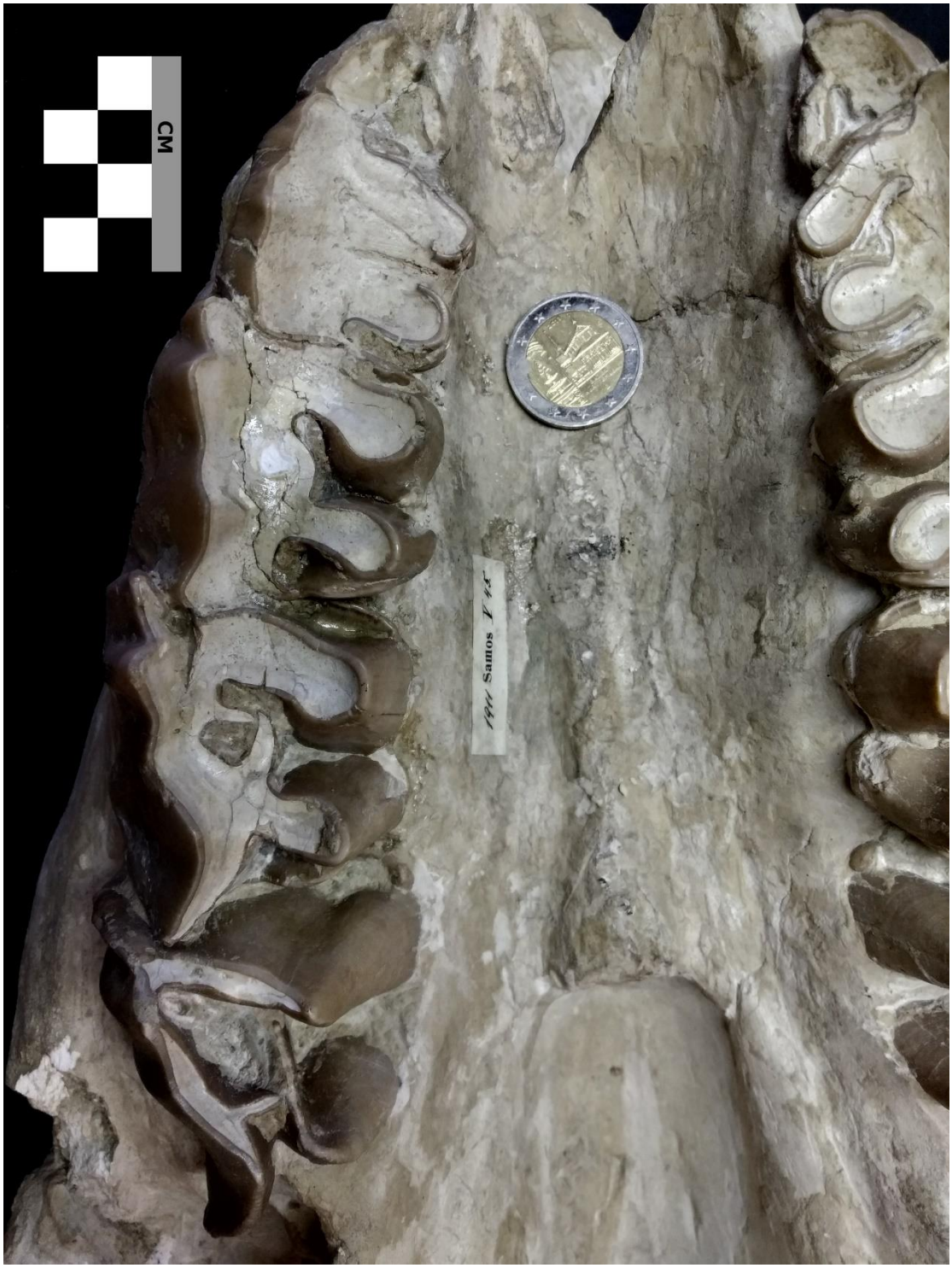

Fig. A6: NHMW-1911/0005/0045, *M. neumayri* adult upper dentition, in occlusal view. Samos Island, Greece. Scale: 4 cm.

Fig. A7: NHMW-1911/0005/0044, *M. neumayri* skull, in lateral view. Samos Island, Greece. Scale: 4 cm.

Fig. A8: NHMW-1911/0005/0030, *D. pikermiensis* juvenile upper dentition, in occlusal view. Samos Island, Greece. Scale: 4 cm.

Fig. A9: NHMW-1911/0005/0128, *C. schlosseri* adult skull, in lateral view. Samos Island, Greece. Scale: 5 cm.

Fig. A10: NHMW-1911/0005/0128, *C. schlosseri* adult skull, in occlusal view. Samos Island, Greece. Scale: 5 cm

Fig. A11: NHMW-2020/0014/0003, *C. persiae* adult skull, in occlusal view. Maragheh, Iran. Scale: 5 cm.

Fig. A12: NHMW-2020/0014/0002, *C. persiae* adult skull, in occlusal view. Maragheh, Iran. Scale: 5 cm.

Fig. A13: NHMW-2020/0014/0006, *C. persiae* juvenile skull, in occlusal view. Maragheh, Iran. Scale: 5 cm.

Fig. A14: NHMW-1911/0005/0032, *C. schlosseri* mandible, in occlusal view. Samos Island, Greece. Scale: 5 cm.

Fig. A15: NHMW-2020/0014/0096, *C. persiae* mandible, in occlusal view. Maragheh, Iran. Scale: 5 cm.

Fig. A16: NHMW-2020/0014/0033, *C. schlosseri* mandible, in occlusal view. Maragheh, Iran. Scale: 5 cm.

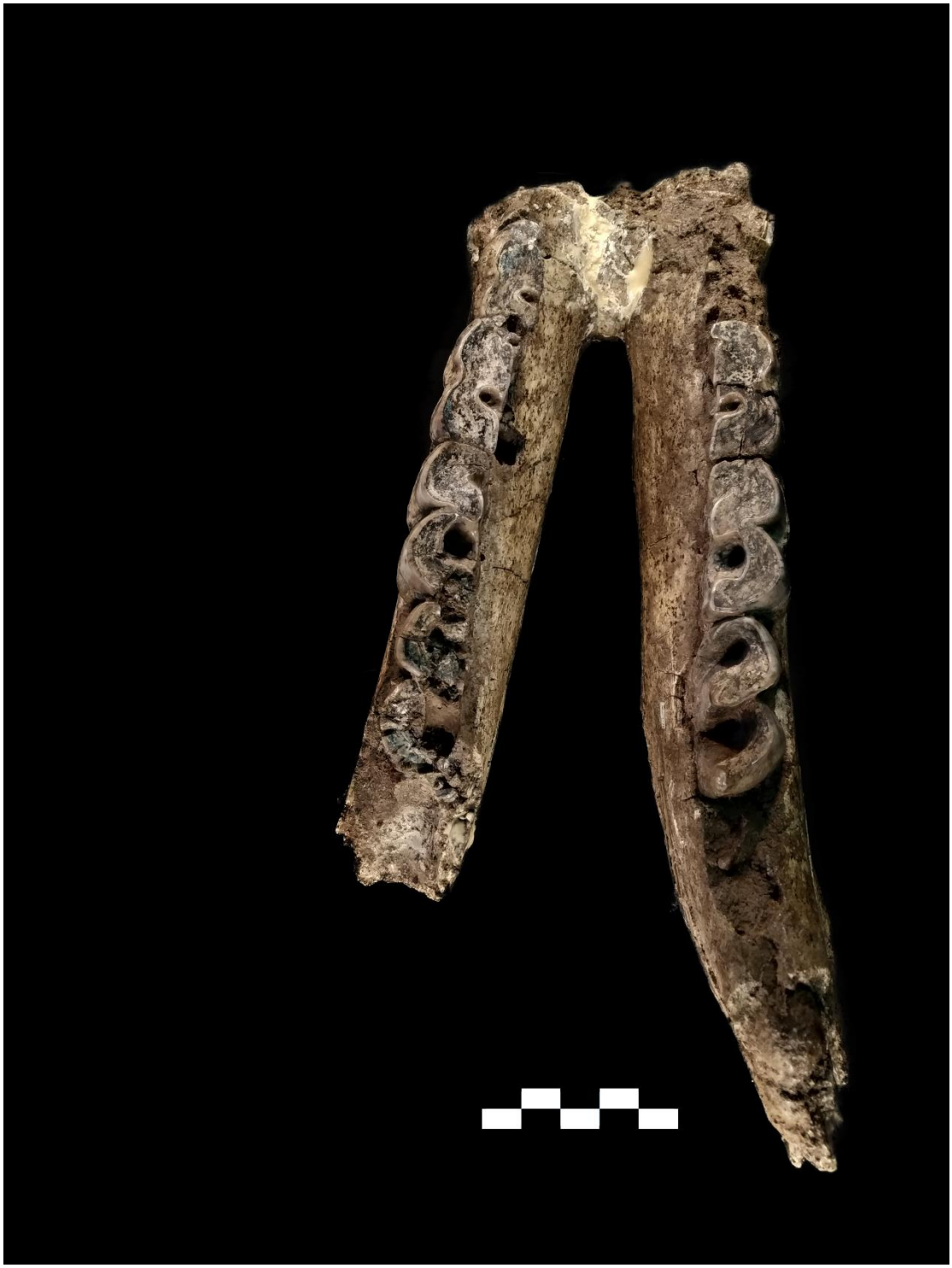

Fig. A17: NHMW-2020/0014/0100, *C. persiae* mandible, in occlusal view. Maragheh, Iran. Scale bar: 5 cm.

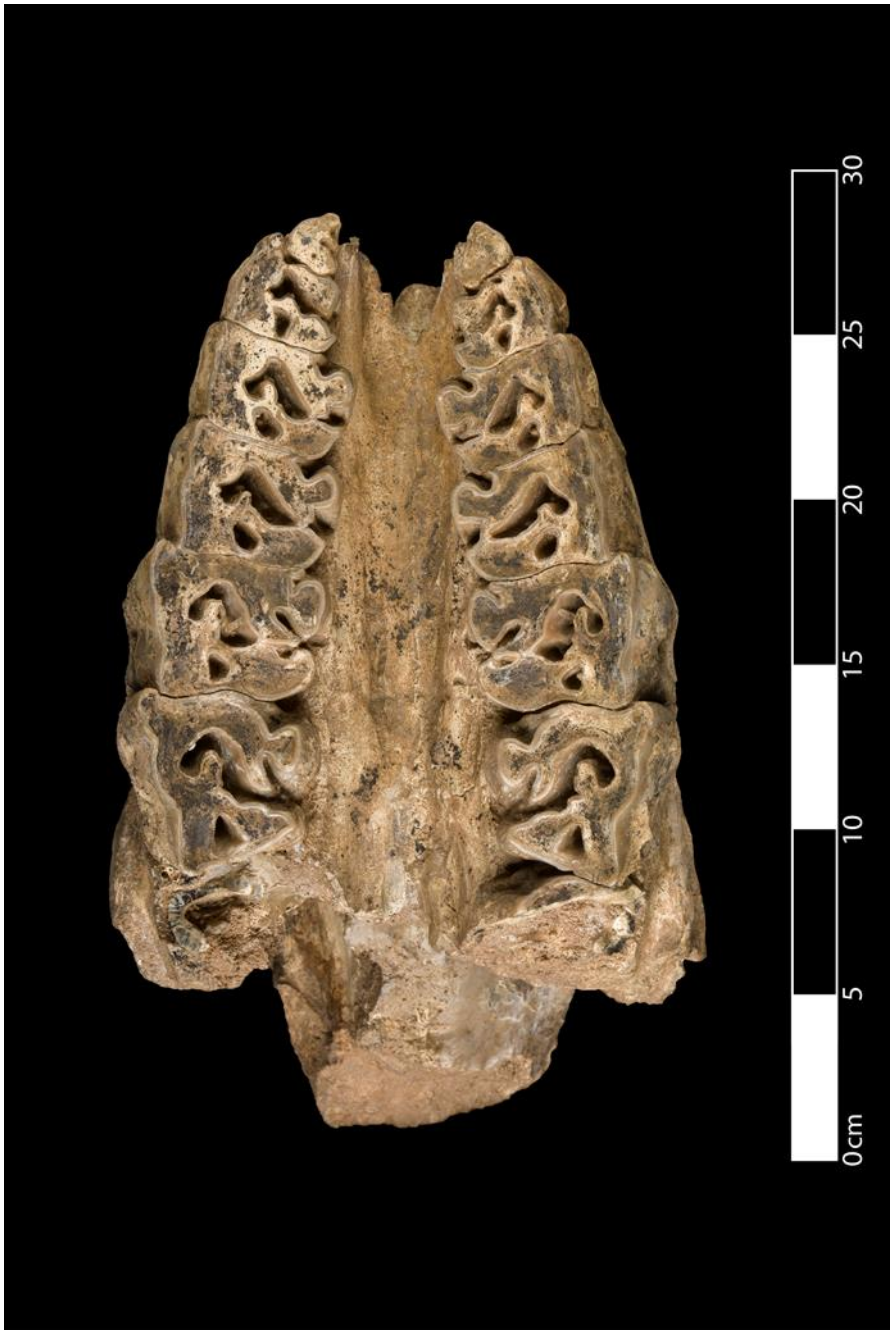

Fig. A18: MNHN.F.MAR3822, *C. persiae* skull, in occlusal view. Maragheh, Iran. Scale bar: 30 cm. Source: https://science.mnhn.fr/all/list?full_text=chilotherium+persiae

Fig. A19: MNHN.F.MAR3053, *C. persiae* skull, in occlusal view. Maragheh, Iran. Scale bar: 20 cm. Source: https://science.mnhn.fr/all/list?full_text=chilotherium+persiae

Fig. A20: MNHN.F.MAR3859, juvenile *C. schlosseri* mandible, in occlusal view. Maragheh, Iran. Scale bar: 30 cm. Source: https://science.mnhn.fr/all/list?full_text=chilotherium+persiae

Fig. A21: MNHN.F.MAR3889, juvenile *C. schlosseri* mandible, in occlusal view. Maragheh, Iran. Scale bar: 35 cm. Source: https://science.mnhn.fr/all/list?full_text=chilotherium+persiae

Appendix D: Macroscopic evaluation of the fossil matrix

Code	Species	Matrix type
AMPG-SAM501	*M. neumayri*	Calcitic sandstone
AMPG-SAM502	*D. pikermiensis*	Tuffaceous conglomerate
AMPG-SAM503	*C. schlosseri*	Calcitic sandstone
AMPG-SAM504	*C. schlosseri*	Calcitic sandstone
AMPG-SAM505	*C. schlosseri*	Tuffaceous conglomerate
AMPG-SAM506	*C. schlosseri*	Calcitic sandstone
AMPG-SAM508	*C. schlosseri*	Calcitic sandstone
AMPG-SAM509	*C. schlosseri*	Calcitic sandstone
AMPG-SAM510	*C. schlosseri*	Calcitic sandstone
AMPG-SAM513	*C. schlosseri*	Calcitic sandstone
AMPG-SAM515	*C. schlosseri*	Calcitic sandstone